

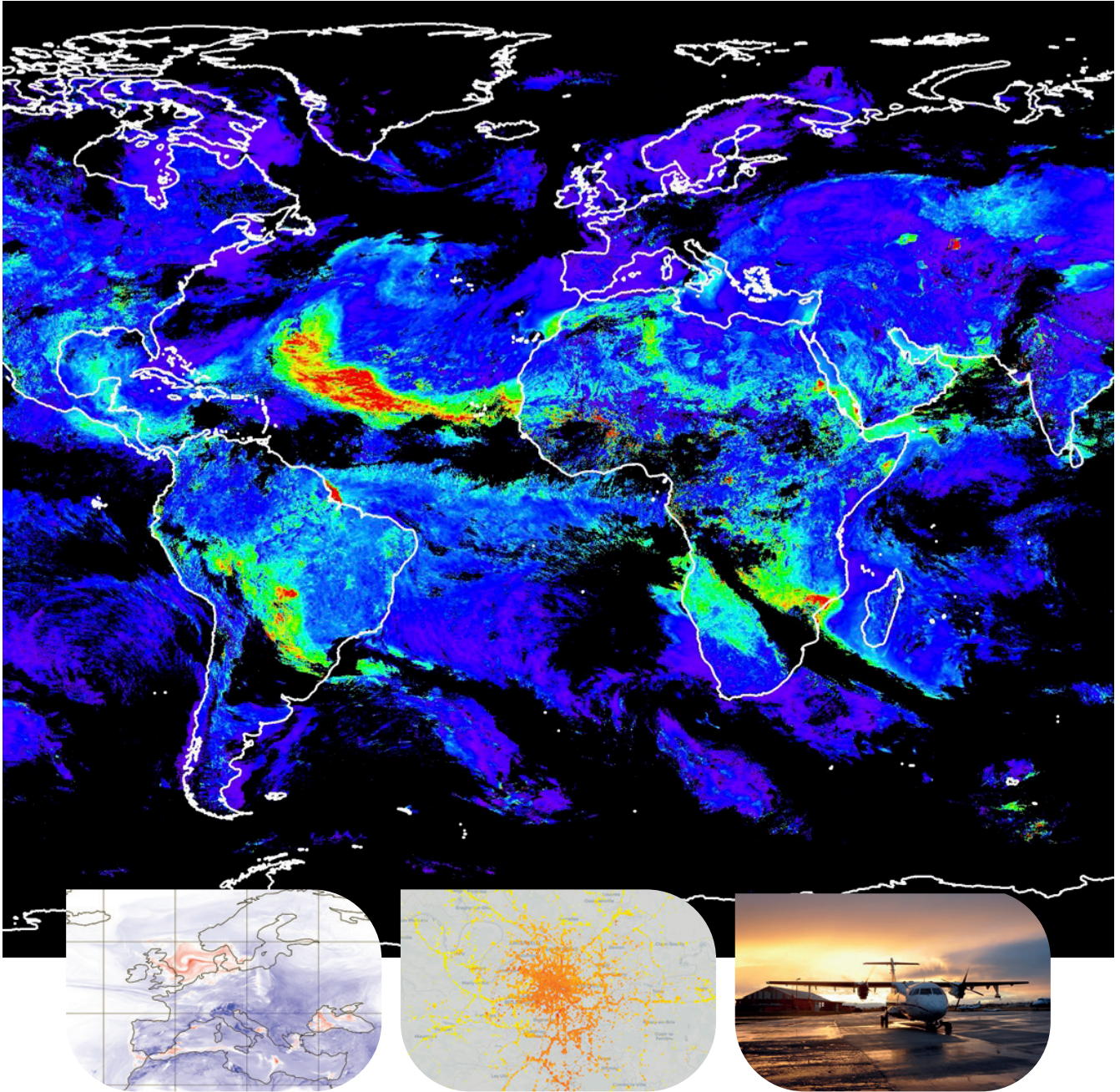


RÉPUBLIQUE  
FRANÇAISE

*Liberté  
Égalité  
Fraternité*



METEO  
FRANCE



Research **Report**  
**2020**



# Research Report 2020

---



# Table of contents

---

**Numerical weather prediction and data assimilation** ● page 6

**Process studies and modelling** ● page 14

**Climate** ● page 20

Climate modelling  
Diagnostic, study and impacts  
Seasonal forecast

**Chemistry, aerosols and air quality** ● page 30

**Snow** ● page 36

**Oceanography** ● page 40

**Engineering, campaigns and observation products** ● page 44

Observation engineering and products  
Campaigns

**Research and aeronautics** ● page 52

**Appendix** ● page 54

Research occupies a special place within Météo-France, as it supports all of the establishment's activities. It is the source of the progress that is then implemented in terms of observation and numerical weather and climate forecasting. It enables the Establishment to constantly improve the quality of its operational products and to open up new areas of work to meet the expectations of society and public authorities.

A major element for any international Meteorological Service is the arrival at the end of 2020 of two new supercomputers which, since the very beginning of 2021, have offered an increase in power of a factor of 5.5. The forecasting suits have been installed there. The first major upgrade is under construction and will be tested from mid-2021. It should be validated -normally- at the beginning of 2022 and should bring significant progress in terms of global forecasts as well as forecasts for metropolitan France and the French overseas territories. It should be noted that these two new machines based on CPU processors are also equipped with a few GPU processors, which will enable new approaches to be tested for the adaptation of numerical codes to future architectures, as well as integrated post-processing of ensemble forecasts.

The year 2020 saw the consolidation of the Scientific Strategy 2020-2030, with new exchanges with the members of the COMSI and a presentation to the Governing Board. Now approved, this Scientific Strategy will be used by the institution to build its next Contract of Objectives and Performance for the period 2022-2026. This Strategy is based on five main areas:

- Progress in the knowledge and anticipation of extreme phenomena and their impacts, in a context of climate change
- Continuing the transition towards integrated environmental modelling systems shared between forecasting and climate
- Adapt modelling tools to the operational requirements of tomorrow's computing architectures
- Enhance the value of weather and climate forecasts, in response to the expectations of internal and external beneficiaries
- Strengthen the dynamics of national and international cooperation, ensuring convergence with ECMWF



These areas will be fed by a series of studies on the generalisation of ensemble forecasting and its valorisation, on a new regional integrated system ("Earth system") to go as far as the impacts, on a hectometric system for the sites at stake and on the city, which brings together a number of meteorological and climatic issues. There will also be a commitment to participate in the IPCC exercises, to determine climate change on a local scale, both in mainland France and overseas, in order to deal with extreme phenomena, and to improve seasonal forecasting and its use. In the mountains, the period ahead will prepare a breakthrough with the development of a new avalanche risk forecasting system for the massifs, represented at a resolution of 250 metres and integrating new space-based observations. More broadly, for all subjects, the work will focus on taking into account the major space programmes announced up to 2030, but also the opportunities offered by 'low-cost' space observation and mass data. Artificial intelligence will be a major tool for processing these observation data, for post-processing ensemble forecasts and for optimising our numerical models. Our efforts will also focus, in European and national coordination, on adapting our numerical codes to the new architectures of the next high-performance computers.

At the international level, Météo-France is implementing its policy of privileged cooperation with the ECMWF on the Arpège/ IFS global model, particularly on various



aspects of physics that will soon bring progress to our global forecasts. Météo-France is seeing the completion of the merger of the Aladin and Hirlam consortia with the establishment on 1 January 2021 of the new ACCORD consortium, which brings together 26 countries around the AROME-HARMONIE-ALARO regional model. The management of this new consortium has been entrusted to an engineer from Météo-France.

The Establishment is continuing its policy of active participation in Eumetsat programmes, which will be reflected in our involvement in CDOP 4 of five of the “Satellite Application Facilities”. In 2020, in a complicated context linked to the COVID, ADM-Aeolus observations (assimilation of wind profiles in the global model) and CFOSAT observations (assimilation of wave observations in the sea surface model) were taken into account in the different models. Preparations for the future MTG and METOP-SG missions, which will carry new high-potential instruments, will continue, as well as the preparation of certain instruments carried by the Sentinel programmes. Météo-France is maintaining its strong participation in European projects, including Copernicus, and is preparing its involvement with its ACCORD partners in the DestinE project led by the ESA-EUMETSAT-ECMWF triumvirate.

At the national level, Météo-France continues to be involved in the scientific community, which is reflected in its various links with the CNRS, CNES and Universities, as well as its

participation in AllEnvi. It is a stakeholder in the Data Terra Research Infrastructure with its AERIS and THEIA Data and Services Centres, in Kalideos-Alpes under the aegis of CNES, and participates in the ACTRIS-FR and CLIMERI-France Research Infrastructures. In particular, AERIS is an opportunity and a vector to facilitate the access of the research world to the operational data of the Establishment.

In terms of experimental and measurement campaigns, the activity was strongly impacted by the COVID context. It is gratifying that, despite this major difficulty, the SOFOG-3D campaign, included in the 2017-2021 Contract of Objectives and Performance, was able to achieve its objectives. On the other hand, we regret the postponement to 2021 of the LIAISE campaign, which aims to gain a better understanding of semi-arid regions and improve our forecasts, particularly for the water budget. SAFIRE, for its part, has had to postpone to 2021, or even cancel, the campaigns planned between March and September 2020. Nevertheless, the EUREC4A campaign, before the first lock-down, was able to proceed perfectly. For the replacement of the Falcon 20 high-altitude research aircraft, Météo-France, along with the other supervisory bodies of SAFIRE, supported the approach implemented, which was selected within the framework of PIA3+. Météo-France will support the project by maintaining its resources at the SAFIRE Unit but will not be able to participate financially in the initial investment.

Much of the research work of direct interest to Météo-France is carried out by the CNRM. This is an opportunity to salute and wish the best to the new CNRM management team (Samuel Morin and Nadia Fourrié), which takes up its duties on 1 January 2021. Other research work is also being carried out within the LACy and in certain Directions of the Establishment. All this work is detailed in the rest of this document. They are numerous, diverse, innovative and exciting. They perfectly illustrate the broad spectrum of our research activities, all of which are essential to the Establishment and its future.

But 2020 was the year of COVID with its difficulties and complications. This report is the opportunity to salute all those involved, researchers, engineers, technicians, administrative staff, post-doc, PhD, trainees and particularly those who have had to lead teams or supervise colleagues. It is also important to salute the support teams and in particular the IT department which played a crucial role during this period. Many thanks to all of them and let's hope that 2021 will see the end of the pandemic.

« Bonne lecture »



Marc Pontaud  
Météo-France  
scientific director,  
Head of Higher Education  
and Research

# Numerical weather prediction and data assimilation

---

A significant part of the research and development activities carried out in numerical weather prediction (NWP) during 2020 was devoted to the implementation of evolutions in the operational suite and the migration on the new Bull-AMD supercomputers and the preparation of the next version of NWP systems. New observations have been assimilated into the operational NWP suite, such as AMV (Atmospheric Motion Vectors) wind data from Goes17 satellite, Afirs and Tamdar aircraft data distributed by FLYTH, wind measurements by ESA Aeolus space-borne Doppler lidar and data from several global positioning systems by radio occultation (GNSS-RO). The latter two types of data have had a very positive impact on the objective scores. Many activities have been conducted to prepare the next e-suite to align specifically the spatial resolutions of the ensemble prediction systems (PEARP and PEARO) with the ones of the deterministic systems (Arpege and Arome-France), to increase the horizontal resolution of the Arome overseas systems and to transfer several important technical and scientific improvements from research to operations.

Research activities have been performed in parallel to prepare the long-term evolutions of NWP systems. An « EnVar » assimilation scheme combining the variational and the ensemble approaches has been developed to improve the representation of the background error covariances and to take into account the temporal dimension in the « 4DEnVar » version. This « EnVar » algorithm is particularly relevant for the analysis of new variables, such as the hydrometeors of the Arome model. Some research activities on the dynamical cores have been conducted to improve the performance of the Arome model on massively parallel machines. The use of the ozone field from the Mocale model improves the radiative transfer in the data assimilation, anticipating the benefits of an integrated Earth system. Several researches have been successfully accomplished to improve the use of ensemble prediction systems (post-processing using artificial intelligence techniques, integration into decision support tools, etc.).

---

## Accounting for hydrometeors in the 3DEnVar AROME scheme

The role of hydrometeors in convective scale data assimilation is a sensitive issue.

These three-dimensional variables of the AROME model describe atmospheric water in condensed form: mass contents of cloud water, ice crystals, rain, snow and graupel. Until now, they were not affected by data assimilation. After the assimilation process, the adjustment of hydrometeor fields to the other analyzed variables such as specific humidity and temperature was expected to be done implicitly through the time evolution of the numerical model. This behavior is sub-optimal, and prevents from directly assimilating observations sensitive to cloud and precipitation (radars, microwave

imagers...). The implementation at CNRM of a prototype of 3DEnVar for AROME has allowed these variables to be accounted for, the ensemble approach allowing a real-time description of hydrometeor forecast error statistics. However, adapted methods of localization had to be implemented to filter the sampling noise in the estimation of these errors.

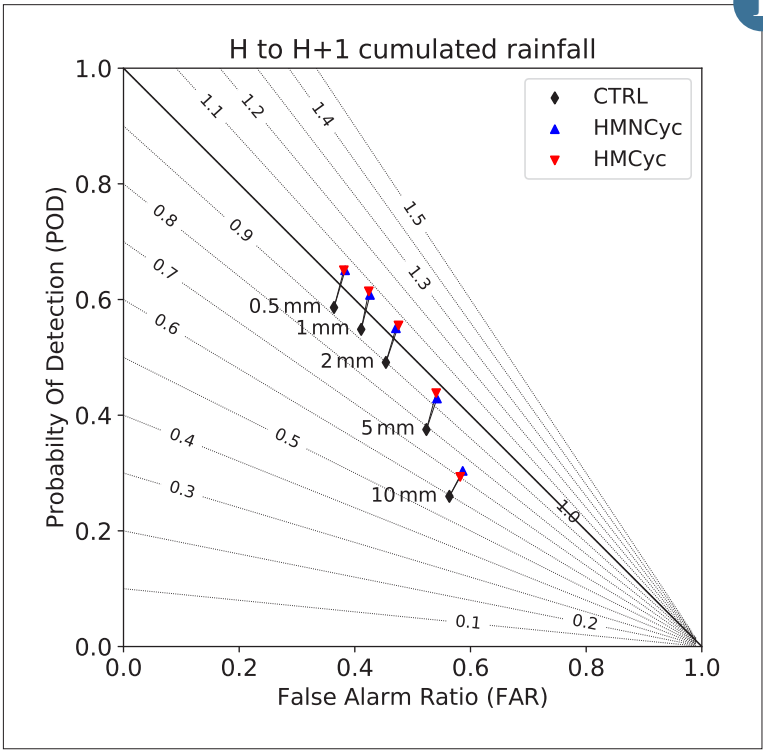
The addition of hydrometeors as control variables of the analysis has been evaluated in a near-operational framework. The spatial resolution has been degraded (3.2 km instead of 1.3 km), thus allowing the evaluation period to be extended to 3 months (May – August 2018). Even without

assimilating additional observations, the impact is positive at nowcasting lead times. In particular, the improvements are statistically significant for cloud positioning (up to 6 hours) and precipitation (first hour). The robustness of these results is confirmed by their relative independence from the localization scheme used in the 3DEnVar.

1



1



▲ The impact of adding hydrometeor in the analysis is globally positive in the cycled (HMCyc) and non-cycled (HMNCyc) experiments compared to the control experiment (CTRL). The contour lines show the value of the frequency bias.

## AEOLUS: Operational use in the global weather forecasting model

The European Space Agency's AEOLUS satellite has been in sun-synchronous orbit since 22 August 2018.

The use of a LIDAR Doppler for the measurement of wind profiles from space was the first of its kind and required considerable calibration/validation work. Thus, from April 2020, AEOLUS wind products have been provided in real time to operational weather forecasting centres, with a quality level sufficient to be assimilated in the global numerical forecasting model ARPEGE. The CNRM/GMAP, strongly involved in this preparatory work, was able to use these data as soon as they were made available. Thus, after having shown a very positive impact on the quality of the forecast scores (cf. Figure), their operational assimilation took place shortly afterwards: on 30 June 2020.

The operational use of these data was particularly relevant since it compensated for the lack of aircraft data caused by the Covid-19 pandemic (cf. the positive impact in the northern hemisphere which had not been shown until then). The AEOLUS data

represent only 0.42% of the total number of data assimilated in the ARPEGE model, but they contribute 2.5% in terms of information content brought by the observations to the model and they are the third most efficient (by individual observation) to reduce the 24-hour forecast error.

Météo-France has thus joined the ECMWF and the DWD (German meteorological service) in the group of the first meteorological centres to assimilate these data operationally.

The importance of AEOLUS winds for numerical weather prediction led ESA to extend this innovative mission for more than a year (end of 2022).

2

## Tracking and assessment of tropical cyclones in the global ensemble forecasting system PEARP

This study focusses on the global ensemble forecasting system PEARP operated at Météo-France, which is based on the global ARPEGE model. So far, there is no deep assessment of PEARP yet about its ability to properly predict tropical cyclone tracks and intensity. For that purpose, an original approach was carried out in which oriented-object scores are calculated based on a dedicated tracking tools developed at CNRM and adapted to the PEARP ensemble. The tropical cyclones included within the period between 5 July and 14 December 2019, over all bassins, were simulated with PEARP, and then forecasts were compared to Best-Track analyses.

The obtained results are fairly comparable to the state of art with track errors reaching in average 500-600 km at 120h of forecast time (Fig a), albeit a simulated slow bias. These track errors are consistent with the ensemble spread. Finally, the case of tropical cyclone Dorian shows that PEARP is able to capture fairly well the uncertainty and the possibility of an intense tropical system impacting Bahamas and Southeastern USA three or four days ahead (Fig b).

This oriented-object approach will be able to further improve the PEARP system for TC assessment as for tropical cyclone forecasting and offer a potential use in the future high resolution ensemble system with Arome Over Seas.

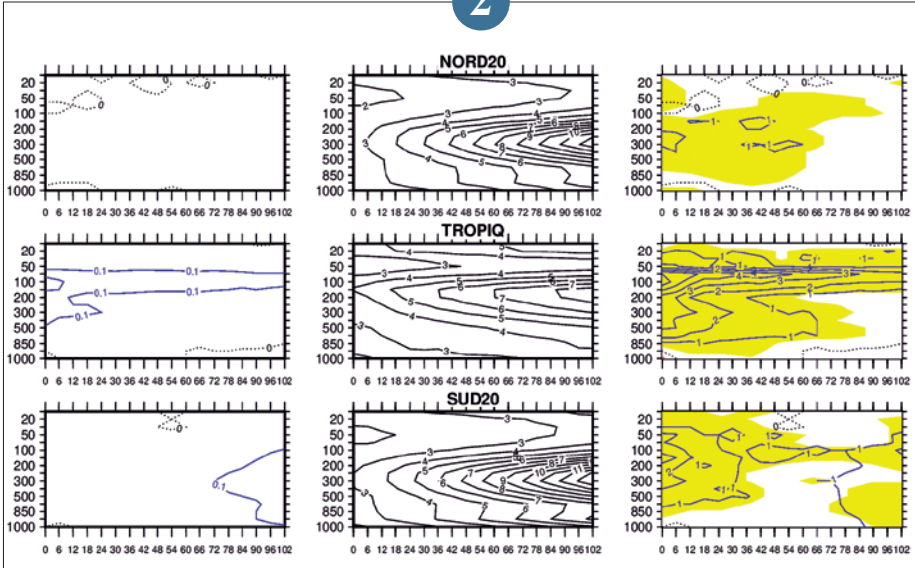
4

## Use of variable ozone in a radiative transfer model for the global Météo-France 4D-Var system

To extract information from satellite observations useful for the global numerical weather prediction model ARPEGE, the fast radiative transfer model RTTOV is an essential numerical tool. It enables to simulate these observations from realistic information on the state of the atmosphere (temperature, water vapour) as well as on its chemical composition. For numerical weather prediction, the concentration of some gases and aerosols is approximated by climatological profiles. At Météo-France, the Chemistry Transport Model (CTM) MOCAGE realistically simulates the concentration of many gases and aerosols present in the atmosphere. A coupling of the ARPEGE and MOCAGE models would improve the assimilation of infrared satellite observations into ARPEGE. Thus, the use of realistic ozone fields provided by MOCAGE in RTTOV has made the simulation of the ozone-sensitive channels of the IASI hyperspectral sounder on board the Metop satellite more accurate. An improved simulation of some channels within the CO<sub>2</sub> or water vapour absorption bands has also been observed. From experiments to assimilate these data into the ARPEGE model, it appears that the changes made to the simulations of these channels gradually improve the quality of meteorological analyses. An indirect positive impact on the assimilation of other observations, independent of ozone, such as radiosondes, microwave satellite observations or GNSS Radio-occultation observations has also been noted thanks to better short-term forecasts of the ARPEGE model. Longer range weather forecasts (up to 102 h) are also improved for different parameters (wind, temperature, humidity). Work continues to make the operational model ARPEGE benefit from these innovations and to extend it to other atmospheric constituents.

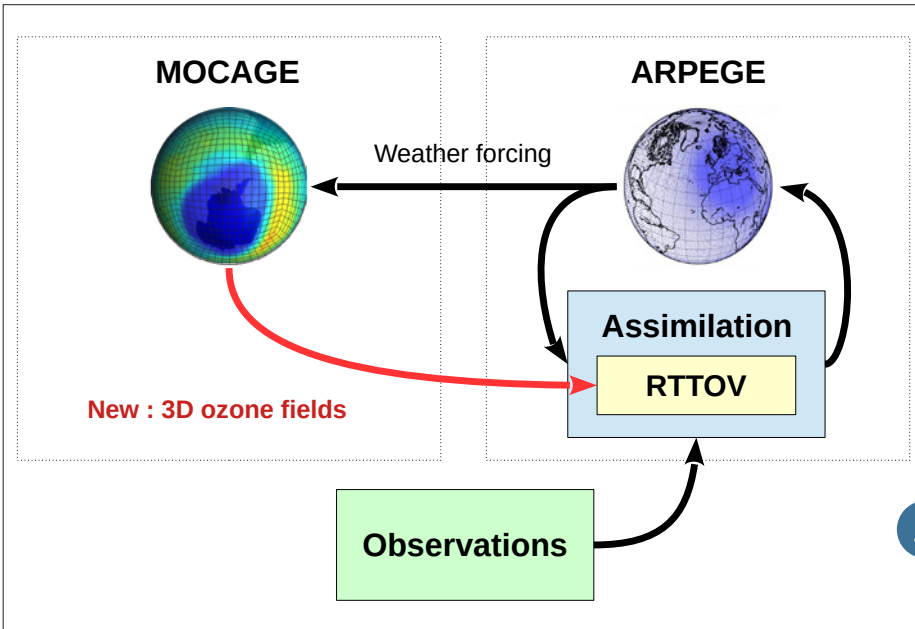
3

2



Relative impact of AEOLUS wind measurements on the reduction of wind forecast errors of the ARPEGE model over the Northern hemisphere (top line), the Tropics (middle line) and the Southern hemisphere (bottom line) (April to May 2020). The left panel displays the variation of the wind root mean square error (in m/s) with respect to ECMWF analyses from 0 to 102 hours (x-axis) and as a function of the pressure level (y-axis in hPa) compared to a reference experiment without assimilation of AEOLUS data. The middle panel displays the root mean square error for the reference experiment, and the right panel displays the ratio of the left panel to the middle ones (in percent). The blue level lines indicate a reduction in forecast error. The yellow background indicates areas where the statistics are considered significant.

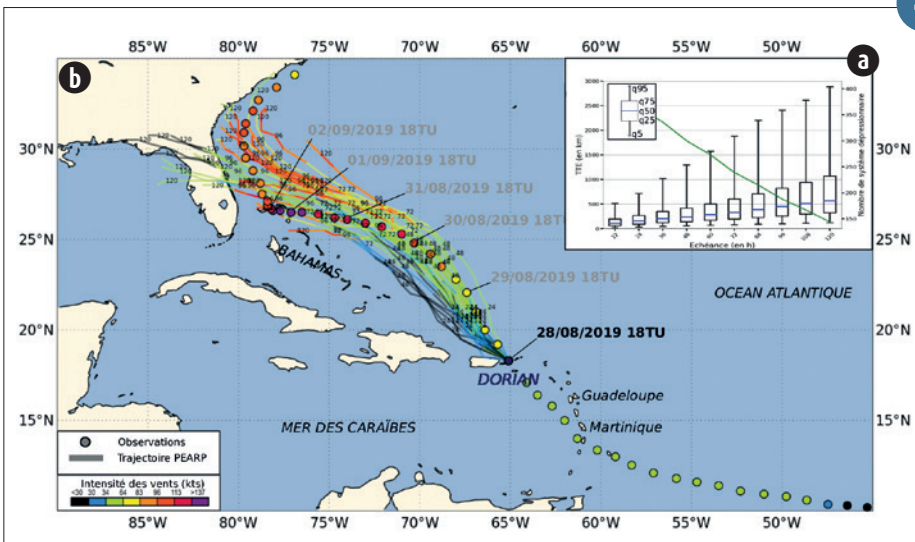
MOCAGE ARPEGE



Synthesis scheme summarising a first step of the coupling between the ARPEGE (numerical weather prediction) and MOCAGE (atmospheric chemistry) models for the Earth system. The red arrow indicates the new addition of tridimensional (3D) ozone fields in the radiative transfer model RTTOV.

3

4



(a) Error track distributions as a function of forecast time (period 05/07/19 - 14/12/19) and (b) Track - Intensity plume of PEARP forecasts for Dorian starting on 28/08/19 at 18 UTC.

---

## Developing a grid point dynamics for the AROME model

The AROME operational model has a very efficient dynamics thanks to the use of long time steps that can be obtained by maintaining the stability and accuracy of the model due to the use of a semi-Lagrangian and semi-implicit algorithm. The semi-implicit scheme requires the inversion of an elliptical problem on the horizontal at each time step. This problem is inverted very efficiently in a so-called “spectral” space. Thus at each time step a transform from the grid point space to the spectral space is performed, different calculations are done in spectral space and then the inverse transforms is performed to continue the calculations in grid point space. The spectral also allows to compute the derivatives with a great precision, and

to apply a filtering to efficiently diffuse the variables of the model. Spectral transforms being very expensive in communications, we would like to be able to avoid using them to improve the performance of the model on massively parallel machines.

We have therefore sought to achieve the inversion of the implicit grid point problem with an iterative method using solvers working in Krylov’s space. The results obtained show that it is possible to get the same quality of forecast as shown in the figure, for a small computer cost of only three iterations on the average.

5

---

## First results from a 4DEnVar assimilation scheme for AROME-France

The AROME-France Data Assimilation system has been providing hourly analyses, using the most recent observations, since April-2015. Some of these observations, for example radar measurements, are available at higher frequency (every 15 mins). In order to optimise usage of these observations, we will replace the current 3D assimilation scheme with a 4D version, able to deal with the temporal dimension during the analysis building.

This change is investigated in the EnVar framework, the association of variational approaches, which have been traditionally used at Météo-France, with ensemble techniques, increasingly used operationally at a number of numerical weather prediction centres around the world. These schemes allow background error statistics to be directly deduced from perturbations provided by an assimilation ensemble, which thus depend on the meteorological situation. Moreover,

temporal error correlations manage the temporal dimension during the assimilation process, without the need of tangent linear and adjoint versions of the forecast model. A prototype of a 4DEnVar system, assimilating the observations available every 15 minutes has been developed and its promising performances evaluated on some case studies. For example, the location and the intensity of the stronger precipitations are better simulated during the convective event of the 28th May 2018.

6

---

## Adaptation and evaluation of RTTOV to IR and MW satellite observations from the 1970s and 1980s

In the framework of the C3S 311c project for the rescue of satellite data from instruments that flew in the pre-1970s to 1980s, the satellite observation operator RTTOV was adapted and evaluated for these old instruments. The main objective is to digitize, reformat, recalibrate and homogenize these observations to be assimilated in the next ECMWF ERA6 re-analysis.

These instruments were mainly on US Nimbus, TIROS and DMSP satellites, including multi-spectral infrared sounders (SIRS, THIR, MRIR, HRIR), a hyperspectral infrared sounder (IRIS) and microwave sounders (MSU, SSM, SMMR). These instruments had much coarser spatial resolutions than current instruments (ranging from a few tens to a few hundred kilometers as opposed to a few hundred meters to a few tens of kilometers currently) but are a unique source of Earth observations during these periods.

To simulate these observations, RTTOV has been adapted from the information found in the archives on the instrumental spectral response functions. An evaluation of the quality of the RTTOV simulations was proposed from a large base of atmospheric profiles covering the globe which allowed to highlight latitudinal biases of the RTTOV model. The evolution of the spectroscopic databases essential for RTTOV simulations were compared to the instrumental noise to see if these instruments were sensitive to it. The attached figure shows for example that the IRIS instrument had such an instrumental noise that it is not sensitive to spectroscopy. The C3S project should be renewed in phase 2 to work on other old instruments.

7

---

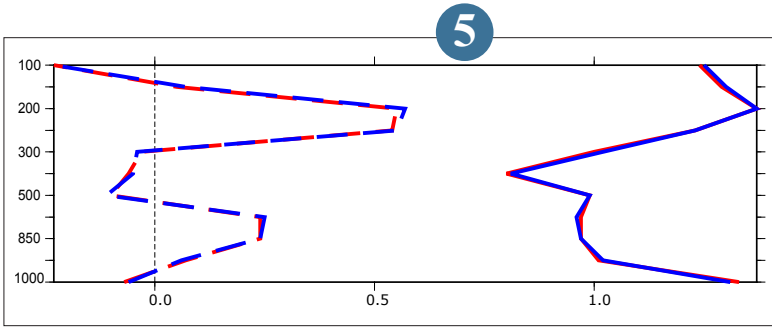
## Automatic texture-based classification of high-resolution precipitation forecasts

The high-resolution Arome model provides very realistic rainfall forecasts. However, these forecasts cannot be interpreted at the model grid scale. To characterize rainfall at a point, it is necessary to consider the forecast rain field around this point. This is particularly true when one is interested in the texture of the predicted rainfall, i.e. whether it is continuous or intermittent.

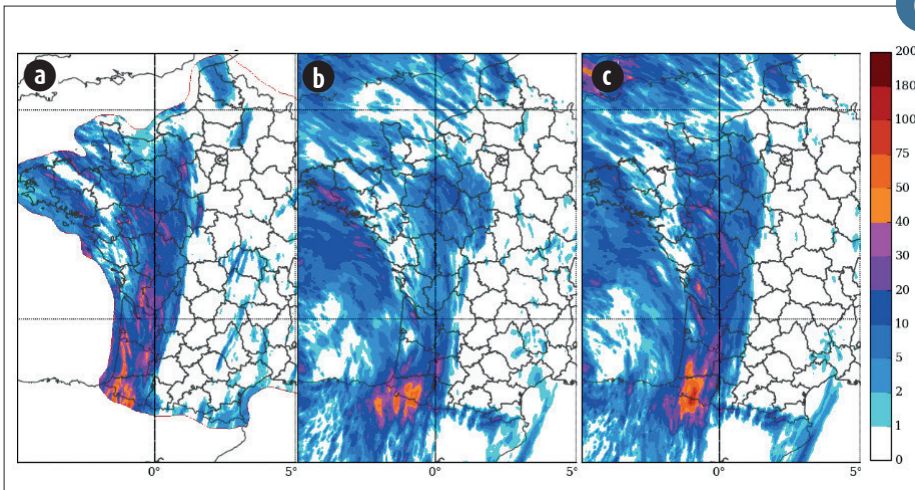
Taking this specificity into account, we have developed an automatic method for segmenting rain fields according to their texture. The method is based on tools from the field of machine learning: random forests and convolutional neural networks. The results obtained are very close to the zoning performed by the experts. They thus pave the way for the use of this segmentation

method for the verification of forecasts, or the automatic drafting of weather maps.

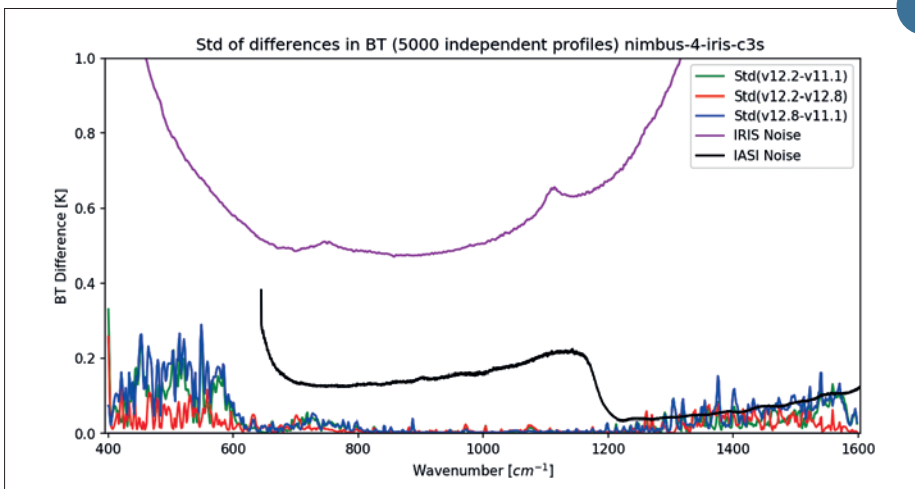
8



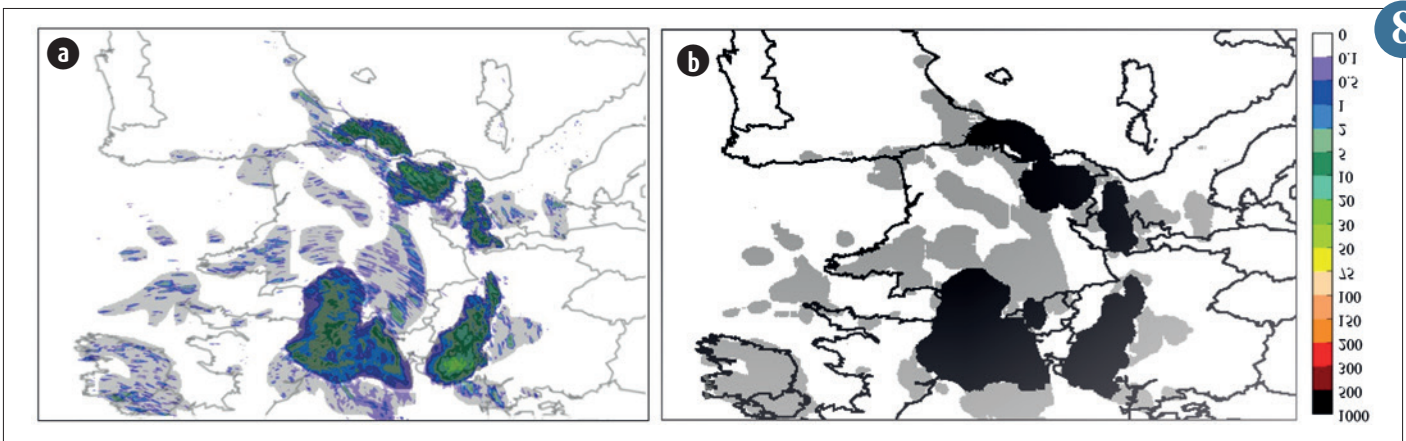
5  
 Comparison of the quality of the model between the spectral method (red) and grid point method (blue) as a function of the height (y-axis in pressure). Dotted line is the bias and solid line is the root mean square error, both with respect to the radiosonde observations.



6  
 24h accumulated precipitations on the 28th May 2018 observed by radars (a) and simulated by the sum of the 1h range forecasts from the 24 assimilation cycles using 3D-Var (b) and 4D-EnVar (c).



7  
 Example of the evaluation of the variability of spectroscopic databases evolutions between 3 versions of LBLRTM1 line-by-line codes based on 3 versions of HITRAN 2004 (v11.1), 2008 (v12.2) and 2012 (v12.8). Comparison of these variabilities to the IRIS instrumental noise (in pink) shows that the IRIS instrument is not sensitive enough to these variabilities. On the other hand the less noisy latest generation of hyperspectral instrument IASI (in black) is sensitive to them in the water vapor band above 1200  $\text{cm}^{-1}$ .



8  
 (a) Cumulative rainfall over 1 hour predicted by the Arôme model. Light grey shaded areas represent intermittent rainfall, dark grey shaded areas represent continuous rainfall. This segmentation was done manually by an expert.  
 (b) Result of the automatic rainfall segmentation with a convolutional neural network. The intermittent rainfalls are shown in light gray, the continuous rainfalls in black.

---

## Application of ensemble predictions in agronomic modelling

In crop protection, the evolution of diseases and pests is highly dependent on weather conditions. Phytosanitary treatments help control part of the epidemics, but they should be used with caution owing to their impacts on the environment and human health. In order to assist farmers in the positioning of treatments, decision support tools (DSTs) are proposed, which are based on the modeling of epidemic dynamics and on weather forecasts. However, the reliability of DSTs remains imperfect, particularly because weather forecasts are uncertain. Several simple approaches are commonly implemented to account for this meteorological uncertainty in DSTs, while the use of ensemble forecasts remains largely unexplored. A first evaluation of the impact of ensemble predictions has been conducted in a DST simulating the evolution of the grapevine worm, and has shown a significant improvement of the prediction of treatment dates compared to existing approaches.

Anticipating the application of treatments is essential and this requires high-quality weather forecasts from very short to medium ranges. This need has motivated the development of an innovative method to combine, without temporal discontinuity, Arome, Arpège and IFS ensemble forecasts. These seamless forecasts then allow DSTs to benefit from the quality of high-resolution Arome forecasts at short lead times. The next step will be the development of a demonstration platform to promote these ensemble forecasts to the agricultural community.

9

---

## Impact of an explicit representation of vegetation on snowpack modeling in forests

The ISBA surface model developed at the CNRM and integrated into the SURFEX surface modeling platform is a so-called composite scheme: it represents the surface soil layer and the vegetation as a homogeneous layer whose physical properties result from an averaging of soil and vegetation properties (e.g.s albedo, roughness).

A new option, Multi-Energy-Balance (MEB), represents soil and vegetation separately. This development allows a more realistic approach to modeling water and energy exchanges above, in and under the canopy with an explicit treatment of each compartment which permits the consideration of new processes (ground shading by the canopy, radiative transfer in the vegetation, interception of snow by the canopy, etc.).

One of the motivations for this development is to model better the evolution of snow cover within the forested regions (Napoly et al. 2020). Indeed, the composite ISBA scheme does not represent the snow cover

between the ground and the canopy. MEB prolongs the snowpack in this example (Fig. 1) by about three weeks in much better agreement with the observations. Indeed, MEB allows the snow to cover the ground under the forest canopy almost entirely and thus cut off direct exchanges between the ground and the atmosphere. Without MEB, the contact with the atmosphere will be able to warm the ground directly at the beginning of spring which in turn will prematurely melt the snow cover. There is also ongoing work with MEB coupled to the detailed CROCUS snow model in SURFEX. The next step is to evaluate MEB on a global scale.

10

## Statistical post-processing of ensemble forecasts using artificial intelligence

Like deterministic forecasts, ensemble forecasts are not perfect and a simultaneous correction for their bias and dispersion is needed in order to provide reliable forecasts. The goal is to train an algorithm on the relationship between past observations and the errors made by the ensemble. For this, we use artificial intelligence techniques, in order to take into account the contribution of many meteorological or even geographic variables. In addition, for global models, a statistical downscaling is performed to reach the kilometer scale.

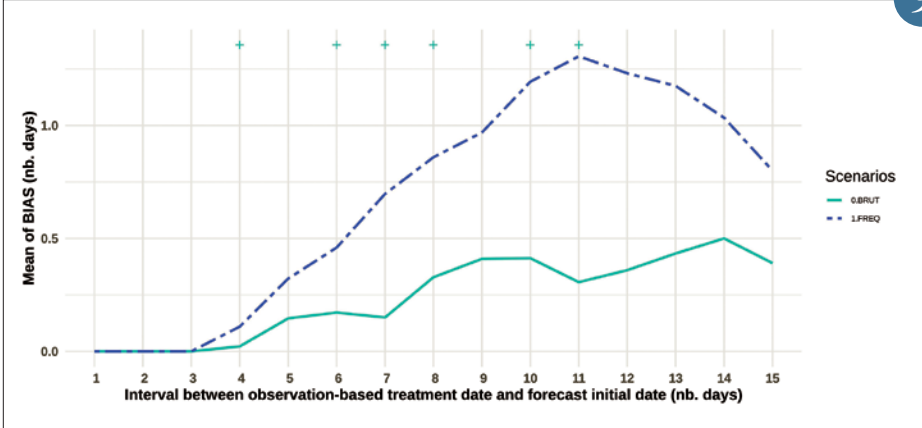
In addition, the operational implementation of these solutions requires original computer architectures to process long archives of past data, and to be able to post-process such ensemble forecasts in a few minutes at a computation cost two orders of magnitude lower than the resources used for the original ensemble model.

These techniques are applied to the ARPEGE and AROME ensemble forecasts. The results show an increased reliability of the forecasts, and we also observe a better detection of extreme events without increasing the false alarm rates.

This work led in 2020 to the operational implementation of the ARPEGE and AROME ensemble post-processing for surface temperature and hourly precipitation. The future is to extend these algorithms to other meteorological variables and to experiment new techniques focusing on predicting extreme events. This work finally shows the strategic interest of having long archives of forecasts to improve the performance of the future algorithms.

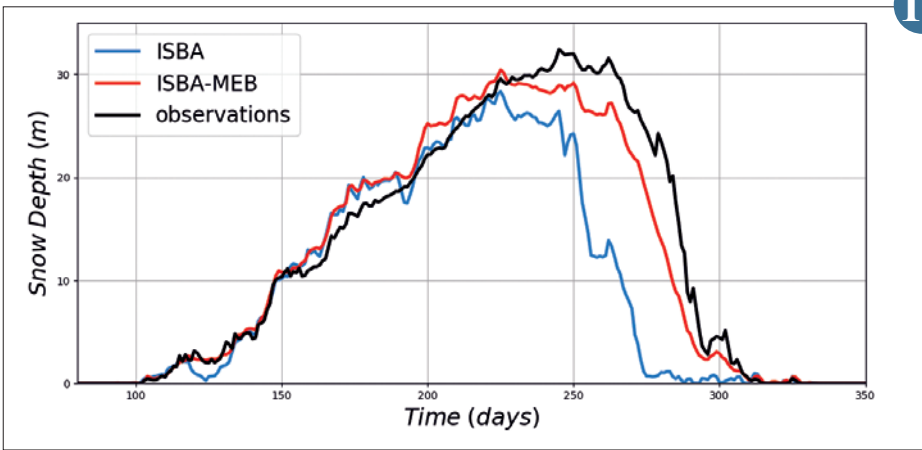
11

9

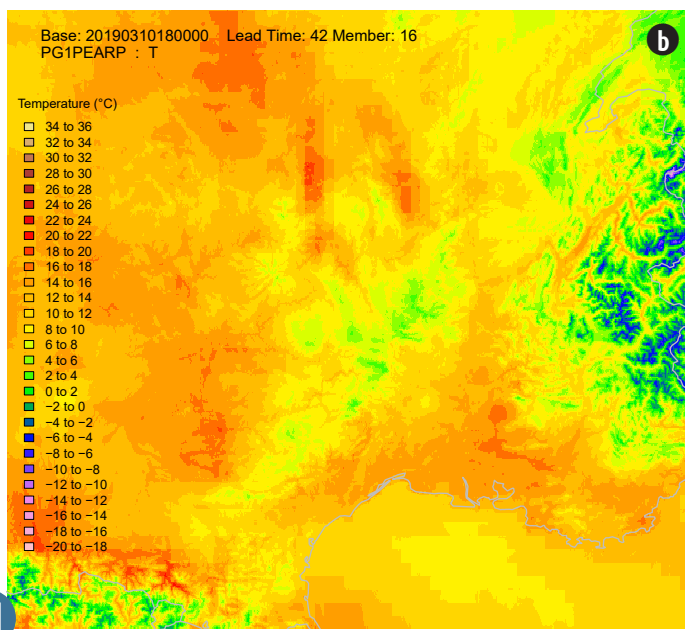
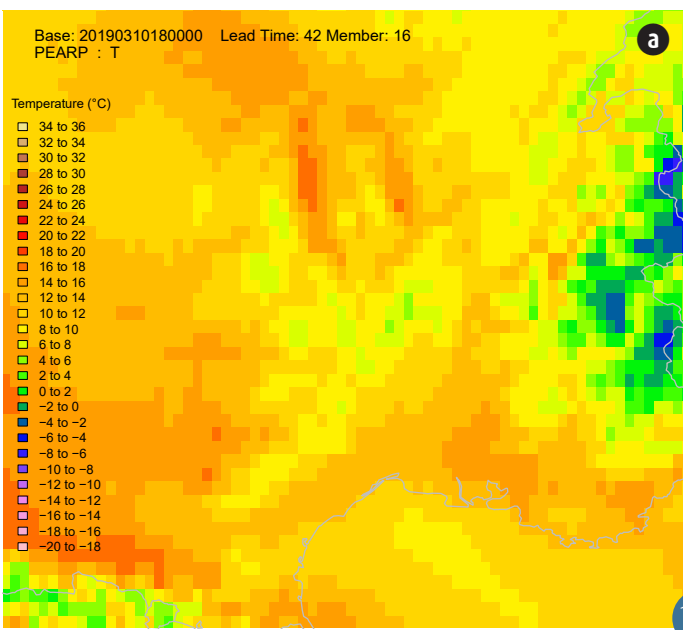


Mean bias of the predicted treatment dates, as a function of the number of days between the reference treatment date and the start of the forecast. The results are averaged over 8 agricultural lands for the years 2018 and 2019. The + signs at the top indicate that the performance of the ensemble forecast (in cyan) is statistically better than the performance of the existing "frequent" approach (in blue).

10



Average annual change in snow depth at one of the BERMS forest sites located in Canada (using 10 years of data).



11

(a) One member of ARPEGE ensemble forecast on the south of France.  
 (b) The same member after post-processing and statistical downscaling.

# Process studies and modelling

---

Research on process studies aims to improve the understanding of phenomena and their representation in numerical weather and climate prediction models, leading to the design of relevant weather-climate services. Process studies are generally based on a complementary approach between observation and modeling: fine-scale numerical simulations, validated with observations, provide a detailed description to better characterize the processes, and thus to better represent them in larger scale models.

All atmospheric simulations presented below are based on the Meso-NH research model. Used at metric spatial resolutions, it allows to characterize complex flows and exchanges at the edges of convective clouds, as well as the processes which govern them, such as the evaporative cooling of cloud droplets.

Closer to the surface, the so-called immersed boundary method makes it possible to explicitly resolve the flow around buildings. The addition of turbulence recycle in a multiscale configuration reproduces the forward energy cascade from larger to smaller vortices, and thus provides an additional degree of realism to simulate aerodynamical effects in urban districts.

At hectometric scales, targeted by numerical weather prediction models over the next few years, the model used as a numerical laboratory makes it possible to analyze heavy precipitation events, such as the Aude floods of 2018, using observations including personal weather stations for validation. For this case, the location of the intense precipitation is determined by the location first of the quasi-stationary cold front, and second of the convective bands downwind of the orography.

Another important issue is aircraft icing by supercooled water, as forecast models have difficulty in predicting significant quantities of water at negative temperature, especially large drops. Expectations are also high in the areas of transport and energy. A new generation of cloud microphysical schemes allows a better representation of particle size distribution, with more finely parameterized processes, and is promising to improve risk prediction.

Heat waves are another type of extreme meteorological event, for which the physical and dynamic mechanisms need to be better documented, as well as their climate evolution. An analysis of simulations on the heat wave of 2010 in the Sahel allows to explain the negative impact of a parameterization of deep convection, which can be overcome at spatial resolutions finer than 5 km.

In the humid tropics, the same model coupled online with aerosol and aqueous chemistry models uses the Bio-Maïdo experimental campaign to better understand the chemical and biological mechanisms in the presence of clouds controlling the formation of organic matter on airborne particles (secondary organic aerosols).

Finally, progress in the understanding and modeling of continental surface processes requires considering anthropogenic factors affecting the water cycle. A step has been taken with the integration of lake dynamics in the SURFEX-CTRIIP model, in order to represent the complete hydrological cycle by coupling with the rivers network. This set will also constitute an essential element of the future kilometric coupled system for meteorological and environmental forecasting, aimed by the Météo-France's scientific strategy for the next decade.

---

## Analysis of the heavy rainfall event of 14 and 15 October 2018 in the Aude department

On 14 and 15 October 2018, heavy rainfall fell on the Aude department and neighbouring departments, causing devastating flash floods that resulted in around fifteen victims and hundreds of millions of euros in damage. This extreme event was studied in detail from a meteorological point of view. To this end, numerical forecast models and operational observation networks were mobilised, as well as research models and observations from personal weather stations. The latter made it possible, among other things, to delimit the various air masses near the ground more precisely and to improve precipitation estimates.

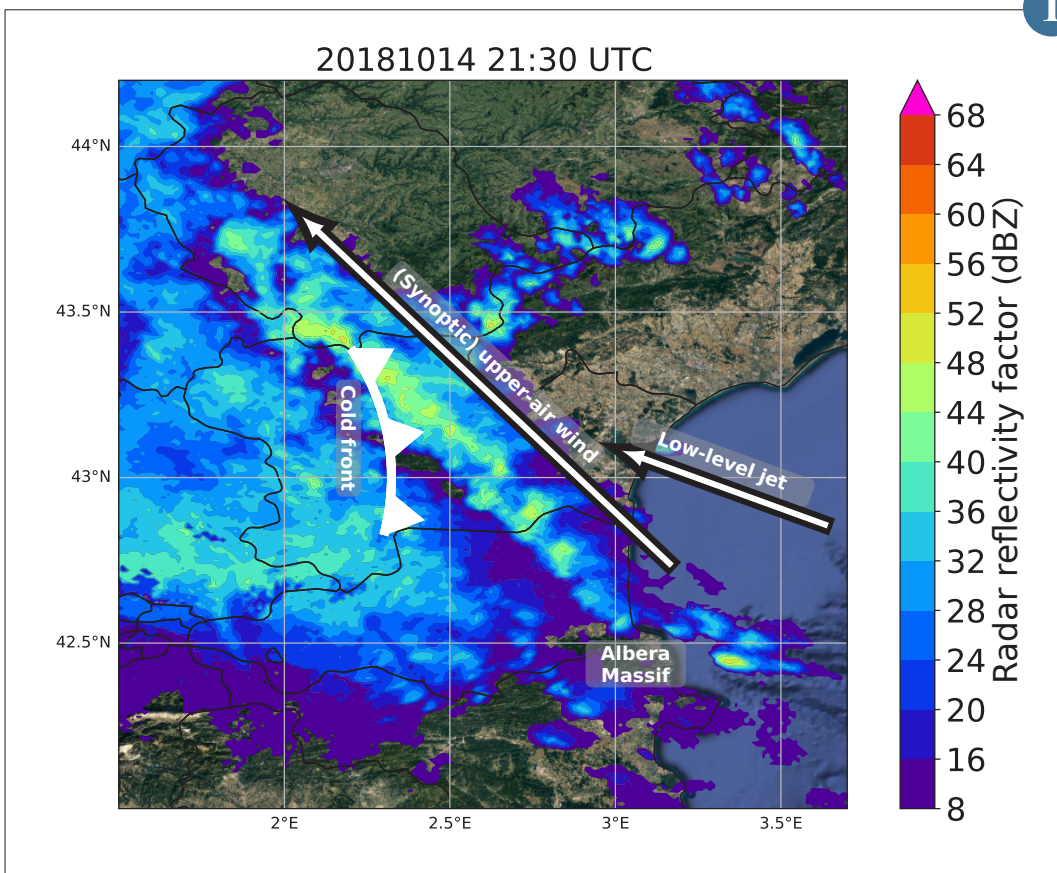
The Meso-NH research model, used with a horizontal resolution of 500 m (compared with 1.3 km for the finest operational model at Météo-France), showed the crucial role of the Albera Massif (see Figure) in the initiation of the storms which then propagated towards the Aude department. It also made it possible to determine the importance of a pre-existing cold air mass in the west on which the warm air coming from the Mediterranean impinged and which contributed to the intensification of precipitation in the northern part of the department. Finally, it has been shown that the remains of hurricane Leslie, which was approaching the Mediterranean basin at the

same time, only played a limited role, and only at the end of the event, in supplying the storms with moisture.

In addition to its contribution to our knowledge of heavy Mediterranean rainfall, this work opens up prospects for increased use of crowdsourced data and prepares the way for the use of future forecasting models with hectometre resolution.

1





▲ Base reflectivity factor (dBZ) of the Météo-France radar network on 14 October 2018 at 21:30 UTC. The upper and lower wind directions are shown schematically (warm and humid low-level jet), as well as the positions of the Albera Massif and the ground footprint of the cold front. The most significant damage was observed to the north of the Aude, near the junction of the cold front and the line of thunderstorm cells fed by the low-level jet.

---

## Fine-scale dynamics and turbulence on the edges of a cumulus congestus

A cumulus congestus has been simulated with the Meso-NH research model at a resolution of 5 meters in order to study the small-scale dynamics and mixing at its edges.

We obtained a very realistic cloud with structures typical of a growing cloud: strong updrafts associated with a core of positive buoyancy, large eddies near the top of the cloud forming a toroidal circulation and a subsiding shell surrounding the cloud.

A partition of the cloud and its environment (Figure a) is used to characterize the dynamics, buoyancy and turbulence near the edges of the cloud. The interior of the cloud is mainly ascending and positively buoyant (Figure b). The edges of the cloud are characterized by an increased presence of subsidence and are marked by an inversion of buoyancy (negative values). Evaporative cooling of the cloud droplets contributes to the buoyancy inversion near the cloud edges and to attenuate the overall convective circulation.

The turbulence at the edges is on a finer scale than that inside the cloud. At a resolution of 5 meters, the dynamic production of sub-grid turbulence (related to wind shear) largely dominates the thermal production (related to buoyancy). The latter is stronger at the edges than inside the cloud.

In order to generalize these results, these studies of physical processes at the interface between the cloud and its environment will be continued by testing in particular different wind and humidity conditions for the environment and by examining more developed clouds such as cumulonimbus clouds.

2

## Obstacle resolving urban climate modelling

Obstacle resolving urban climate modelling is required to represent the complexity of urban geometries and their interaction with meteorological parameters like air temperature, wind, and radiative fluxes, which are strongly heterogeneous in the urban environment. An obstacle resolving version of the Meso-NH model has been developed to enable the quantification of urban districts in terms of thermal comfort and ventilation or to serve as a reference for urban climate models like TEB1, which are based on a simplification of the urban geometry.

The objective of the present study is to investigate the influence of atmospheric boundary layer turbulence on the flow and the dispersion of a pollutant released in an idealised urban environment under realistic meteorological conditions (MUST2 experiment; Figure 1). Two modelling approaches are tested: a fine-scale-only approach, which does not take into account the boundary layer turbulence upstream of the city, an approach similar to the one chosen in common engineering studies, and a multi-scale approach based on the grid nesting in Meso-NH which takes into account all scales of atmospheric boundary layer turbulence. Results show that the multi-scale approach improves the vertical profiles of wind speed and turbulent kinetic energy. Furthermore, due to the increase of turbulence intensity, the multi-scale approach simulates lower values of maximum pollutant concentration, which is in better agreement with the observations than the fine-scale-only approach.

In future studies, similar analyses will be made for a selection of urban morphologies representative of French cities

4

---

## Improving supercooled liquid water forecasts : The ICICLE field campaign

Aircraft icing is a serious hazard that occurs when a plane flies through a cloud containing supercooled (at a negative temperature) liquid water. Supercooled droplets are unstable and freeze easily upon contact with the aircraft, building ice masses that can cause stalls or power losses.

Numerical weather prediction models tend to glaciate clouds too fast and underestimate supercooled liquid water in clouds. In order to better understand this bias and icing-prone conditions, the ICICLE field campaign was conducted in February 2019 in Rockford (USA). 30 flights were performed in icing conditions to provide detailed cloud composition observations for various weather types.

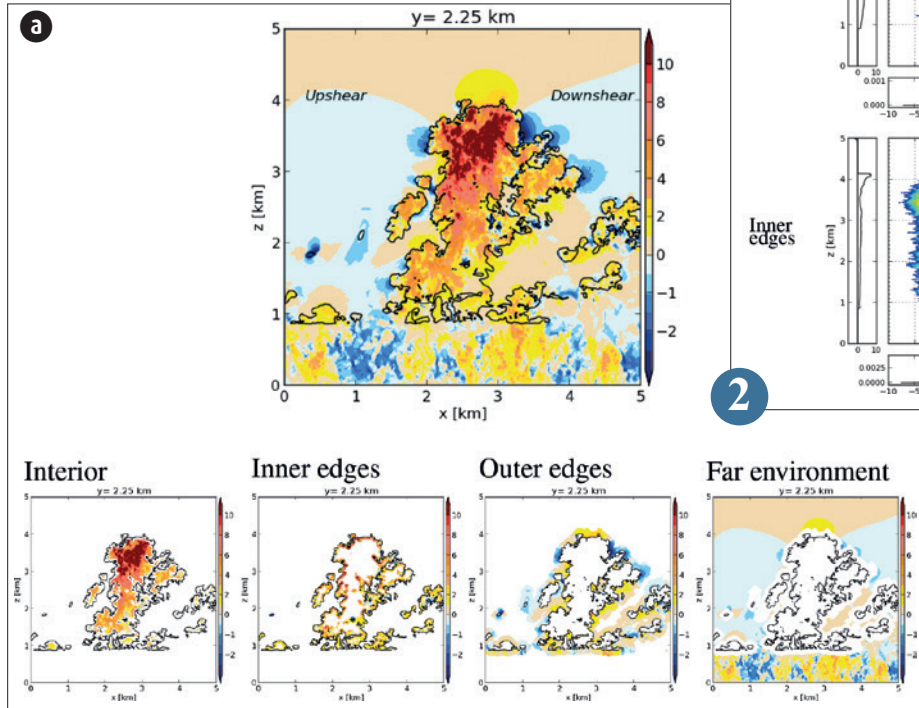
Two cases from the ICICLE campaign were simulated with the Meso-NH research model using various configurations of the ICE3 and LIMA microphysical schemes. Results

from this study showed that the 2-moment scheme LIMA produces more supercooled liquid water than ICE3, thanks to a better description of ice nucleation and vapour deposition on ice crystals. Supercooled cloud droplets sizes, which are important to estimate icing severity, are also quite well estimated. These simulations, at a resolution of 2 km, also showed a strong impact of the subgrid cloud scheme on cloud liquid fraction, which will have to be investigated further with higher resolution runs.

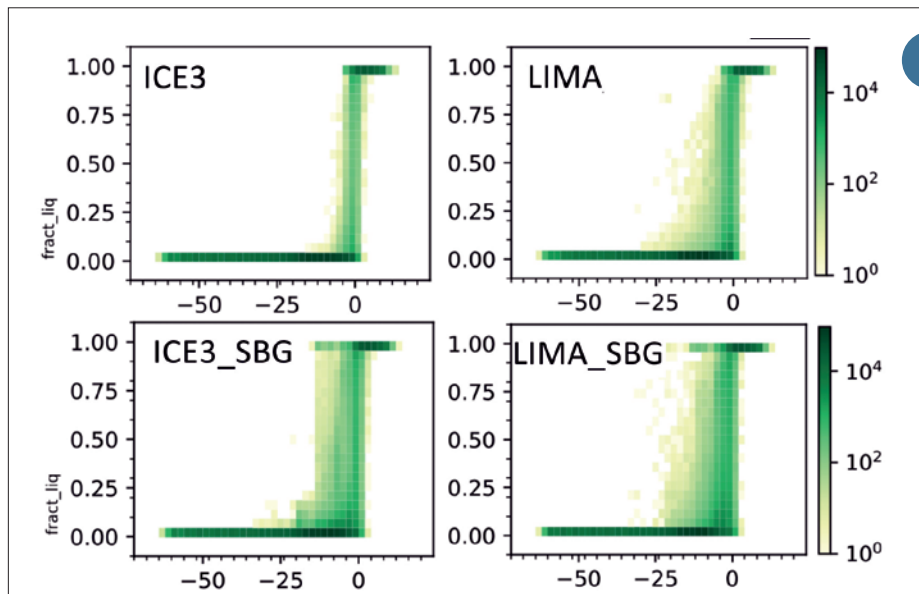
This study will result in improvements in our ability to forecast supercooled liquid water in clouds, enabling better icing forecasts, for aircraft safety as well as other purposes, such as ground transport and energy production management.

3

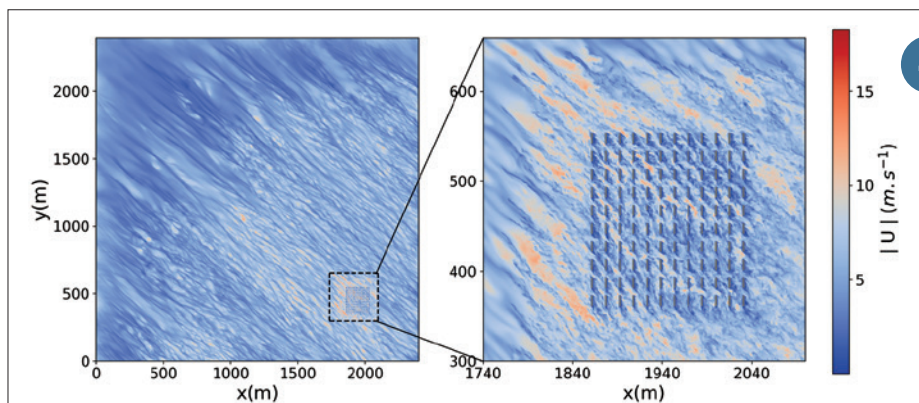
(a) Vertical section of the vertical velocity (m/s) within a cumulus congestus (cloud contour in black lines) and its environment (top panel) and partition (bottom panels) from left to right: inside of the cloud (more than 50 m from the edges), inner edges (50-m thick), outer edges (150-m thick) and in the far environment (more than 150 m from the interface).



(b) Vertical distribution of vertical velocity  $W$  (m/s) (right panels) and buoyancy  $B$  ( $m.s^{-2}$ ) (left panels) for the inside of the cloud (top panels) and for its inner edges (bottom panels). The mean vertical profiles and mean distributions are shown respectively on the left and below each panel.



Number of grid points with a given liquid fraction and temperature, on 2019/02/17 at 12 UTC. SBG denotes simulations using the subgrid cloud scheme.



Modelling the turbulent flow in an idealised urban district by taking into account the atmospheric boundary layer turbulence upstream of the district thanks to the Méso-NH grid nesting approach.

---

## Explicit Representation of lake mass balance within the global hydrological cycle

Earth System modeling at the CNRM represents the global continental hydrological cycle using the coupled ISBA-CTrip system. The new 1/12° resolution hydrographic network represents key processes, such as river discharge, floodplains and groundwater flows. But the performance of such a system can be improved, especially in regions of high lake density such as Northern Canada and Scandinavia, by adding a component representing lake dynamics. Thus, a lake mass balance model (MLake) has been developed to forecast water resource evolution. This model includes processes that contribute to the variation of lake water volume, in particular, precipitation, evaporation (simulated with the SURFEX/FLake model), inflow (CTrip) and outflow (parameterized), surface runoff and water infiltration into the ground (SURFEX/ISBA), as well as water exchanges with aquifers and withdrawals. Lake mapping is derived by cross-referencing the MERIT-HYDRO high-resolution Digital Terrain Model with

the Global Lake DataBase mask. The explicit consideration of the surface water balance requires two masks: one ensuring hydrological consistency and the other guaranteeing a correct distribution of surface runoff between the different hydrological compartments (Fig.a). The model simulates lakes with a surface area greater than 1 km<sup>2</sup> and predicts the evolution of their storage while permitting a diagnosis of water level variations.

A preliminary evaluation of ISBA-CTrip in off-line mode at the global scale including the lake dynamics has shown a clear improvement in regions where the presence of lakes controls the propagation of flows (Fig.b). Moreover, the introduction of Mlake in this coupled system permits modeling the effect of dams on reservoirs.

5

---

## Heat wave and convection scheme: A Sahelian case-study

In spring, the Sahel is prone to heat waves that strongly affect local populations. Over the past decades, these events have been intensifying, at a rate faster than the global warming. This trend is expected to continue into the 21st century. The present study aims at improving our understanding of these events, in particular to better criticize the numerical models used for producing these climate projections. We focus on the April 2010 Sahelian heat wave and perform numerical simulations using the limited area model Méso-NH. Two different configurations are considered, and differ from the activation or not of the deep convection scheme. These simulations are evaluated using a wide set of in-situ and spatial observations. The activation of the deep convection scheme generates spurious precipitating events over the Sahel and a poor phasing of convection in its southern part. Rainfall evaporation cools and moistens the atmospheric boundary layer, limiting the model's ability to reproduce the properties of the heat wave.

The simulation without deep convection scheme better agrees with the observations. In particular, the monsoon surge is well reproduced, thereby allowing an increase in water vapour over the Sahel, an increased greenhouse effect, and ultimately an increase in minimum temperatures. Some biases potentially persist in relation to the high concentration of dust during the episode and an underestimation of cloud occurrence.

In conclusion, a sufficient horizontal spatial resolution allowing an explicit representation of deep convection is unexpectedly important to correctly simulate a heat wave over the Sahel. Such an issue likely impacts current climate models, thus questioning their ability to capture Sahelian heat wave processes and provide relevant projections of their evolution.

6

## Bio-Maïdo

The Bio-Maïdo programme aims to improve our understanding of the formation and transformation processes of atmospheric Secondary Organic Aerosols (SOA). Indeed, uncertainties about the processes involved in the life cycle of these aerosols need to be addressed in order to better understand the impacts of SOA on air quality, health and climate change.

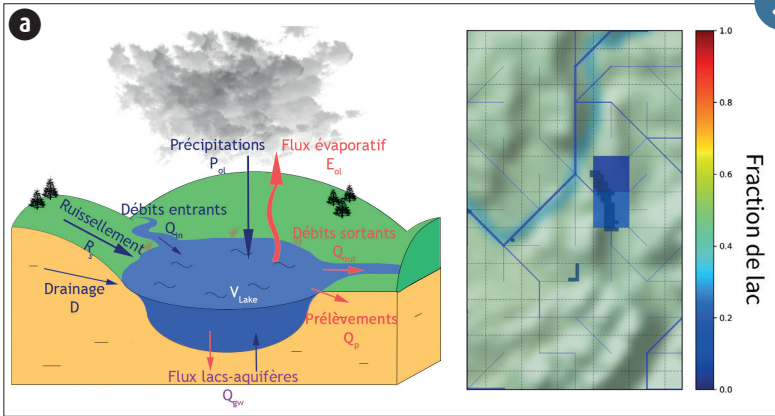
The objectives of Bio-Maïdo are as follows: to understand what are the main routes of formation of SOA in moist tropical atmospheres (respective contributions of the gaseous and aqueous phases); to improve the multiphase processes leading to the formation of SOA in three-dimensional models; to understand how the presence of bacteria in the aqueous phase contributes to the formation of SOA (Figure 1).

Given that the tropical environment of Reunion Island presents optimal conditions for studying these processes, and that Reunion benefits from the presence of OPAR, the proposed strategy is based on a large-scale measurement campaign at several sites in Reunion Island in order to characterize the sources of gas and aerosol emissions, and to assess the multi-phase pathways of formation and oxidation of SOA, including the effect of bacteria present in cloud water. This work is carried out in synergy with modeling studies with an explicit cloud chemistry model and a three-dimensional transport/chemistry model including a cloud chemistry module.

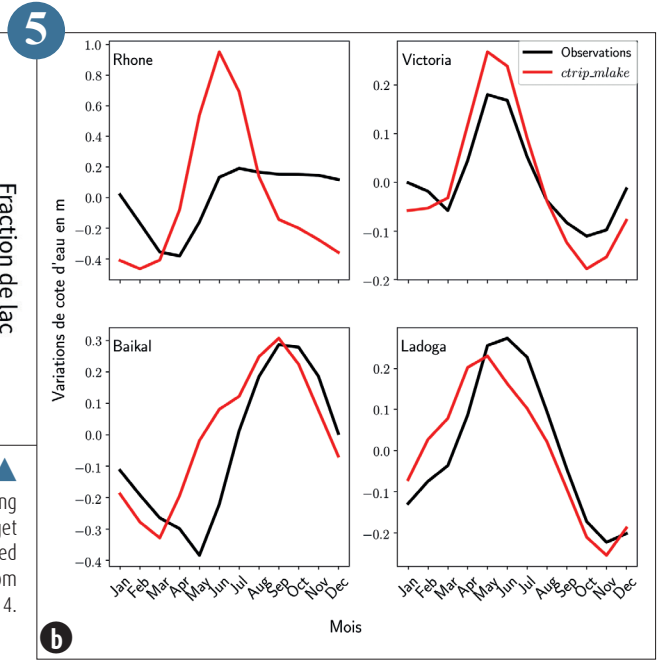
The Bio-Maïdo measurement campaign took place in March-April 2019 and mobilized the entire programme consortium of six partners: LAERO, LACy, LaMP, IGE, LSCE, CNRM and LaRGE.

The data from this campaign are currently being processed and analysed.

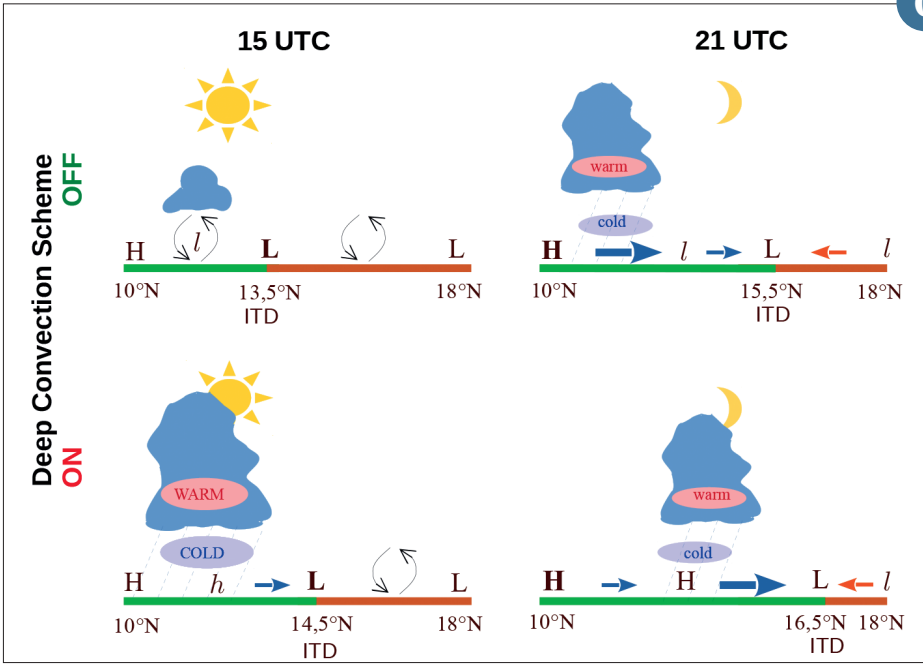
7



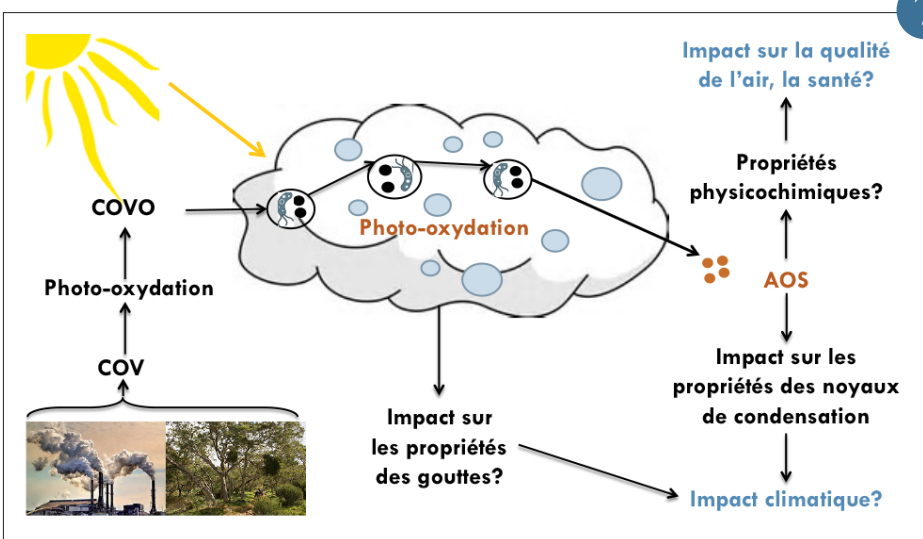
(a) Schematic representing the process participating in a lake mass balance evolution and the implementation of Lac du Bourget in the Rhone watershed  
 (b) Seasonal mean of lake level variations simulated by CTRIP-Mlake and observation from the Hydroweb platform over the period 1993-2014.



(b)



Differences in behavior between the two simulations, the top one without the deep convection scheme and the bottom one with it .  
 In the Sahel, in the low layers, the high pressures ("H") are located in the South and the low pressures in the North ("l") and the minimum at the level of the Inter-Tropical Depression ("L").  
 As soon as the daytime turbulence ceases, the nocturnal jet blows, advecting cold and humid air, which can cause precipitation.  
 While in the simulation with the activated deep convection scheme, its premature triggering causes an overpressure favoring the northern branch of the nocturnal jet to the detriment of its south branch. Then, "cold" and humid air is advected further and further north.



Main processes leading to the formation of secondary organic aerosols in the presence of clouds and the associated impacts.

# Climate

---

Météo-France's ability to model past and future climate change from the global to the local scale, to forecast seasonal climate variability and to perform meteorological observations is unique in France. This places the institution in an excellent position to understand climate, climate change and variability including extremes, and to develop climate services in support of adaptation policies.

Global and regional climate modeling tools are part of a continuum within CNRM, including also numerical weather prediction models. The CNRM-CERFACS platform of global climate models (CNRM-CM) has enabled CNRM to participate in CMIP6 at the highest international level. One of the metrics of success of CNRM's participation in the exercise, in addition to the acknowledged quality of its models, is the fact that, at the end of 2020, the data produced by CNRM-CM remain the most downloaded in the world. Although already significant, the exploitation of CMIP6 results by the research community will continue for several years. Among the studies carried out in 2020 at CNRM, let us point out original results on the changes of groundwater tables from simulations with CNRM-CM, the only CMIP6 model that represents groundwater tables, and another one where the expected future global warming is estimated through combining CMIP6 model output and observations since 1850.

In parallel with the valorization of CMIP6 results, we go on improving our models, with in particular the development and the first tests of an oceanic convection scheme based on parameterizations of atmospheric convection and, further upstream, measurements of the nitrogen and carbon content of peat bogs which will allow to improve the next generation of CNRM climate models.

Regarding seasonal forecasting, the new system 7 is based on CNRM-CM and continues to improve the quality of forecasts compared to previous systems, especially for precipitation over many regions around the world.

In terms of observations, 2020 was the warmest year in mainland France since records began, confirming the long-term warming. Precipitation trends are more difficult to interpret, but work carried out by Météo-France's Department of Climatology and Climate Services shows that an increase in maximum daily precipitation is emerging in several regions of France, particularly around the Mediterranean and the North-East of the country. Generally speaking, the annual cumulative precipitation tends to increase on average over France, but the increase in evaporation tends to reduce soil moisture except in winter.

Finally, the year 2020 has been marked by the finalization of the development of the DRIAS-2020 portal, which provides corrected data over mainland France from a selection of regional EuroCordex models.

1

---

## Climate modelling

### Development of a new Regional Coupled System Model for the study of Mediterranean Climate : CNRM-RCSM6

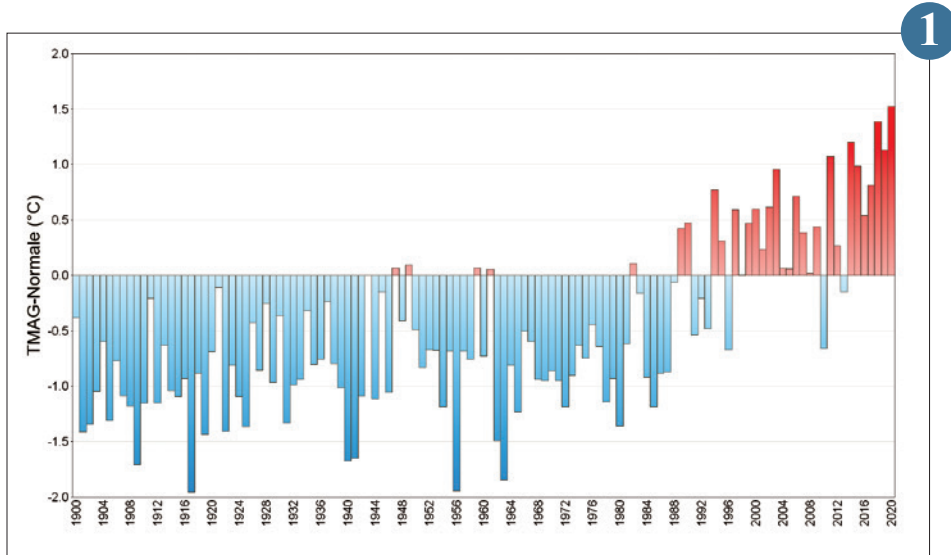
Internationally recognized for its research in regional climate modeling, the CNRM has recently developed the sixth version of its regional coupled system model (CNRM-RCSM6, figure a, <http://www.umr-cnrm.fr/spip.php?article1098>), to improve the understanding of past and future regional climate variability in the Mediterranean.

This system integrates the different components of the climate system, namely the atmosphere (ALADIN v6), continental surfaces (SURFEX v8), the Mediterranean Sea (NEMOMED12) and rivers (CTRIP). Communications between these models are managed by the OASIS-MCT coupler at an hourly frequency. Improvements mainly

concern the implementation of prognostic atmospheric physics, the integration of an interactive aerosol scheme (TACTIC) and the increase of horizontal and vertical resolution (12 km and 91 levels for the atmosphere, 6 km and 75 levels for the ocean). All these developments ensure a better consistency between CNRM-RCSM6 and its global scale equivalent, the earth system model CNRM-ESM2-1, which shares the same components. Following a tuning step of the system the first results show a significant improvement of the surface fluxes representation. The sea surface temperature trend is particularly well reproduced over the historical period (figure 2), thanks in particular to the consideration

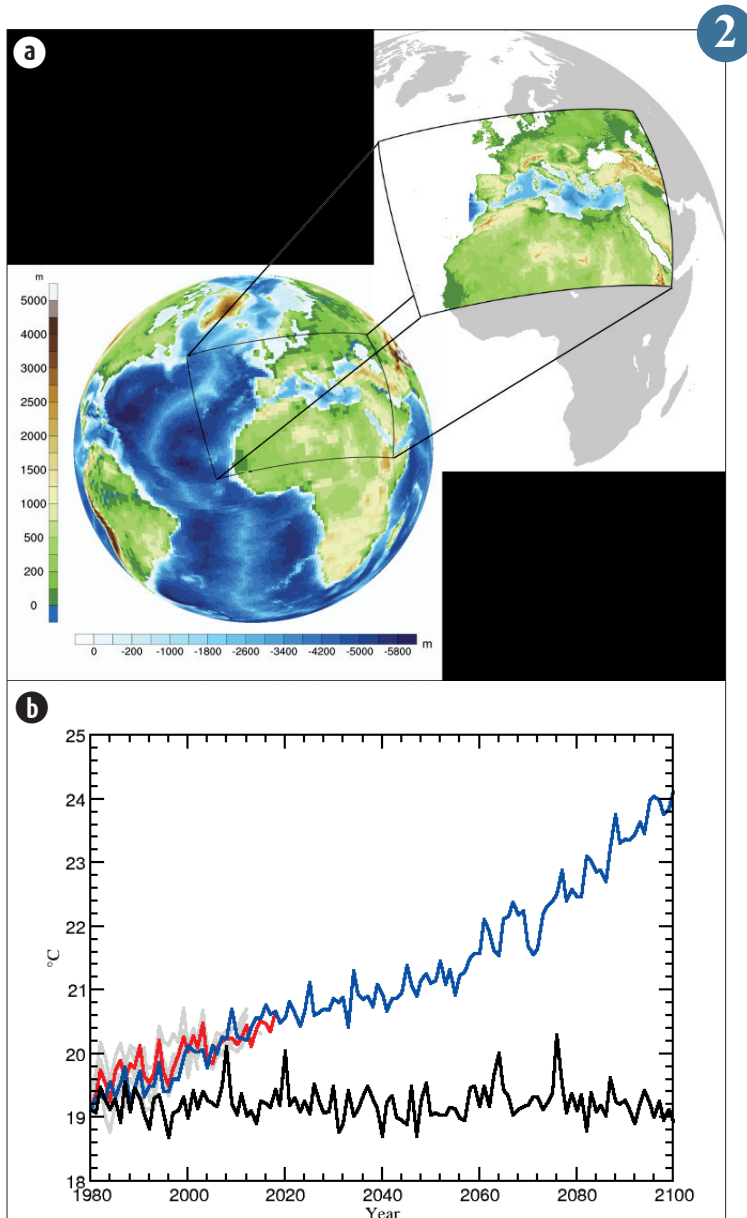
of aerosol evolution. This model was already used to show original results on oceanic heat waves in the Mediterranean. Finally a first simulation of the historical period and of the ssp585 CMIP6 scenario (figure 2) has enriched the multi-model and multi-scenario analysis of the Mediterranean climate in the framework of the Med-CORDEX initiative ([www.medcordex.eu](http://www.medcordex.eu)).

2



1

Annual mean temperature anomalies over France for 1900-2020 with respect to the 1981-2010 reference period. © Météo-France.



2

(a) Orography and bathymetry of CNRM-RCSM6 and its position on the global model [© CNRM/ P. Nabat and A. Voldoire]  
 (b) Annual average Sea Surface Temperature of the Mediterranean : observations (grey), CNRM-RCSM6 simulations (1980-2018 period driven by ERA-Interim in red, historical and ssp585 scenario driven by CNRM-ESM2-1 in blue, and associated control simulation in black)

## An Eddy-Diffusivity Mass-Flux Parameterization for Modeling Oceanic Convection

Oceanic convection is a fine-scale process which plays an important role in deep and intermediate water formation and ultimately in the large-scale thermohaline circulation. Consequently, oceanic convection takes a central place in determining global climate. A new one-dimensional parameterization of penetrative convection has been developed in order to have a better representation of the vertical mixing in ocean general circulation models. Our approach is inspired from atmospheric parameterizations of shallow convection which assumes that in the convective boundary layer, the subgrid-scale fluxes result from two different mixing scales: small eddies, which are represented by an Eddy-Diffusivity (ED) contribution, and large eddies associated with thermals, which are represented by a mass-flux contribution (MF). In the present work, the local (small eddies) and non-local (large eddies) contributions are unified into an Eddy-Diffusivity-Mass-Flux (EDMF) parameterization which treats simultaneously the whole vertical mixing. EDMF is implemented in the community ocean model NEMO. As an illustration, Figure shows the time series of the surface net heat flux (top) at the Lion buoy in the western Mediterranean during winter 2013 and the convective vertical velocity (bottom) simulated by EDMF at this place. Intensity and frequency of surface heat loss events control the plumes variability. In particular the 3 strongest surface heat loss have generated vertical velocities close to 10 cm/s in accordance with glider in-situ estimates. EDMF is a new paradigm of oceanic mixing which leads to more realistic simulations of the hydrological properties of water masses. In the future, it is expected to obtain more reliable climate projections.

3

## Diagnostic, study and impacts

### Measuring carbon and nitrogen content of a Greenland fen to improve global climate models

Peatlands play a major role in the carbon cycle. They contain about a third of the global soil carbon stocks, nearly as much carbon as the atmosphere. During the last millenia, these wetlands accumulated carbon because their inundated soil, poor in oxygen, prevented microbial decomposition of the organic carbon. However, whether they will remain carbon sinks in the future under climate change remains highly uncertain. Nuuk fen (fig a) is a well instrumented site close to Nuuk (Greenland) where meteorological variables, energy balance, and CO<sub>2</sub> and CH<sub>4</sub> fluxes are measured since 2009. This fairly long time series site is particularly well suited to validate the land surface modules embedded in global climate models. But the carbon content of the fen and its vertical profile was unknown. Soil carbon content is one of the main drivers of CO<sub>2</sub> and CH<sub>4</sub> emissions and is necessary to correctly evaluate land surface models.

The PhD student Xavier Morel joined a CENPERM (University of Copenhagen) field campaign in July 2017 to measure for the first time soil carbon and nitrogen profiles and stocks in the fen. Measurements were made along two transects, co-located with the greenhouse gas measurements. Samples were analysed in Nuuk and Copenhagen, and the results are available on the PANGEA database. These new stocks and profiles (fig. b) together with the existing greenhouse gas measurements constitute a unique dataset for the development and validation of climate models. At CNRM, these measurements helped the PhD student test and improve his detailed soil carbon model with CH<sub>4</sub> emissions included in ISBA.

4

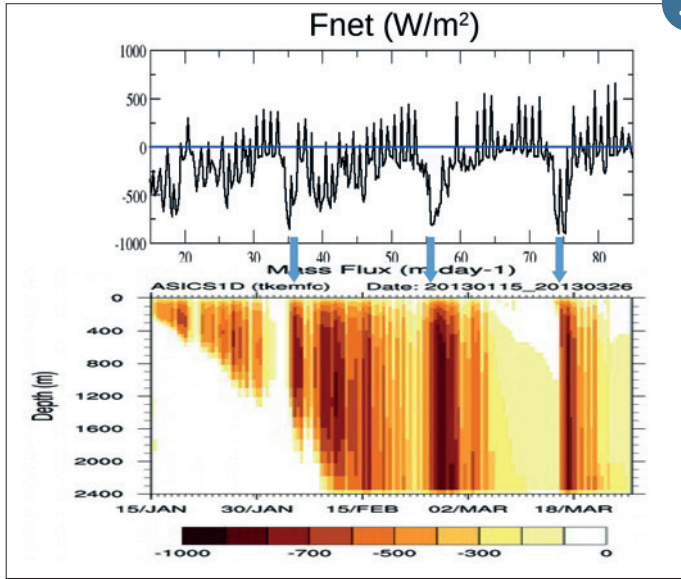
## New climate projections merging models and observations

The scientific community regularly produces climate projections in order to quantify the expected climate changes over the 21st century and beyond. These projections were previously based on climate model simulations. But, as the 21st century is now well underway, the warming is strengthening and observations are becoming more and more informative about the magnitude of past and future climate change. Using a new statistical method, we have calculated the expected global warming in the 21st century by combining the latest climate simulations (CMIP61 exercise) and observations since 1850. Our results suggest that the uncertainty from the climate simulations is significantly reduced by taking into account the observations. This reduction is close to a factor of three in the short term (before 2050), and a factor of 2 in the long term (end of the 21st century). The expected warming in 2100 compared to the

period 1850-1900 is about +2°C (+/-0.6°C) for a low emission scenario (SSP1-2.62), +3°C (+/-0.6°C) for a moderate emission scenario (SSP2-4.5), and +5°C (+/-0.6°C) for a high emission scenario (SSP5-8.5). We also estimate that the current warming (in 2020) reaches +1.22°C (+/-0.15°C), out of which +1.15°C is attributable to human activities. Beyond the interest of these results for adaptation and mitigation strategies, many other applications of the proposed method are envisaged in order to specify climate projections at the regional or local scales, and/or for other variables than temperature.

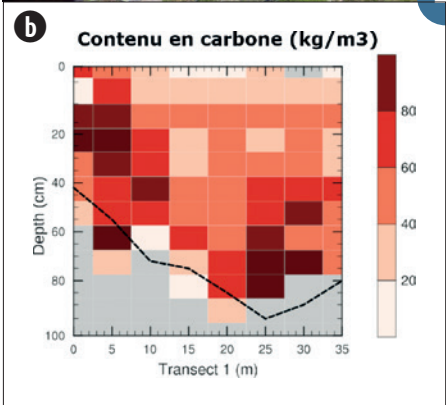
5





3

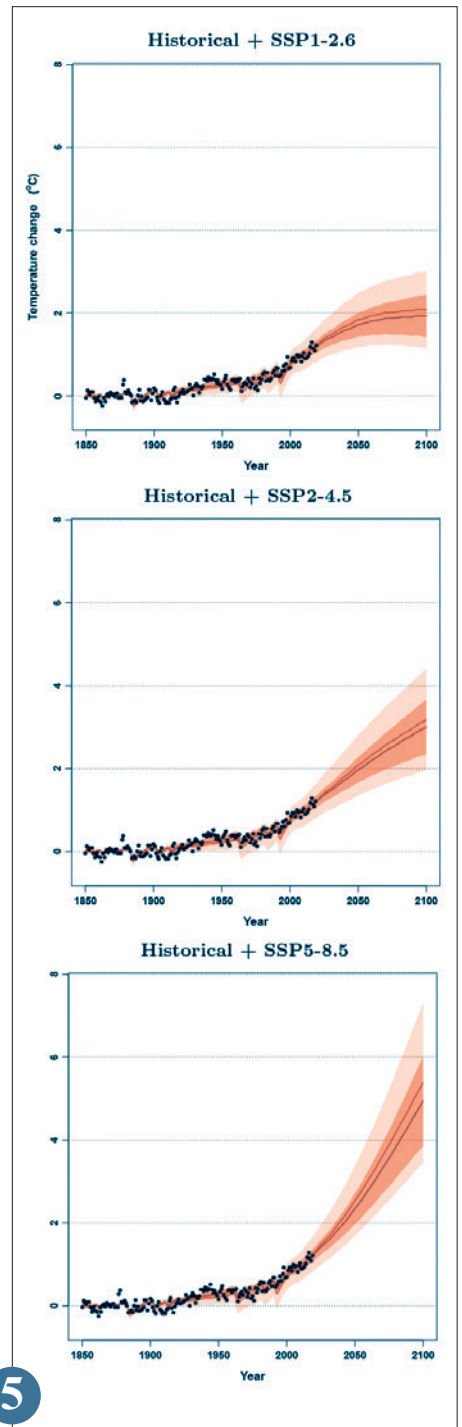
Time series of the Surface Net Heat Flux ( $W \cdot m^{-2}$ , top) and the Convective Mass-Flux ( $m \cdot d^{-1}$ , bottom) at the Lion buoy (Western Mediterranean, Gulf of Lion)



4

(a) View of the fen ( $64^{\circ}7'51.5''N$ ,  $51^{\circ}23'10.5''W$ ) in July 2017 with the greenhouse gas fluxes measuring tools: eddy flux tower and automatic chambers

(b) Soil carbon content ( $kg \cdot m^{-3}$ ) with depth, measured along the first transect along the access boards. The dashed black line represents the bottom of the fen: the limit between the organic and mineral soil (adapted from Morel et al, 2020)



5

Global mean temperature projections, and associated uncertainties (5-95% confidence intervals) obtained from climate simulations alone (pink interval), then using a merging of climate simulations and observations (red interval). The calculation is made from 22 climate models of the CMIP6 exercise, for three emission scenarios (SSP1-2.6, SSP2-4.5, SSP5-8.5). Observed annual global mean temperature values are indicated by black dots. All temperatures are anomalies relative to the 1850-1900 period, used as a reference.

---

## Global scale evolution of groundwater in future climate

Groundwater (i.e. water found in aquifers) plays an important role in the hydrological cycle and it is essential for human activities and ecosystems. In this recent study, conducted at the global scale, we assessed the response of unconfined shallow aquifers to climate change using the CNRM global climate models. They are the only climate models representing the hydrogeological processes involving aquifers. Our analysis is based on CMIP6 simulations – carried out for the IPCC 6th assessment report – following several pathways of greenhouse gases concentration. Here, only the “SSP245” scenario considered by the scientific community as the most probable currently is shown (Fig. 1). It underlines that aquifers should replenish at the global scale on average until 2100. The evolution of annually averaged water table depths (i.e. heads of aquifers) is mostly driven by the precipitation evolutions, and the increase of groundwater stored in shallow aquifers is thus consistent

with the projected global intensification of precipitation. However, similarly to precipitation, the evolution of aquifers is not uniform and shows large regional disparities. Regions that are already arid could experience a strong reduction of their groundwater resources. This latter result, combined with projections of population density and water use, indicates that the water stress risk could increase in some of these already aquifer-dependant regions.

6

---

## Impact of climate change on hydroclimatic variables over France

From 2017 to 2019, Météo-France was involved in the CHIMERE21 project, funded by the water agency of the Rhine and Meuse basins. This project aimed at exploring the future evolution of the hydrological regime of the Meuse river, using climatic data from Euro-Cordex and several hydrological models. After that, we produced an analysis of the impact of climate change over the whole France, considering different hydroclimatic parameters.

The evolution of surface temperature and precipitations obtained with the 5 couples of GCM/RCM models used within the framework of CHIMERE21 were analysed. At the end of the century for the RCP 8.5, the surface temperature increases during the whole year, by around 2,8 to 4,5 degrees, the highest increase occurs in summer. Annual precipitation is also increasing, particularly in winter. However, the evolution of summer precipitation is more contrasted, with strong regional differences between the northern and southern parts of France, the southern regions being affected by summer precipitation decrease.

The soil wetness index (SWI) is driven by the global increase of precipitation

(which increases soil water) and also by the temperature elevation that supports evaporation (which dries soils). At the end of the century, the mean SWI over France slightly increases in winter, but decreases in autumn, spring and up to 20 % in summer. The dry season starts earlier and lasts longer, figure 1 shows that the number of dry days over the Adour-Garonne basin increases by around 30 days at the end of the century for the RCP 8.5.

The snow cover is globally decreasing. Over the Alps, at the end of the century, the winter snow pack decreases by around 20% in the near future, the decline in snow cover reaches 60% by the end of the century.

Within the next few months, this study will be updated using the new DRIAS-2020 data set.

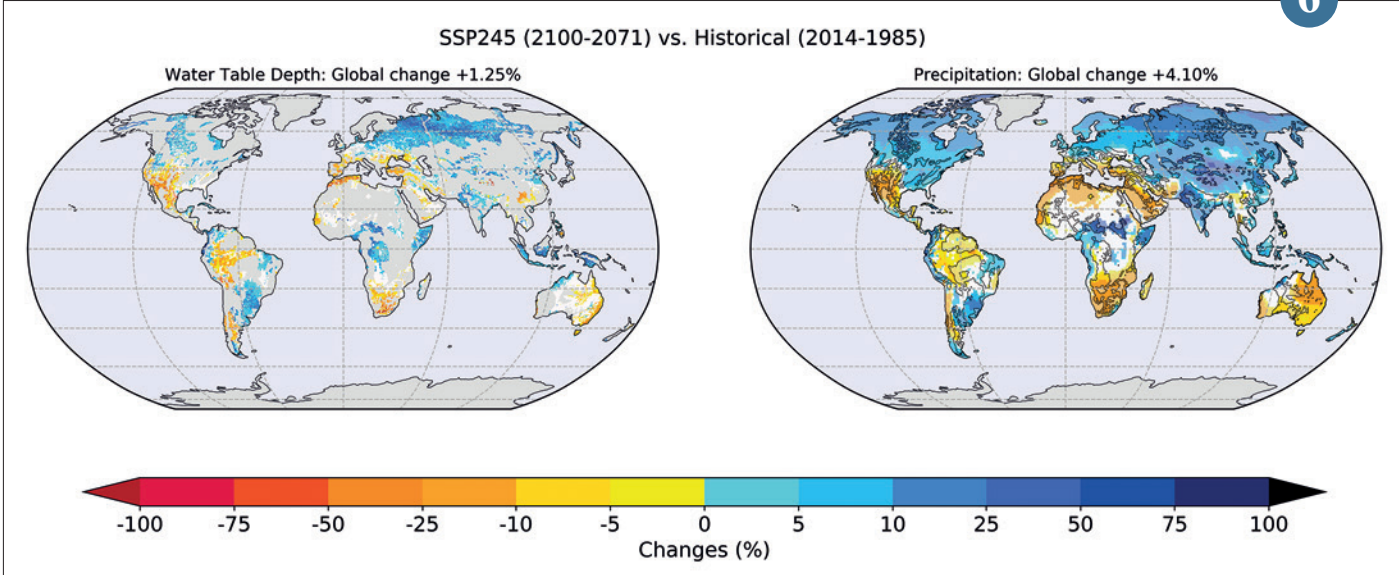
7

## Evolution of rainfall in France

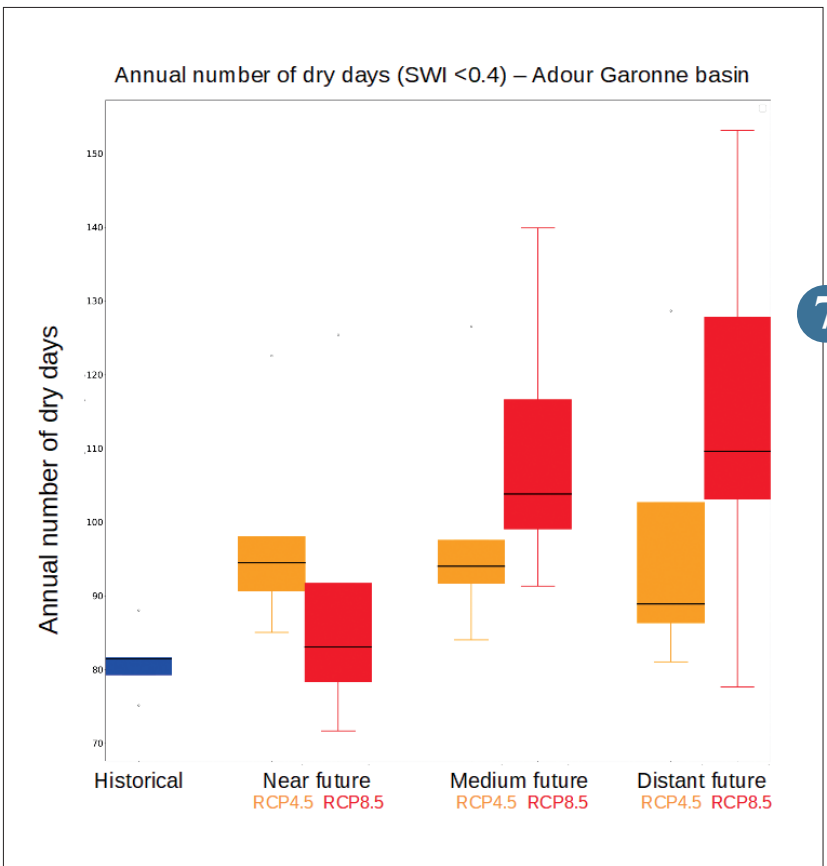
Characterizing the average and extreme changes in rainfall in France is a key societal issue, particularly for agricultural sector. Recent studies have highlighted an increase in the intensity and frequency of extreme rainfall events around the Mediterranean in recent decades. A set of 274 series of daily reference observations is used to establish a diagnosis over the period 1961-2012 over the entire metropolitan territory. These series are selected on criteria of temporal homogeneity and absence of missing data. The study focusses on the evolution of 11 standard indices recommended by the World Meteorological Organization (Expert Team on Sector-Specific Climate Indices), some of which are the subject of a more detailed analysis.

The changes in the intensity of average and extreme rainfall are respectively characterized by the sum of daily rainfall and the maximum daily amount of rainfall. The evolution of frequency is examined via the number of days where the daily amount exceeds a given threshold. Based on local (stations) analysis, few evolutions are significant and it is difficult to draw conclusions on a larger scale. In order to improve the signal-to-noise ratio, we calculate regional trends. Our results confirm the singular character of the Mediterranean rim, known as a “hot-spot” of climate change, and where the increase in precipitation extremes is particularly significant. Whatever the index considered, the intensity of precipitation is also on the rise in Bretagne, Grand-Est, Bourgogne-Franche-Comté and Auvergne-Rhône-Alpes.

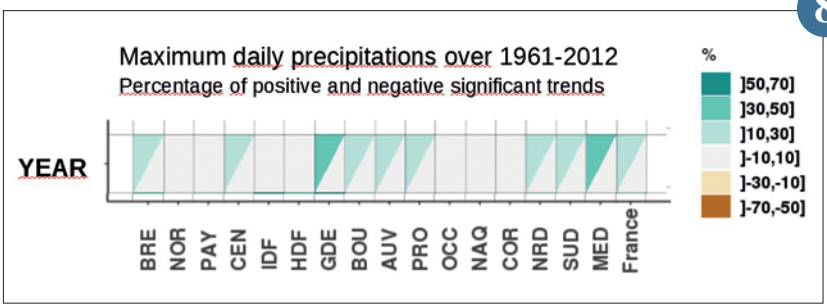
8



▲ Evolution (in %) of aquifers water table depths (left) and precipitation (right) according to the "SSP245" pathways of greenhouse gases concentration. The evolution is computed between the means of water table depths or precipitation rate over the 1985-2014 (present) and 2071-2100 (future) time periods. The global rate of change (in %) between these two periods is also given. White areas indicate places where the difference is not statistically significant.



▲ Distribution of the annual number of dry days (SWI < 0,4) over the Adour-Garonne basin, for the 5 couples of GCM/RCM models over the 1976-2005 period (blue) and for three time horizons (2021-2050, 2051-2070, 2071-2100) for the RCP 4.5 (orange) and 8.5 (red).



▲ Annual evolution of the maximum daily precipitation aggregated by geographical area. On the x-axis, the geographical areas: the 11 administrative regions from north to south, then the North of France (NRD), South (SUD), the Mediterranean rim (MED) and France. A rectangle corresponds to a geographical area and is divided into two: the left triangle characterizes the percentage of significant upward trends, the right triangle the percentage of significant downward trends. The color of the triangle indicates the proportion of significant trends, respectively upward (green) or downward (brown).

## Dissemination of CNRM climate simulations performed for CMIP6

The 6th IPCC synthesis report will be published in the second half of 2022. This report will be based in particular on the work presented in the special reports published in 2018 and 2019 as well as on the work carried out by Working Groups 1 to 3 which will deliver their conclusions in 2021.

CNRM is involved in these reports through the direct contribution of several colleagues but also through the realization of global climate simulations within the framework of the intercomparison exercise CMIP6.

Begun in 2014, this exercise is coming to an end for the CNRM and a first assessment can be made: 35,000 simulated years, about 300 Million computing hours over 2016-2020 on Météo-France computers having generated about 1.3 Po of data (310 simulations performed with the 3 model configurations of the CNRM-CERFACS group). Respecting the standards required by CMIP6, these simulations are distributed in free access through the CNRM ESGF3 datanode. Thanks to the commitment of CNRM engineers and researchers in collaboration with CERFACS4 and IPSL5, the CNRM CMIP6 simulations were the first to be distributed in the summer of 2018.

Although the CNRM ESGF node only distributes its own climate simulations, it is the 3rd node worldwide to have distributed the largest volume of data since 2018. It is surpassed by only two nodes that offer, in addition to their own data, copies of most of the existing CMIP6 simulations including those of the CNRM-CERFACS. Among the 39 institutions contributing to CMIP6, the most downloaded data from the ESGF Federation, all nodes combined, are those of the CNRM-CERFACS.

9

## Extreme event attribution

In order to estimate the influence of climate change on the occurrence of extreme events, a new attribution method has been developed. This method uses climate models (the CMIP5 or CMIP6 ensemble) - which provide a prior of reality - to estimate the probability of occurrence of these events, which is then constrained by observations.

This new approach has been applied to the July 2019 heat wave, allowing to infer a probability multiplied by (20 to  $+\infty$ , interval 95%) in 2019, and a temperature increase of  $+2^{\circ}\text{C}$  ( $+1.5^{\circ}\text{C}$  to  $+2.7^{\circ}\text{C}$ ) compared to a world without human influence. The projection in 2040 (for the RCP8.5 scenario) estimated that the probability is multiplied by 3500 (75 to  $+\infty$ ), and a temperature increase of  $+3.6^{\circ}\text{C}$  ( $+2.6^{\circ}\text{C}$  to  $+4.6^{\circ}\text{C}$ ). These developments have been published, and the source code allowing the example treated to be reproduced has been made public.

This method has been applied internally at Météo-France to several extreme events: the French heat waves of August 2003, June/ July 2019 and the heat wave of September 2020. In the framework of the Copernicus C3S-62 project, in collaboration with the KNMI, Oxford University, the Met Office, the Deutsche Wetterdienst, and the Dutch e-science center, a prototype rapid service for extreme event attribution is being developed using this new attribution method, as well as a method developed by KNMI. In the framework of this service, an exercise for the attribution of the Siberian heat wave of July 2020 was conducted. These results have been the subject of a first publication in the WWA (without a review committee), and a second publication is currently being reviewed.

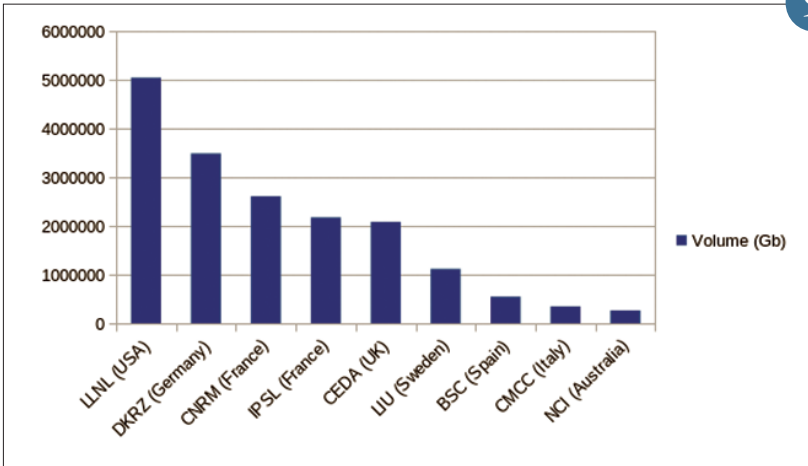
10

## Climate indicators for wind energy in France

The actions for the energy transition led in many countries, including France, are based on the development of wind energy and require climate indicators adapted to both historical references and climate projections in order to verify the relevance of projected energy production. Until the last few years, the climate data available for the wind energy sector only concerned local data or global reanalyses. More recently, a replay of the AROME model was carried out to produce a 2.5 km wind atlas over France, covering the period 2000-2019. Work was initiated in 2020 to extend these analyses to the SAFRAN reanalysis available at 8-km resolution over France since 1958, as well as climate projections from the DRIAS-2020 dataset. As the height of wind turbine hubs is around 100 m, energy companies need wind measurements at 100 m. So, after assessing the quality of the SAFRAN 10 m wind by comparing it with observations and the AROME replay, a reconstruction of a 100 m wind was performed using different methods, then an analysis was carried out on change in wind potential in France between 1958 and 2019. The study also explored the evolution of wind in future climate in France using climate indicators based on wind data from the DRIAS-extrapolated 100 m wind set. It is about 12 climate projections in scenario RCP8.5 debiased by the ADAMONT method. These data are planned to be published on the DRIAS portal in 2021.

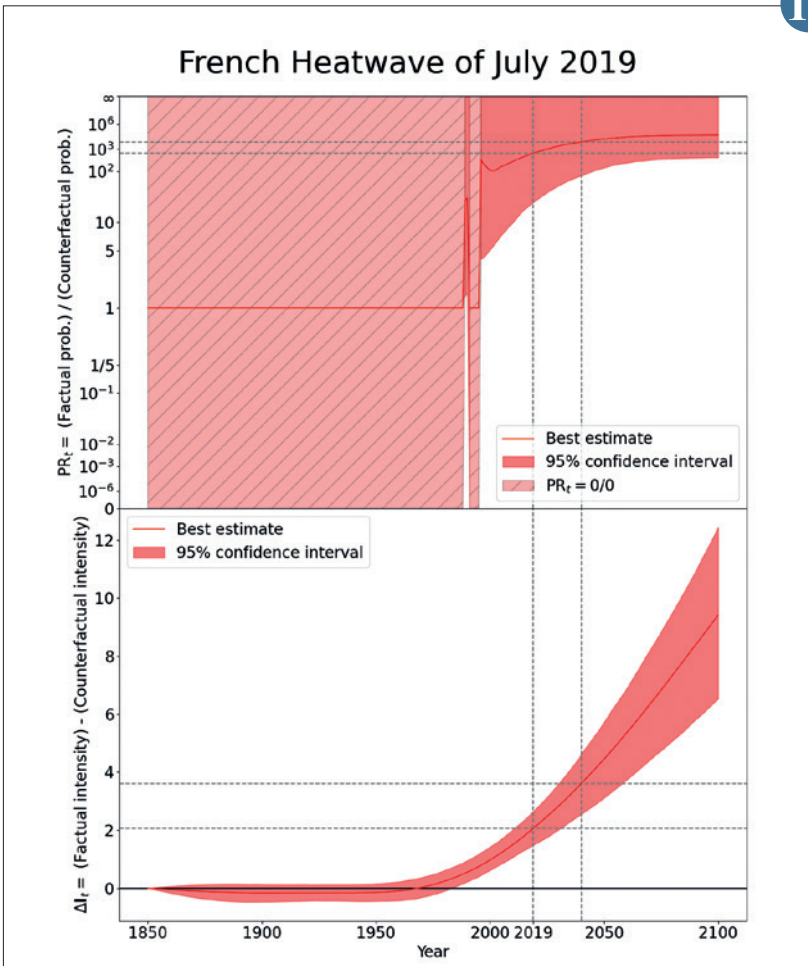
11

9



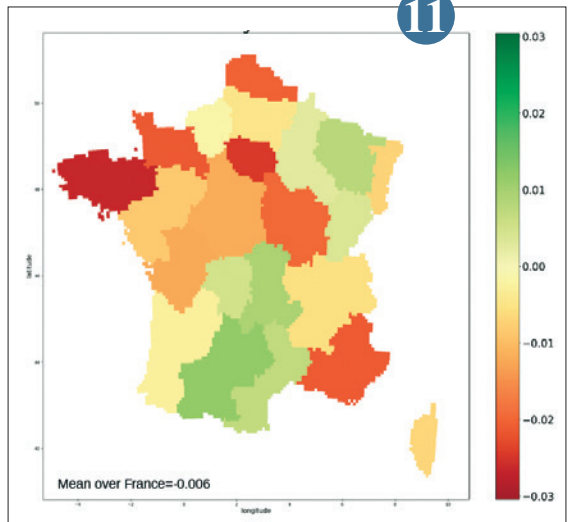
downloaded data (Gb) since 2018 by majors ESGF datanodes (source <http://esgf-ui.cmcc.it/esgf-dashboard-ui/>)

10



In both figures, the red line indicates the estimated value, the red zone the 95% confidence interval, the grey dashed lines highlight the years 2019 and 2040. Top: Increased risk due to climate change. The crossed out red zone corresponds to a period when the probability that the heat wave is impossible in the factual and counterfactual world is at least equal to 5%. Bottom: Temperature change due to climate change.

11



Regional trend of mean wind at 100 m for the period 1959-2019 in France, calculated with SAFRAN data extrapolated from the seasonal vertical profiles of the ERA5 reanalysis.

## Climate change in France in the 21st century based on the DRIAS-2020 dataset

The new DRIAS-2020 dataset for climate projections in France is based on a selection of thirty regionalised climate simulations, corrected with the ADAMONT method applied on the SAFRAN observations. This subset of the simulations available in the Eurocordex database was selected for its representativeness of future changes in temperature and precipitation over France. A diagnosis on climate change in the 21st century was established from this set of simulations covering three socio-economic scenarios RCP2.6, RCP4.5 and RCP8.5:

- The mean temperature is increasing for all three scenarios, with a continuous rise until the end of the century (period 2071-2100) for RCP4.5 and RCP8.5, with median values reaching +2.1°C and +3.9°C respectively. This warming, more marked in the summer, presents a geographical variability with a stronger increase in the east of the country. This change in temperature is also reflected in the extremes, with a dramatic rise in the number of heat wave days in all three scenarios.
- The evolution of annual precipitation amount, stable or slightly increasing depending on the horizons and scenarios, is accompanied by model uncertainty, which can reverse the sign of the trend. This evolution is subject to seasonal (increase in winter, decrease in summer) and geographical variations (increase in the northern half and decrease in some regions of the South). The evolution of extreme precipitation and summer droughts also presents strong uncertainties. All of the results are detailed in the DRIAS-2020 report, which is available on the DRIAS portal ([www.drias-climat.fr](http://www.drias-climat.fr)).

12

## Seasonal forecast

### Research Report 2020: Evaluation of precipitation re-forecasts in Météo-France System 7

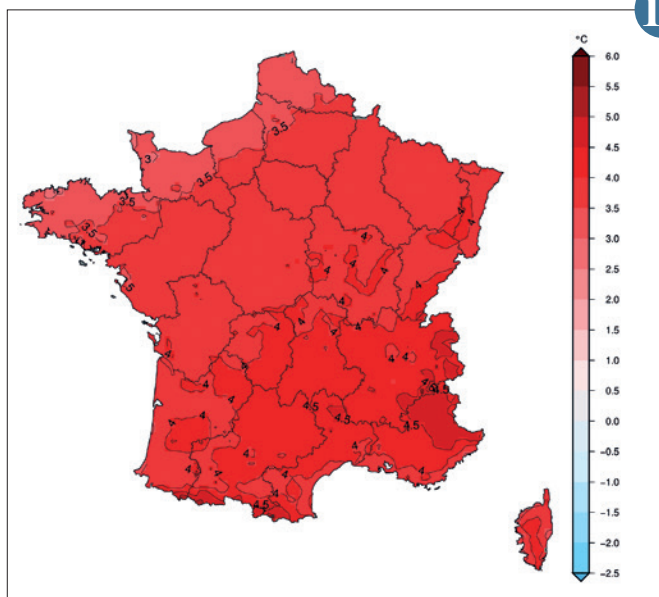
The Météo-France seasonal forecasting system 7 uses the CNRM-CM6-1 high resolution coupled climate model to provide ensemble forecasts at a 7-month range. Beyond typical deterministic scores, a probabilistic evaluation is performed using the re-forecast over 1993-2016.

To measure the accuracy of the precipitation re-forecasts, we compute the Brier score for June-July-August (JJA) re-forecasts initialized in May in the below, near, and above normal categories derived from 25 ensemble members at each grid point. The Brier score is the mean square error in probability space between the forecast probability and the observed outcome. The lower the score, the better the forecast. Here we use the GPCP global precipitation analysis as a reference. The spatial distribution of the Brier score depends significantly on the method used to define the category thresholds; in figure (a), category thresholds are determined by the GPCP precipitation anomalies. The Brier score therefore encompasses a mean bias in probability space. In figure (b), the re-forecasts are used in cross-validation to define the category thresholds for each year, therefore correcting the distribution error. Errors over the tropical deserts, rainforests, and West Antarctic are much lower.

Work has also been undertaken to characterize the impact of observational uncertainty on the robustness of evaluation metrics. Using two references (e.g. GPCP and MSWEP) to define an observed probability, the Brier score is further reduced over the West Pacific and Eurasian continent (not shown). Future work includes extending this evaluation to probabilistic scores assessing the ranked distribution of the ensemble.

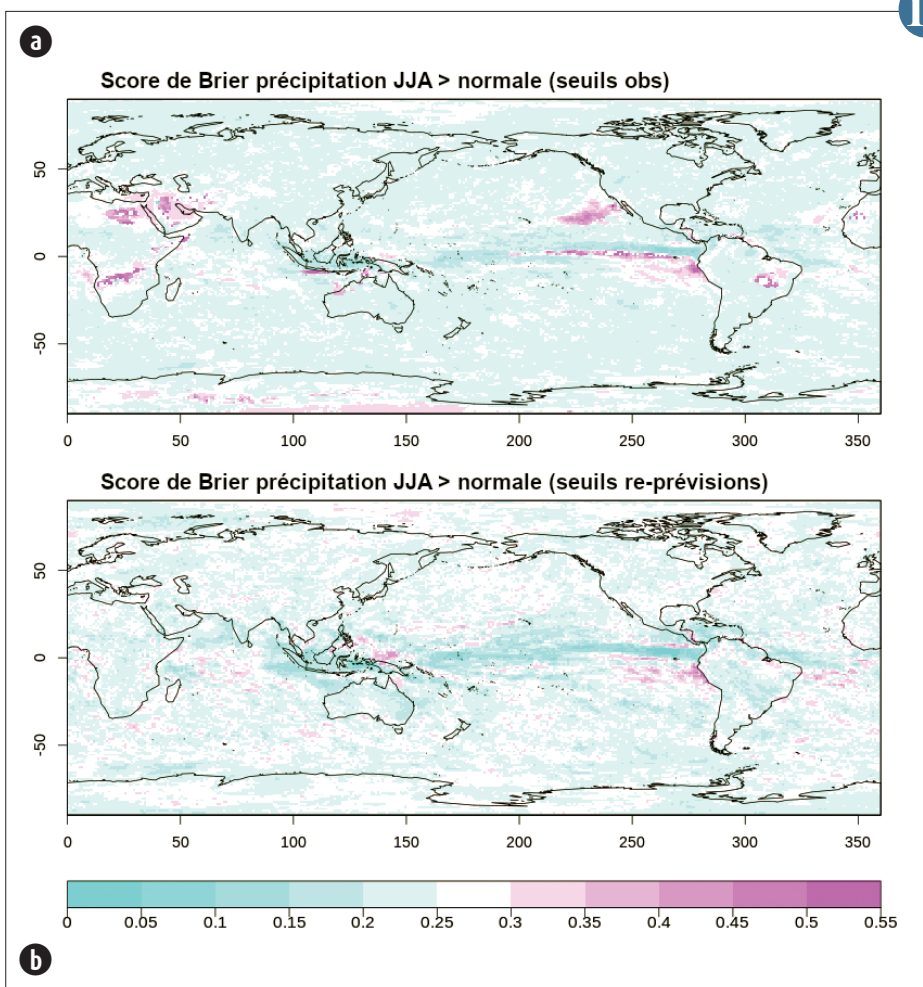
13

12



Mean temperature difference for the period 2071-2100 (reference 1976-2005) according to the RCP 8.5 scenario for the median of the DRIAS-2020 dataset

13



Brier score for above-normal June, July, August (JJA) precipitation (exceeding the second tercile) for Météo-France System 7 re-forecasts initialized in May, over the 1993-2016 period. The thresholds for the re-forecast probabilities are computed using the GPCP climatological distribution (a) or the re-forecast ensemble in leave-one-out cross-validation (b).

# Chemistry, aerosols and air quality

---

The forecast of the chemical composition of the atmosphere is part of the missions of Météo-France and responds in particular to the needs of the French army (sand dusts), air traffic (volcanic ashes) or Prév'Air (health issues). CNRM contributes strongly to these missions by conducting upstream research to better understand the chemistry and particles (aerosols) in the atmosphere, both through its observation activities, and modeling and data assimilation approaches.

In terms of in situ observations, new results have been obtained on the aging of black carbon aerosols emitted by biomass fires, explaining their very high solar radiation absorption capacity, with implications for improving the representation of aerosols in air quality or climate models.

Moreover, thanks to its expertise at the best international level in aerosol optical depth retrievals from satellite measurements, a CNRM team has combined data from a belt of 5 geostationary satellites to produce daily quasi-global maps of aerosol optical thicknesses.

Downstream of the observation activities, the use of aerosol data assimilation in MOCAGE allows to improve the analyses and reanalyses of atmospheric composition, but also to anticipate the added-value of future space missions. This year, the data assimilation of the CALIOP lidar of the CALIPSO satellite has been successfully tested in order to build an aerosol climatology. In addition, the use of MOCAGE has allowed to document the impact of volcanic eruptions on air quality, or the impact of the Covid-19 pandemic by taking into account the reduction of human emissions in Europe. Finally, simulations of several decades carried out with MOCAGE in the framework of the international CCMI-2 project have confirmed the good capacity of the model to simulate the mean states and the interannual variability of tropospheric and stratospheric ozone.

Concerning operational applications, it should be noted that the two former air quality forecast systems based on MOCAGE for the regional Copernicus service and the national Prév'Air system have been merged into a single system, resulting in better forecasts. This new channel also provides forecasts for the entire globe.

1

---

## Quasi-global maps of aerosol optical depth and surface albedo from the combination of five geostationary weather satellites

Geostationary weather satellites are recently receiving a great deal of attention from the remote sensing community due to their increasingly advanced performances for the continuous monitoring of aerosols and surface properties. However, geostationary missions are limited by their partial coverage of the Earth, which makes them inappropriate for monitoring long-range transported aerosols or assimilating the derived satellite products into global models, for example. This shortcoming was overcome in a recent collaboration between CNRM and the ICARE Data and Services Center thanks to the simultaneous use of the geostationary missions GOES-West, GOES-East, MSG,

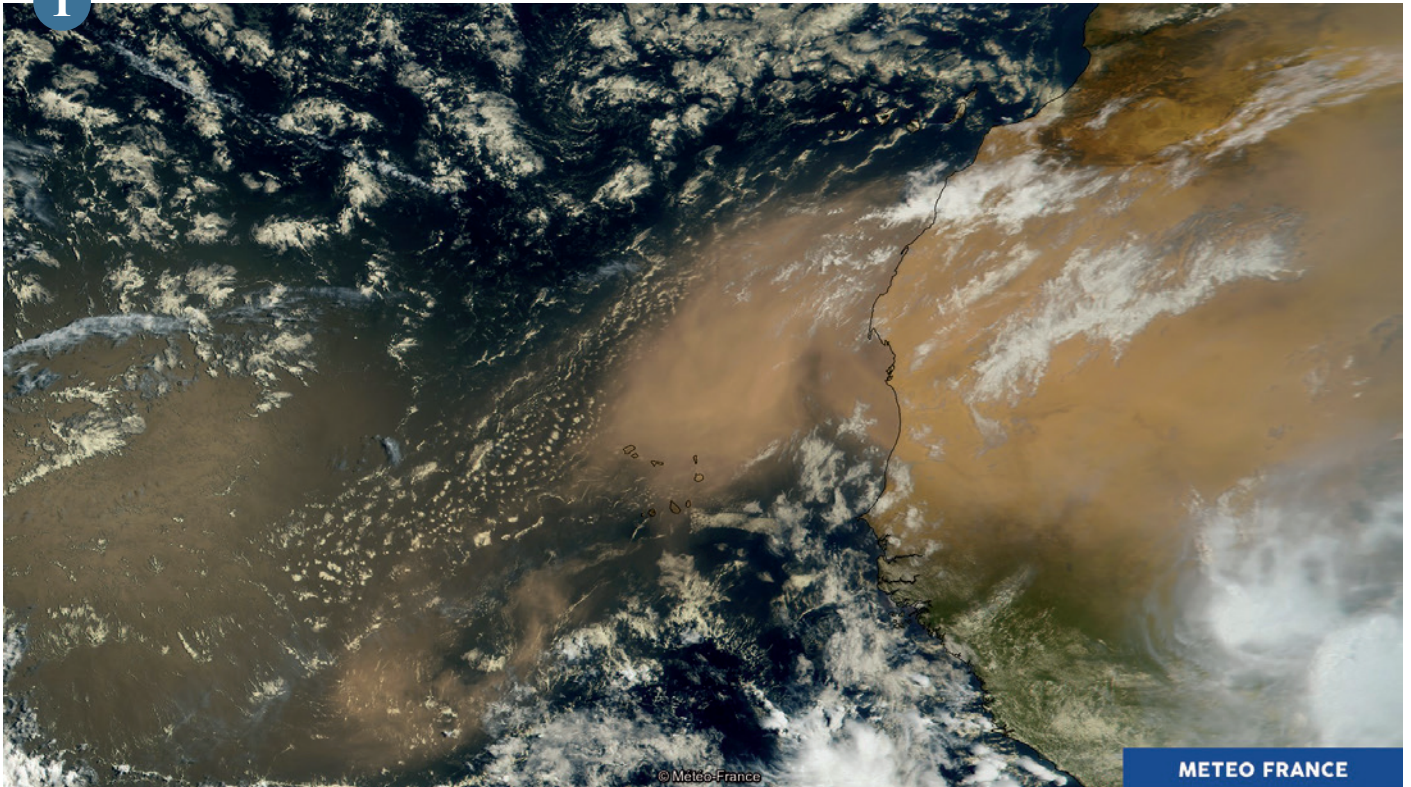
IODC, and Himawari. The combination of these five operational weather satellites evenly located around the planet gives a ring of geostationary satellites (aka. GEO-ring) covering the full globe except for the poles, which are not seen from the geostationary orbit. The data acquired by this GEO-ring are currently being processed by ICARE in near real time using the retrieval algorithm AERUS-GEO, which is developed at CNRM. As an example, the figure below shows the quasi-global maps of daily average aerosol optical depth and surface albedo retrieved by AERUS-GEO for August 31<sup>st</sup> 2020. These satellite outputs have strong potential for aerosol and land surface studies thanks

to their completeness and accuracy. In the future, CNRM will work on the improvement of these results thanks to the upcoming MTG-I mission, which will complete a GEO-ring exclusively made of next generation spacecrafts.

2

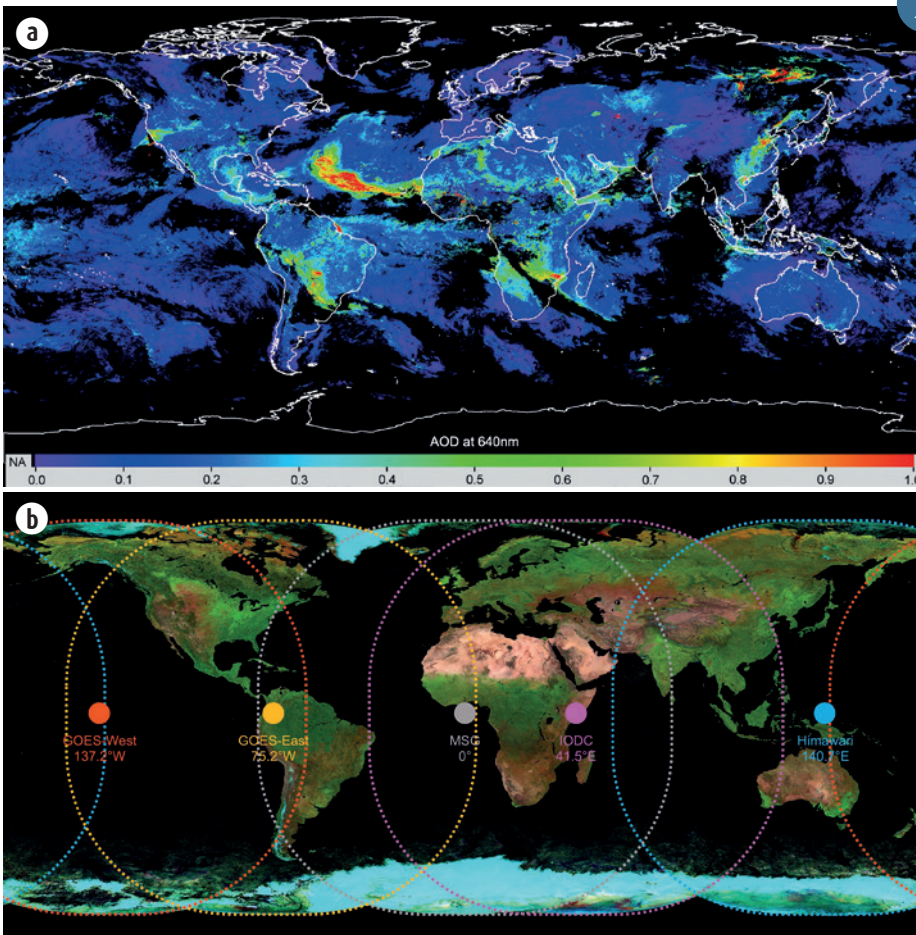


1



GOES-16 satellite image, 09/06/2020 at 1:15 UTC: winds have been blowing strongly over the Sahara for the past three days, lifting sand particles and creating a plume west of Africa. This type of event contributes to fertilizing the Amazon forest. © Météo-France..

2



Quasi-global map of daily aerosol optical depth (a) and surface albedo (b) obtained by AERUS-GEO on August 31st 2020. Sub-satellite point and coverage of each satellite forming the GEO-ring are superimposed. The albedo map is obtained by combining the albedo retrieved at 0.6 (blue), 0.8 (green), and 1.6 (red) microns.

---

## Importance of CALIOP lidar data on board the CALIPSO satellite for the construction of an aerosol climatology based on data assimilation

Given their effects on the Earth's radiation balance, human health and various economic sectors (energy, transport, etc.), aerosols are monitored using modelling and observation tools. The assimilation of aerosol observations allows the quantification of their concentrations as well as their forecasting, which is important for air quality monitoring within the framework of Copernicus as well as the development of pre-operational tools for volcanic ash forecasting within the VAAC (Volcanic Ash Advisory Centre) responsibilities of Météo-France.

The aerosol assimilation module coupled to the MOCAGE model allows the assimilation of aerosol observations in terms of optical thickness or lidar measurements individually or jointly. The CALIOP lidar on board the CALIPSO satellite provides information on the vertical structure of aerosols. In order to build an aerosol climatology from the assimilation of CALIOP observations, we have assimilated CALIOP data over the whole measurement period since 2007. This climatology will be used to evaluate the impact of different types

of aerosols during extreme events and also provide a complete and accurate picture about their vertical structure.

The attached figure shows the temporal evolution for the 4 seasons of 2016 of the backscatter coefficient derived from the assimilated fields CALIOP data over the African Sahara. Periods of high desert dust emission are characterised by high values of the backscatter coefficient. The dust emission activity intensifies during spring and summer (between March and August) when desert dust can rise quite high in the atmosphere.

This research using the CALIOP instrument also helps to prepare future space lidar missions such as the European Space Agency's EarthCare programme or the international ACCP study in partnership with CNES.

3

---

## Impact of anthropogenic emissions reductions due to COVID-19 on air quality

Air quality forecasting is an important health and societal issue. Operational forecasts are carried out daily at Météo-France over Europe as part of the European Copernicus CAMS\_50 program, as well as over France as part of the national Prév'Air consortium.

The particular health context of 2020 and the restrictions on travel and activities that have been imposed have greatly reduced the associated anthropogenic emissions. This has had a measurable impact on air quality in major cities across Europe. In the framework of the European Copernicus CAMS\_50 project, in order to determine the impact of these restrictions at the European scale, a posteriori modelling was conducted using, among others, the transport-chemistry model MOCAGE, developed at CNRM and operational at Météo-France.

Emission reduction factors depending on the emission sector, the country and the simulated day were developed at the Barcelona Supercomputing Center (BSC) and applied to the emission cadastres used as input to the MOCAGE model. The study period covers the different European

confines (21 February 2020 - 31 July 2020). Simulations performed with the MOCAGE model show a significant decrease of around 15% in ozone concentrations over Europe as a whole, as shown in Figure 1, representing the relative difference in ground-level ozone on May 1, 2020 at 12:00 noon, between two simulations with and without emission reductions. However, this decrease in atmospheric concentrations of chemical compounds is not noticeable on PM10 (aerosol particles less than 10 microns) because in spring, particles are mostly due to agricultural activities, which have not been impacted.

4

---

## What is the impact of volcanic SO<sub>2</sub> emissions on the global tropospheric budget in sulfur species?

Together with human activities, natural sources such as volcanoes contribute to the injection of pollutants into the atmosphere. Using global emission inventories and chemistry-transport models (here MOCAGE), it is possible to estimate the amount of sulfur species emitted, deposited and remaining in the troposphere: this is the calculation of the tropospheric budget.

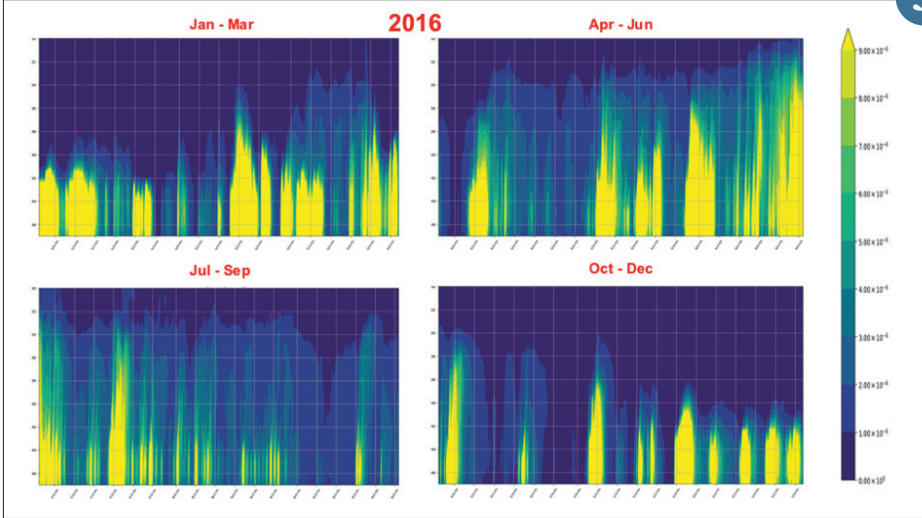
The study is carried out over the year 2013; a year with not much eruptive events, which supposes that only passive degassing influences the budget (Tab. 1). By comparing two simulations, one with and the other without volcanic emissions, it is possible to estimate the contribution of these emissions to the sulfur budget. At the global scale, about 81 Tg of sulfur are emitted, of which 15 % by volcanoes. But, the tropospheric burden in SO<sub>2</sub> and sulfate aerosols (SO<sub>4</sub>) due to volcanic emissions represents 14 and 27 % respectively. This difference in the ratio shows the greater capacity of volcanic emissions to form sulfate aerosols.

These results show the impact of volcanic emissions on the atmospheric chemical composition. In the vicinity of volcanoes, these sulfur emissions play a predominant role, contributing very strongly to the presence of sulfur species in the atmosphere (Fig. 1). Volcanoes can significantly impact local air quality, causing environmental and health problems.

In the future, a similar study will be carried out, but over the year 2014. Unlike 2013, this year inventories much more eruptive events, which will allow to compare the additional contribution of this type of emission on the tropospheric budget in sulfur species

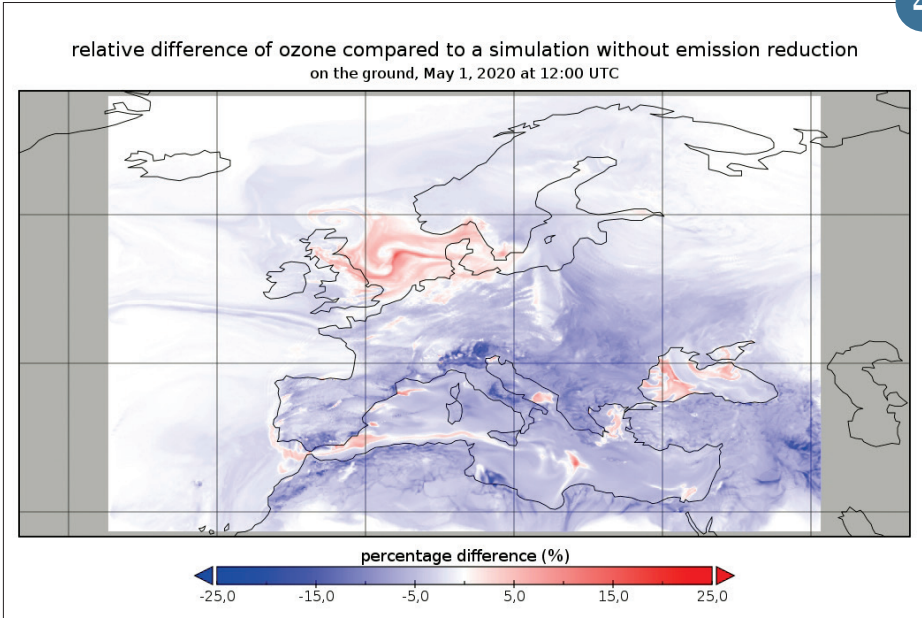
5

3



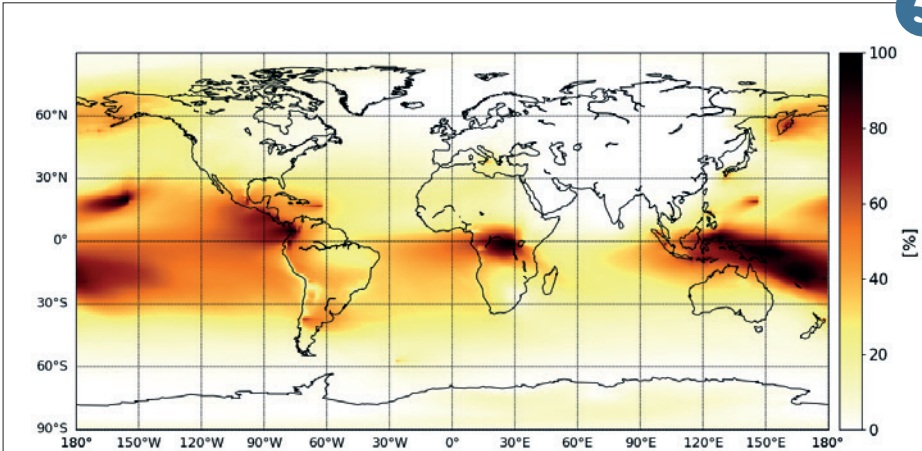
Temporal evolution of the analysed backscatter coefficient resulting from the assimilation of CALIOP lidar data over the African Sahara and corresponding to the 4 seasons of the year 2016.

4



Relative difference in surface ozone concentration on May 1, 2020 at 12:00 noon, between a reference simulation without emission reductions and the simulation taking into account reductions due to the health situation.

5



Annual mean 2013 tropospheric column contribution of sulfate aerosols due to volcanic emissions (in %).

	Sulfur Emission	SO <sub>2</sub> Burden	Sulfate Burden	Sulfur Deposition			Efficiency
				Wet	Dry	Sedim	
Total (Tg)	81.41	0.17	0.82	42.41	27.81	9.80	-
<i>Sources contributions to the total budget (%)</i>							
Volcanoes	14.5	13.8	27.4	7.9	2.3	23.0	1.89
Other	85.5	86.2	72.6	92.1	97.7	77.0	0.85

Global tropospheric budget with 2013 annual mean sulfur emissions, sulfur burden and deposition quantities in Tg. The contribution of sulfur species due to the different sources of emissions are presented in %. Efficiency is the ratio between the contribution to the sulfate aerosol burden and the contribution to sulfur emissions for a specific source.

## Participation in phase 2 of the international CCMi exercise

The international CCMi initiative (<https://blogs.reading.ac.uk/ccmi>) aims to improve our knowledge of chemistry-climate interactions for the past, present and future projections. To this end, intercomparison exercises between models are carried out. The CNRM is once again participating in the exercise, this time for phase 2. One of the objectives of this phase 2 is to support the preparation of the WMO/UNEP Scientific Assessment of Ozone Depletion Report 2022.

For this purpose, a new version of MOCAGE has been developed in order to better describe stratospheric levels, with an upper limit now at 0.1hPa, instead of 5hPa in the previous version. The chosen resolution is 2°x2°, and the meteorological forcing comes from the CNRM-CM model. Several simulations have to be carried out.

On the one hand, the capacity of the models to reproduce the past is evaluated, by carrying out simulations from 1960 to 2018. On the other hand, future projections of the evolution of the chemical composition are simulated, with two projected scenarios. In 2020, the past simulations have been carried out, and the projections will be made in 2021. Another new feature is also the request by CCM-I to provide a set of simulations rather than just one, in an attempt to estimate uncertainties. For each of the simulations, a set of 3 or 4 realizations is thus carried out with MOCAGE.

The figure below illustrates the evolution from 1970 to 2017 of the total ozone column, averaged over the longitudes, with time as the x-axis. On the left, the observations from SBUV-MOD, on the right one of the MOCAGE simulations on the past. The model reproduces satisfactorily the evolution of ozone over the last 60 years.

6

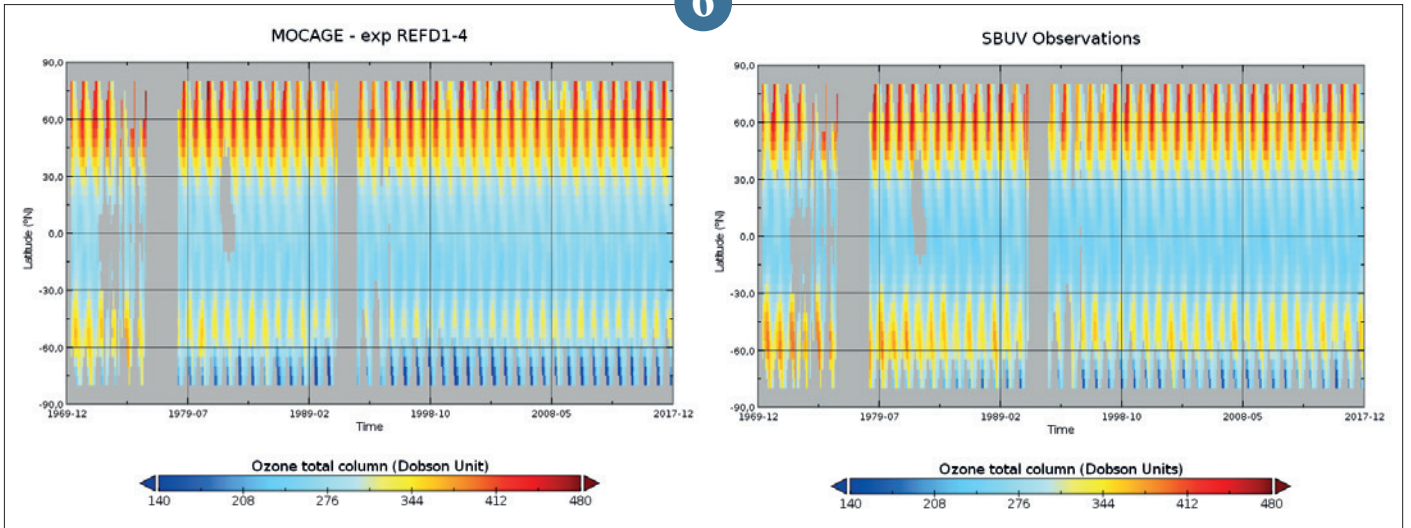
## Unexpected biomass burning aerosol absorption enhancement explained by the measurement of black carbon ageing

Extensive seasonal fires over southern Africa result in the transport of massive amounts of biomass burning aerosols over huge areas of the eastern Atlantic Ocean. Recent field observations highlight that biomass burning aerosols transported from the coast of southern Africa to the far north over southern West Africa were characterized by very strong absorption. This finding is of paramount interest, because radiative heating within the absorbing aerosol layer is hypothesized to affect the low cloud deck over this specific region and may ultimately influence the large-scale circulation. However, debate remains about the causes of the strong absorption observed in biomass burning plumes, causing ambiguous parameterizations of their properties in climate models. As part of the DACCWA project, the GMEI group from CNRM deployed a large set of instruments onboard the ATR-42 airborne platform

to measure the physical properties and chemical of aerosols over southern West Africa. Using these measurements coupled to the radiative transfer model EcRad, our findings indicate that black carbon particles dominate the light absorption by biomass burning aerosols. The ageing (mixing state) of black carbon particles plays a significant role in the aerosol optical properties and may be an important modulator to be considered in climate models for simulating direct and semi-direct radiative effects of biomass burning aerosol over southern West Africa.

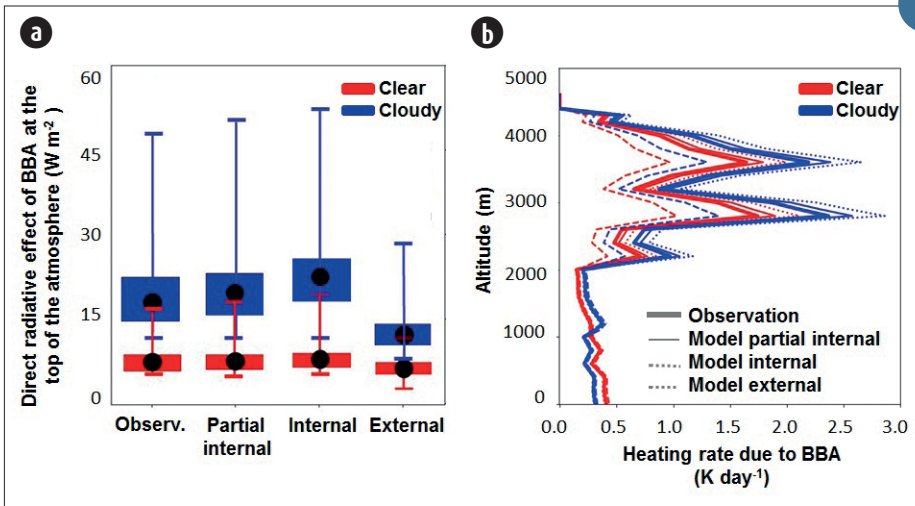
7

6



Evolution of the total ozone column, as a monthly average and over time (along the x-axis), from 1970 to 2017. On the left, according to the observations of SBUV\_MOD ([https://acd-ext.gsfc.nasa.gov/Data\\_services/merged/](https://acd-ext.gsfc.nasa.gov/Data_services/merged/)), on the right according to the MOCAGE model for one of the four realizations of the set calculated for the CCM-I project.

7



(a) Direct radiative effect (DRE) at the top of the atmosphere and (b) heating rate profile due to the transport of BBA, calculated from measured and modelled BBA optical properties assuming different representation of rBC mixing state. On the left, the boxes mark the respective median values (middle points), the 25th and 75th percentiles (left and right box edges), and the minimum and maximum values (error bars). On the right, heating rate profiles are averaged over the campaign.

# Snow

---

Snow is an essential component of the Earth's climate system. Snow plays a major role in climate regulation, as a water resource and a key element of the landscape, for human societies and natural environments. Snow plays an important role in many natural hazards such as avalanches and floods. Météo-France, and in particular the Centre d'Etudes de la Neige (CEN, Météo-France - CNRS, CNRM), conducts research to better understand and predict the evolution of the snow cover in the mountains.

In 2020, several major advances have been concretized and published. The assimilation of satellite data in snowpack models will play a crucial role in the coming years; since it drastically reduce the uncertainties of snow cover simulations. Satellite data offer the unique possibility of obtaining information on the state of the snowpack over large areas but remain incomplete (clouds, shadows for example). An innovative methodology has been set up to transfer information from observed areas to unobserved areas via an assimilation system. The PROSNOW and CLIMSNOW projects have enabled the development of weather and climate services for the winter sports industry. The important impact of Saharan dust deposits on the duration of the snow cover has been studied in detail for several years and mountain massifs. Finally, at a small scales, several issues in our current understanding of mass and heat transport in snow have been solved, paving the way for new decisive advances in physical models of snowpack evolution.

---

## Assimilation of satellite and in-situ observations in snow cover simulations

The knowledge of physical properties of the snowpack in mountainous areas is critical to forecast snow-related hazards and optimize water resources management. Available observations only offer an incomplete overview of the snow cover. The use of numerical models is a mandatory supplement providing all physical properties of snow at any time and any point. However, their large inconsistencies with the reality of the field strongly limit their current use. Assimilation of observations to constrain simulations is the most promising alternative for all groups operating numerical modelling systems for snow cover. To this aim, CNRM has developed an original algorithm so

called "k-localized sequential particle filter". It consists in sampling the members of a simulation ensemble the most consistent with observations, working iteratively on the most relevant subdomains. The algorithm is easy to apply on the most complex snowpack models such as Crocus. It allows to propagate information from observed to unobserved pixels (Figure) and guarantee a realistic spatial variability of snow cover despite the heterogeneity of observations coverage. The added value has been proven for the assimilation of optical satellite reflectances, in situ snow depths, and snow depths obtained by stereo images from the Pléiades satellites.

Developments in progress intend to apply this algorithm in high resolution simulations (250 meters) allowing to take the best benefit from available satellite observations. The expected improvements of simulations will be beneficial for all forecasting systems relying on these simulations over French mountain ranges.

1

## Innovative weather and climate services for the ski tourism industry

The tourism economy in mountain areas relies heavily on ski resorts activities. They exploit the snowpack, a resource that varies greatly at low and medium altitudes, and which undergoes reductions under the effect of climate change. Winter sports resorts manage the snowpack, in particular through grooming and snowmaking. Recent scientific advances have improved the means of anticipating snow conditions on various time scales. The H2020 PROSNOW project, coordinated by Météo-France at CNRM/CEN from 2017 to 2020, brought together 13 partners in the European Alps countries and 9 pilot resorts. It has developed an innovative tool combining meteorological observations and forecasts, modelling of the natural and managed snow cover (grooming and snowmaking), and in-situ observations (snow depth measured by snow groomers, water consumption for snow production) and satellite remote sensing.

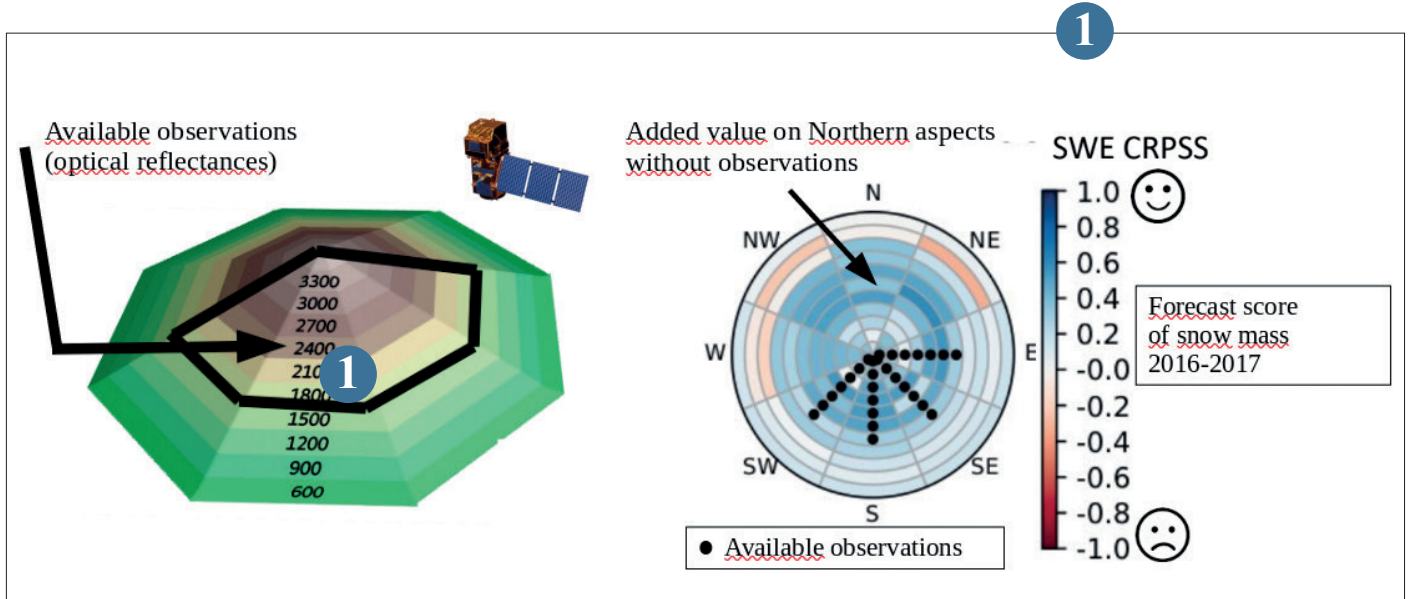
This tool quantifies the impact of daily snow management decisions, at time scales ranging from a few days to a few months. This service has started operations in the winter 2020-2021 in the Alps and Pyrenees by a consortium involving Dianeige, CGX and Météo-France.

In 2020, the CLIMSNOW service, operated by Dianeige, Météo-France and INRAE, has been launched. It provides ski resorts tailored information on the impact of future climate change on their operating conditions, thereby enabling a relevant inclusion of such input to the design of climate change adaptation strategies for this sector, at the scale of several decades. Furthermore, Météo-France coordinated and produced pan-European natural and managed snow cover indicators under a Copernicus Climate Change Service contract, available on the C3S Climate Data Store.

*Useful links:*

<http://prosnow.org/?lang=en>  
<https://www.climsnow.com/>  
<https://cds.climate.copernicus.eu/cdsapp#!/dataset/sis-tourism-snow-indicators>

2



▲ Impact of assimilation of optical reflectances available once a week and only on sunny slopes above forest line, on the forecasts scores of snow mass in Grandes Rousses massif (Isère) during 2016-2017 winter. Blue: improvement Red : degradation. The massif is represented as a pyramid, elevation increases going closer to the center of the circle. Compared to simulations without assimilation of observations, a very significant added value is obtained not only on observed slopes but also on Northern slopes, without any observation.



◀ Example of snow production and overview of the PROSNOW visualization. PROSNOW was featured in the European Commission contribution to the GEO Week 2020 and referred to in the statement by Dr Patrick Child, Deputy Director General for Research & Innovation ([https://www.youtube.com/watch?v=\\_RJzWwSFhsw](https://www.youtube.com/watch?v=_RJzWwSFhsw)).

---

## Impact of dust deposition on snowpack evolution

In March 2018, the Caucasus Mountains were covered with an orange deposit. The phenomenon of high intensity was widely reported by the media. A strong storm coming from the Libyan coasts transported the Saharan sand mineral particles that had been deposited in the Caucasus. This type of phenomenon is sometimes visible in France, particularly in the Alps and the Pyrenees. This deposition has a strong impact on the evolution of the snow cover, especially at the end of the season when the orange layers reappear on the surface. The dark colour, compared to the usual white colour of snow, causes an increase in the solar energy absorbed by the snow, energy that is necessary and then available for an accelerated melting. To follow the evolution of dust concentrations at the snow surface (Figure 1), we used images from the optical satellite Sentinel-2 and detailed numerical simulations of the snow cover. Whatever the altitude, the simulations show that the dust deposition caused an accelerated melting of

the snow cover by one to two tens of days. The impact is more pronounced at higher altitudes, with an advanced melting date of  $23 \pm 7$  days (2200m), than at lower altitudes,  $15 \pm 3$  days (1600m), which is explained by the fact that at higher altitudes the melting naturally occurs later, at a time of the season when more solar energy is available. In France, this type of phenomenon is observed almost every winter with very variable intensities. At the Lautaret pass in the Alps, we studied the phenomenon in detail for two winters and showed that dust combined with carbon soot had shortened the duration of snow cover by about ten days for these two winters.

3

---

## Heat and mass transport in the snow microstructure

Characterizing mass and heat transport in snow is essential for predicting the evolution of the snow microstructure as well as the energy and mass balance of this key component of the Earth system, at the interface between the atmosphere and the ground. In current models, these transports are often treated in an uncoupled manner, for simplicity.

We studied the coupling between mass and heat transport in dry snow, and its homogenization into equivalent macroscopic properties. Combining theoretical developments, measurements, and numerical simulations based on 3D tomographic images, we showed that, contrary to a 60 year-old idea, water vapor diffuses less in snow than in air. Nevertheless, as illustrated in the Figure, diffusion increases with the kinetics of phase change at the ice surface. Moreover, our results show that in the case where this kinetics is very fast, an hypothesis supported by several experimental results, mass and heat transport become inextricably entangled. Indeed, vapor molecules carry

a small amount of energy, that is released when vapor deposits on the surface of the ice matrix. This energy carried by vapor is an integral part of the heat flux, and can increase snow effective conductivity by up to 50 % for certain snow types.

Our work shows that the quantification of the phase change kinetics at the ice surface is required to improve the modeling of heat and mass transport, which in fine govern the evolution of the snow cover.

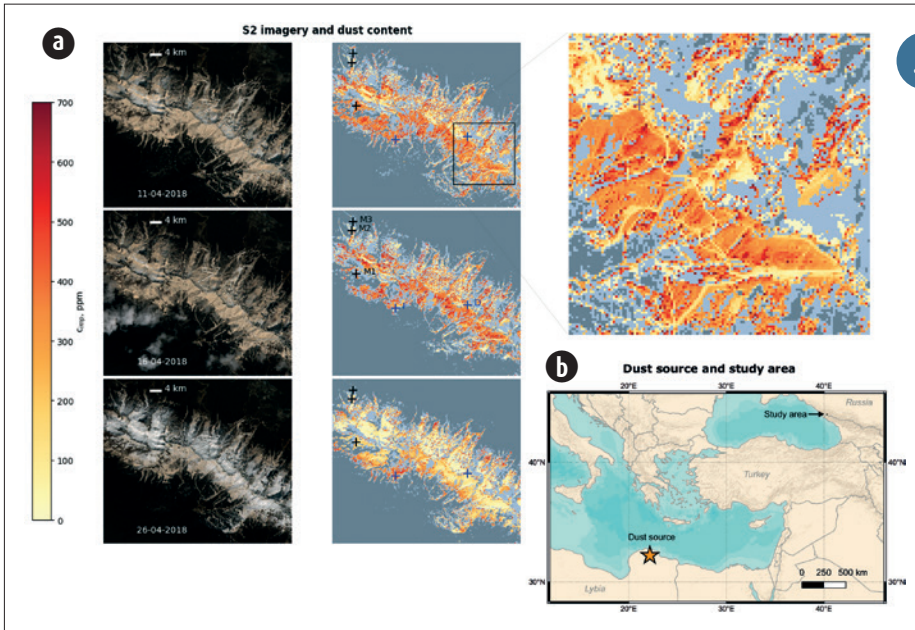
4

## Impact of satellite-based irradiance products on mountain snowpack

Mountain snowpack monitoring is essential for many applications, but remains very challenging because the snowpack is strongly influenced by a variety of factors, including incoming shortwave and longwave radiation. In this study, an evaluation of the solar and longwave downwelling irradiance products (DSSF and DSLF) derived from the Meteosat Second Generation satellite in the French Alps and the Pyrenees is presented. The satellite-derived products were compared with forecast fields from the meteorological model AROME and with reanalysis fields from the SAFRAN system. A new satellite-derived product (DSLNew) was developed by combining satellite observations and AROME forecasts. An evaluation against *in situ* measurements showed lower errors for satellite based products in terms of solar irradiances. For longwave irradiances, it was difficult to identify the best product due to contrasted results falling in the range of uncertainty of the sensors. Spatial comparisons of the different datasets over the Alpine and Pyrenean domains highlighted a better representation of the spatial variability of solar fluxes by DSSF and AROME than SAFRAN. We also showed that the altitude gradient of longwave irradiance is too strong for DSLNew and too weak for SAFRAN (see the attached figure). All datasets were then used as radiative forcing together with AROME near-surface forecasts to drive distributed snowpack simulations by the model Crocus in the French Alps and the Pyrenees. An evaluation against *in situ* snow depth measurements showed higher biases when using satellite-derived products, despite their quality. This effect is attributed to some error compensations in the atmospheric forcing and the snowpack model that needs to be investigated further.

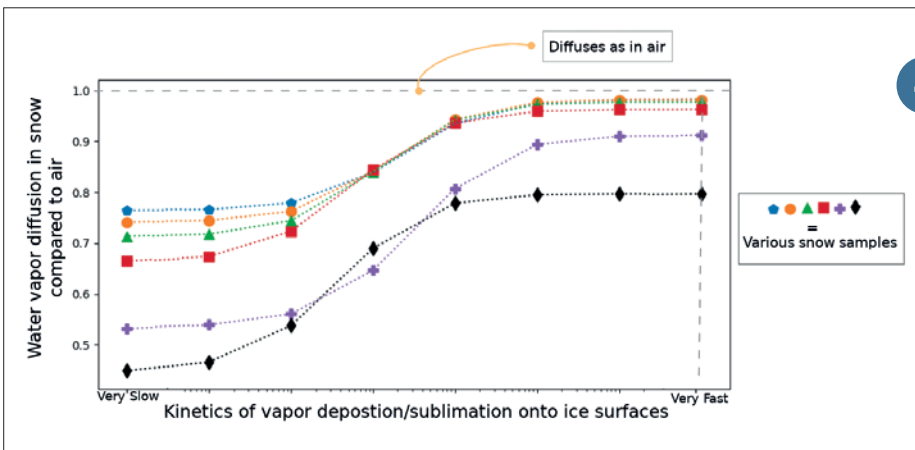
5





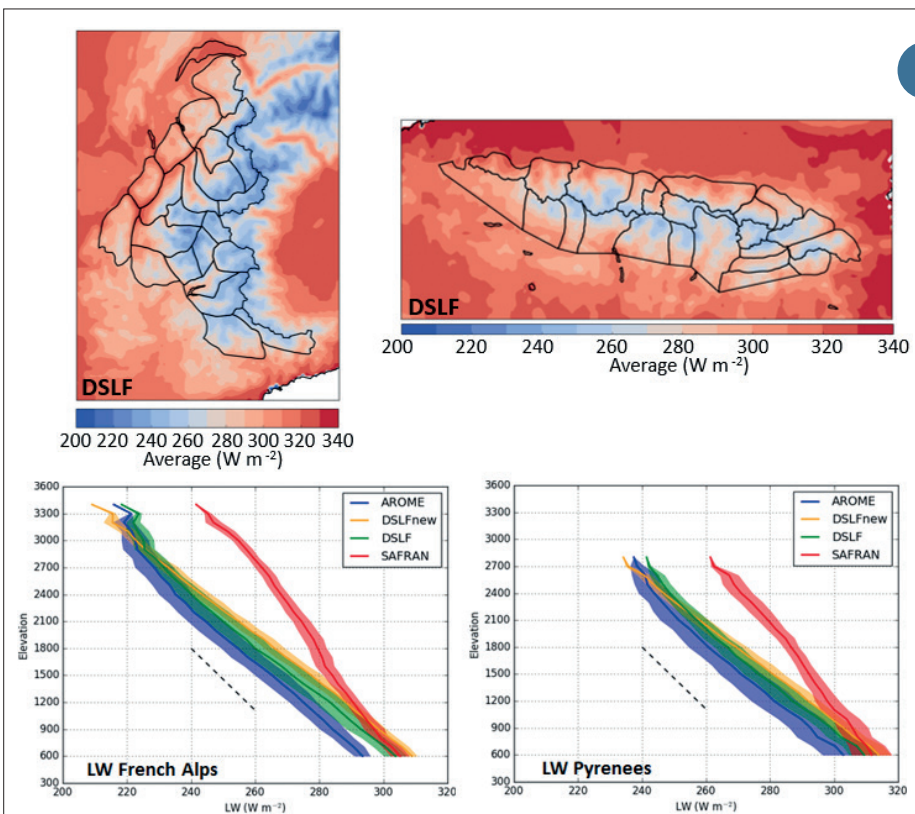
3

(a) Location of the study site and of the dust origin region, (b) S2 time series, left column RGB composite, right column, estimated dust content in ppm. Shaded areas are clouds or no snow (dark grey) or mixed, inclined or noisy pixels (light grey). The 4 locations correspond to snow depth measurement sites (M1, M2, M3), dust content measurement site (D) and a reference flat area (F). On the top right, a zoom of the dust content maps is provided for the black rectangle. Cleaner ski slopes are visible on the map (see zoom).



4

Impact of surface kinetics on the diffusion of water vapor in snow. In all cases, water vapor diffuses less in snow than in air.



5

(top) Average of the DSLF (Alpes and Pyrenees) from 1 August 2010 to 31 July 2014. (bottom): Vertical gradient of LW products in the French Alps and Pyrenees, with LSA SAF in green, AROME in blue, SAFRAN in red, DSLFnew in orange. The envelopes represent the mean  $\pm$  the standard deviation. The dashed black line represents the climatological LW $\downarrow$  vertical gradient of  $-29 \text{ W m}^{-2} \text{ km}^{-1}$  from Marty et al. (2002).

# Oceanography

---

Two kinds of research work in oceanography are presented this year. The first one highlights different and original developments in the field of observation. Innovative observation of sea state along the coast using simple cameras ranges in the category of ‘opportunity systems’, a well-established practice in meteorology. The retrieved data are compared to the operational wave models. This work is being carried out with the Institut de Recherche pour le Développement and a start-up company housed in the incubator located at the Météopole. The second illustration takes advantage of the satellite observation infrastructures in order to combat plagues such as sargassum algae. Météo-France innovates and makes the most of its know-how, its processing chains and digital modelling systems to constantly develop its contributions to understanding our environment and its disruptions, and to prevent risks.

Major hazards and striking events are also a key motivation for work addressing the complexity of air-sea interactions and their role in coupled ocean-atmosphere phenomena. This applies to sea surface temperature fronts and the associated atmospheric response – like the fog associated with the tide-related excursions of the Ushant front, and the heavy maritime traffic sailing in and out of the Channel -, but also to Mediterranean events and tropical cyclones. In all cases, more sophisticated modelling of the coupling between the atmosphere and the ocean is a determining factor in improving our understanding of these phenomena and our forecasting capabilities.

Research efforts range from processes, which are revisited in depth, to modelling tools, from those reserved for the laboratory to models used in operations. Ocean-atmosphere interactions, taking sea state into account, are a key to a number of phenomena with high stakes for our coastal territories and maritime activities, both in mainland France and in the overseas territories.

---

## Remote sensing of Sargassum for operational early warning bulletins.

Remote sensing of Sargassum is a relatively new field of the remote sensing studies becoming the more and more important with more frequent hazardous impact on the coastal communities, especially in the Caribbean sector.

Since 2020, we have started developing a system of early satellite monitoring of the Sargassum mats in the deep-ocean sector. This early detection of Sargassum is necessary as the preparatory information for the numerical predictions of the Sargassum

shoaling, but also for the local decision makers who can choose a good strategy to cope with this problem. At present we develop a set of algorithms for different satellite sensors (MODIS, OLCI, VIIRS, and others) using visual, infrared and near-infrared wavelengths. The task is, thus, challenging as one of the most problematic features is the clouds that should be filtered out. The main goal of our team is a multi-sensor algorithm providing the most precise information on the Sargassum mats positions

at different spatial and temporal resolution. The first results of the algorithm development for MODIS sensor are promising and are being validated by a team of local experts and some expedition data. The new sensors will be added to the operation algorithm next years to increase the temporal resolution and the quality of delivered information.

1

---

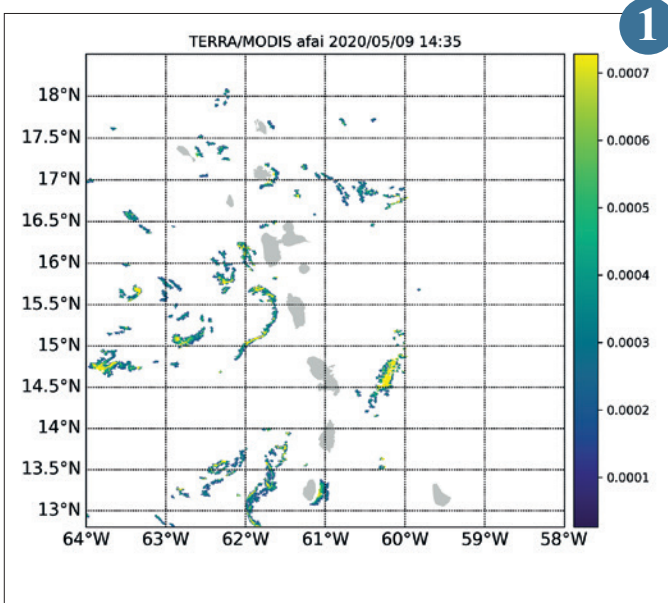
## WASP (Wave-age dependant stress parameterization) a new parameterization of air-sea turbulent fluxes accounting for the wave impact

Representing accurately the surface turbulent exchanges between the ocean and the atmosphere is important for a number of numerical weather prediction of climate applications. Intensification of tropical cyclones for instance is known to depend both on the amount of heat extracted from the sea and the shear due to surface friction. A polyvalent parameterization of momentum and turbulent heat fluxes at sea has been developed for the SURFEX v8.0 surface model. This wave-age dependent stress parameterization (WASP) combines a close fit to available in situ observations, including estimates of drag coefficient and transfer coefficient for heat fluxes up to

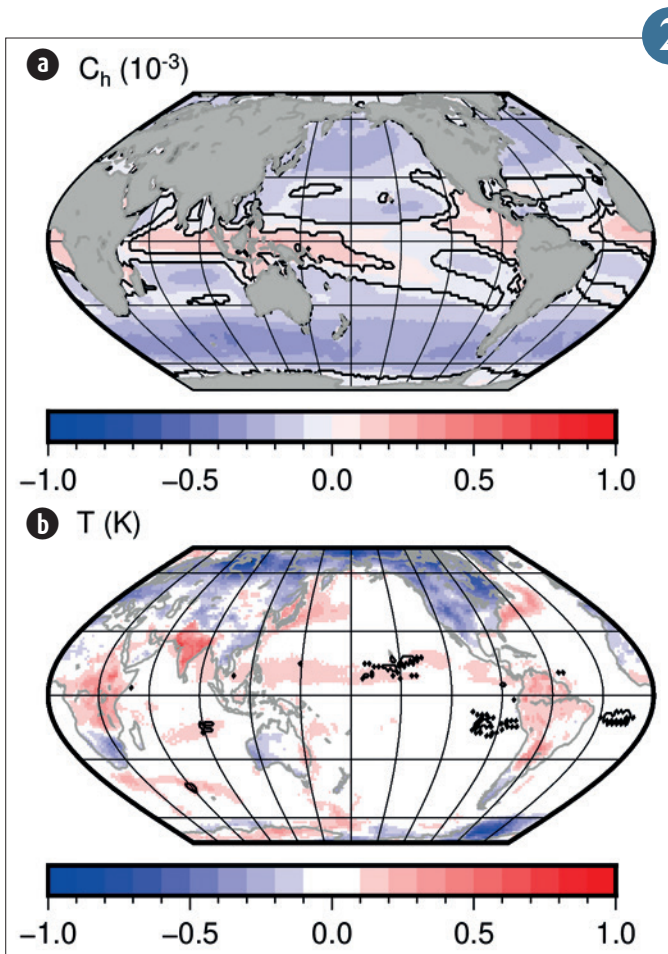
wind speed of 60 m s<sup>-1</sup> with the possibility of activating the impact of wave growth on the wind stress. It is based on different physical principles depending on the surface wind range considered and the state of the art of the associated surface processes. It can be used with the different atmospheric models in use at Météo-France coupled with the surface model SURFEX, namely AROME, ARPEGE and Meso-NH. It has been validated in several case studies covering different surface conditions known to be sensitive to the representation of turbulent fluxes: i) the impact of a SST front on low-level flow by weak wind; ii) the simulation of a Mediterranean heavy precipitating event where waves have

been shown to influence the low-level wind and displace precipitation; iii) a tropical cyclone; and iv) a climate run over 35 years. It shows skills comparable or better to the different parameterizations in use in the SURFEX v8.0 so far.

2



◀ The Sargassum mats and their AFAI (Alternative Floating Algae Index) detected in the Western Atlantic Ocean on May 9, 2020 using MODIS/Terra sensor



◀ Difference of (a) sensible heat transfer coefficient and (b) 2-m temperature between the atmospheric 35-year climate run with WASP and the present parameterization ECUME. Black lines indicate differences significant at 95 % uncertainty.

## Validation of a video processing system for sea state observations

Coastal sea state observations are crucial for Météo-France's wave and flooding alert system, for continued monitoring and for improving the wave model. For more than ten years, the use of coastal cameras to make these observations has been an area of active research within the scientific community. This measurement technique was tested in 2020 in collaboration with Waves'n See, a start-up hosted on-site at Météo-France in Toulouse.

Their algorithms, developed from research undertaken at IRD, derive sea state parameters from webcam images. The study focused on two existing cameras at Capbreton (from Viewsurf, in partnership with IRD). The wave period is computed using temporal samples and by processing of the images' luminosity. Blurry images because of sea-spray are detected and removed. Then, without prior knowledge of the camera's characteristics, a georeferencing of the image is performed allowing the calculation of wave heights.

Data from a coastal wave model correlate well with the camera's parameters, though there is still need for improvement. These results are all the more encouraging because the cameras were part of an existing network intended for leisure activities and its technical specifications (focal length, height,...) were unknown.

The validation has been limited by a lack of in-situ observations. This will be addressed by validating cameras from other sites against nearby buoy measurements.

3

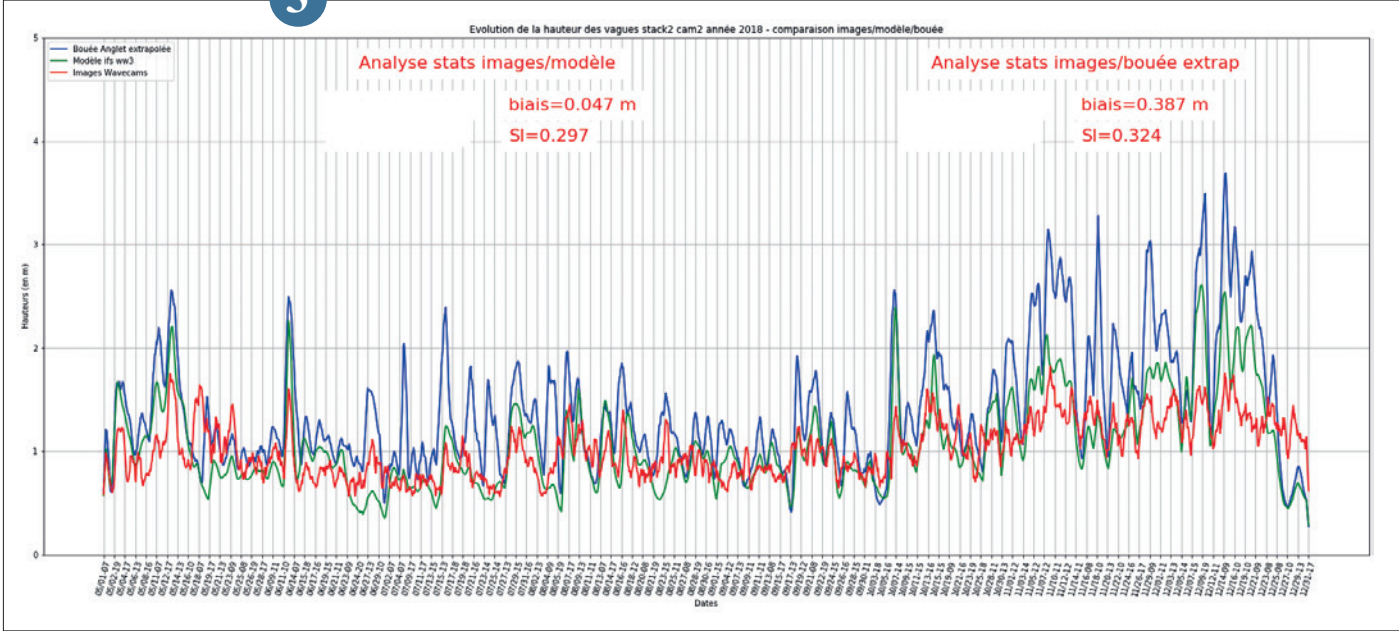
## Coupling the AROMES-OM with NEMO

5 AROME models have been operational since 2016 in the Indian Ocean, the Caribbean, Guyana, New Caledonia and Polynesia. The AROMES-OM domains are mainly covered by a tropical ocean on which tropical cyclones can develop. Since 2017, the surface scheme of the AROMES-OM includes a 1D parametrization of the Ocean Mixed Layer (OML) which allows to take into account the rapid changes in ocean temperature induced by cyclones. The coupled simulations initially carried out at LACy with MesoNH and the NEMO or CROCO ocean models had shown that the OML parametrization tends to underestimate the cooling under cyclones. A coupled configuration of AROME-Indian Ocean-NEMO was developed this year in order to test the impact of the 3D coupling on a larger number of cyclones and to evaluate its interest in an operational context. The first simulations show that the coupled model can lead to very strong oceanic cooling in areas where the cyclone is quasi-stationary for several hours (see Figure). Sensitivity tests on the mixing processes in the ocean model are underway in order to optimise the NEMO configuration for the resolutions used and the forcing by strong cyclonic winds. However, given the extreme scarcity of ocean data in Indian Ocean cyclones, it is difficult to validate the state of the ocean at a scale of a few tens of kilometres in areas covered by clouds.

The AROME-OI/NEMO configuration will be further enriched in 2021 thanks to the coupling with the WW3 wave model, which will allow to test new parameterizations of the flux at the ocean-atmosphere interface integrating the wave characteristics provided by WW3.

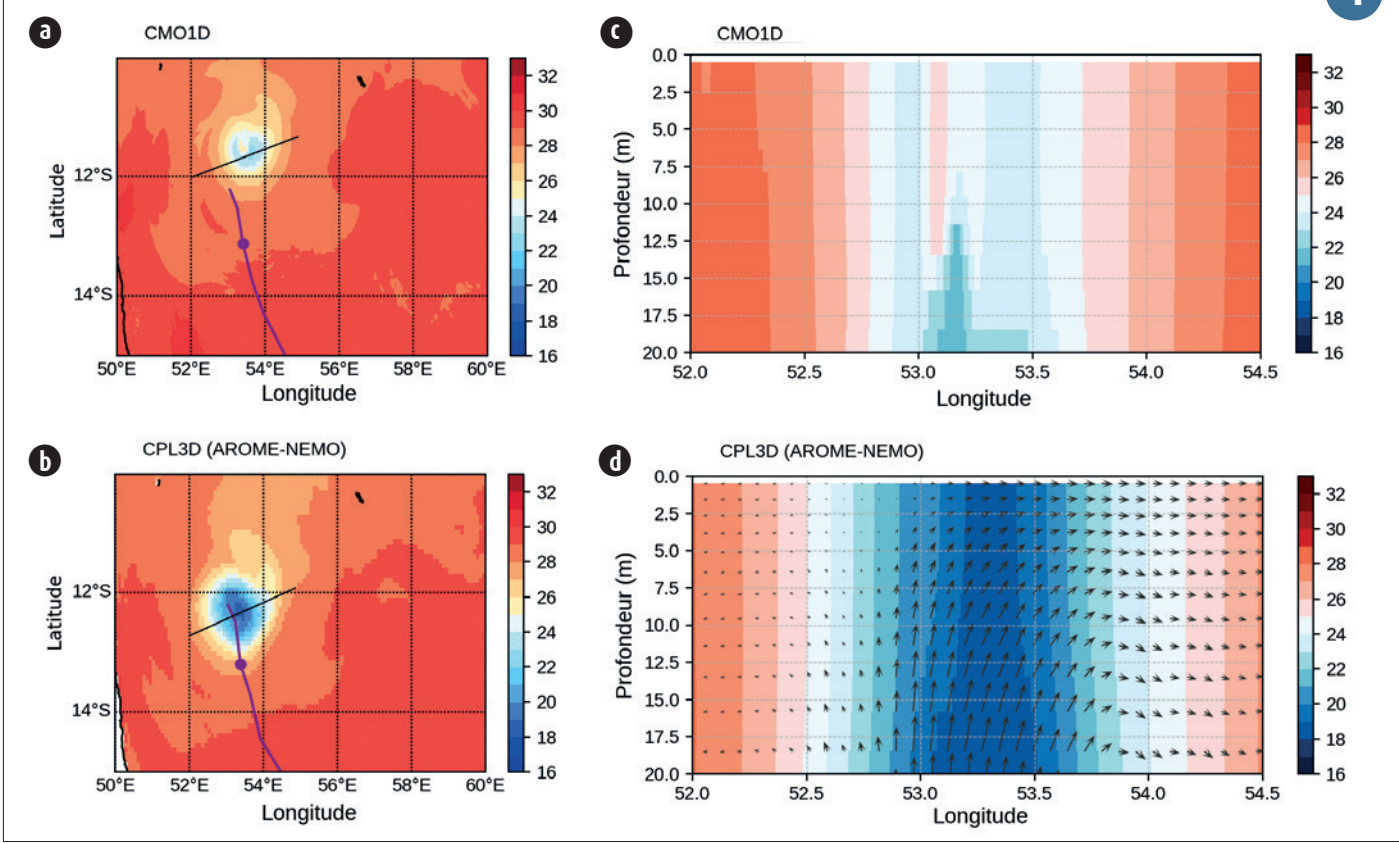
4

3



Graph of the wave height (m) of the camera (red), of the WW3 Météo-France model (green) and of the Anglet buoy (blue - Cerema and Pau university), at the south camera of Capbreton in 2018

4



SST (left panels) and cross-section of the ocean temperature in the OML and of the currents (right panels) after 12 hours of simulation for cyclone Gelena (07/02/2019) (a)-(c) operational configuration with the 1D parameterization of the OML (b)-(d) coupled simulation AROME-NEMO; an ocean warm-up of 24h prior to the simulation is used in this case.

# Engineering, campaigns and observation products

---

Experimental research activity at Météo-France has been severely disrupted by the pandemic. Most of the campaigns planned for 2020 had to be postponed. The campaign on fog in the Landes region, started in 2019 (SOFOG3D programme) had to be interrupted slightly early. It enabled the acquisition of valuable data on the 3D structure of fog thanks to an original instrumental device. The international EUREC4A campaign in Barbados on trade wind clouds and oceanic eddies took place at the very beginning of the year. It involved SAFIRE's ATR42, operating far from its bases, and CNRM's ultralight and light drones, the former flying in swarms, the latter carrying out long-range, low-altitude flights over the sea, all in coordination with air traffic. Instrumental development activities were less disrupted. Thanks to an innovative technological solution borrowed from the GSMA laboratory, a probe for the rapid measurement of humidity in a tethered balloon was successfully tested. Turbulent latent heat fluxes can now be measured at altitude. The adaptation of the MAP-IO observation system to the harsh sea conditions and the low bandwidths of the telecommunication system available on the ship Marion-Dufresne has been validated. The preparation of Meteosat Third Generation is underway. Data from the meteo-pole's permanent observation station were used by the DSM to evaluate vegetation wetting models for the benefit of agricultural services. Finally, the study of the urban heat island, a concern of cities faced with global warming, benefited from the observations of autonomous stations deployed in a network in Toulouse, as well as from temperature measurements carried out in personal cars, which are increasingly connected. These techniques, which are expected to develop, offer great potential for documenting climate conditions on a very fine scale in cities.

---

## Observation engineering and products

### Measurement and modeling of wetting duration

Liquid water is frequently found on the surface of the leaves. This phenomenon is called humectation and promotes fungal and bacterial diseases. Its duration is a key factor in decision-making tools for the agricultural end-users.

Based on experiments carried out on the Toulouse site, with the support of the CNRM / GMEI research group and the DOS/SENSORS unit, the DSM/CS/AGRO team confirmed the strong variability in the wetting duration measurements according to the sensor used or its installation configuration (figure a).

The final objective of this study is to build a model based on meteorological parameters in order to overpass this variability.

Wetting duration measurements and meteorological parameters from the METEOPOLE-FLUX instrumented site, available since mid 2012, were used as reference for the three following models :

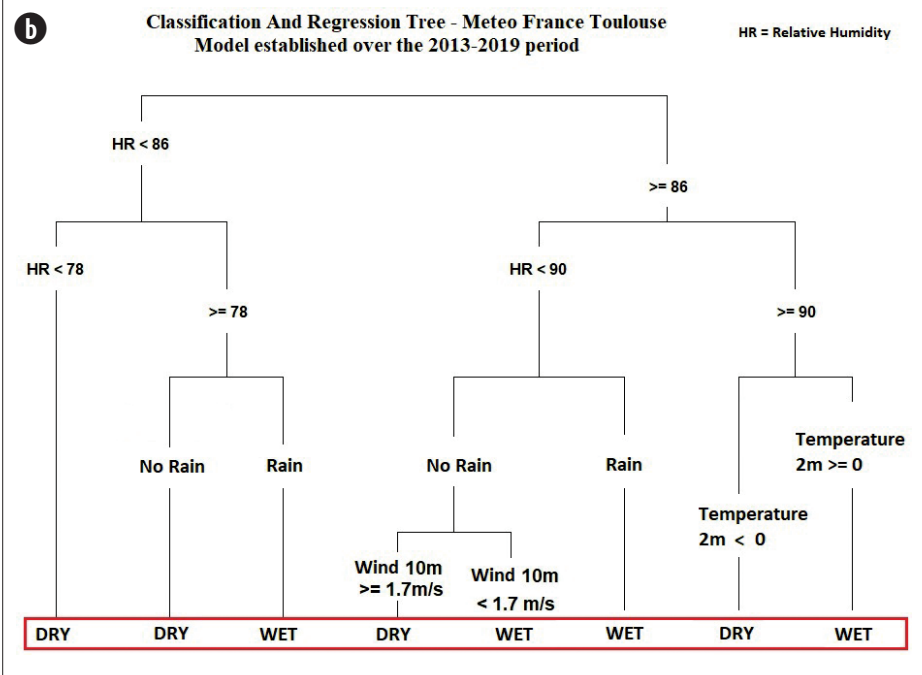
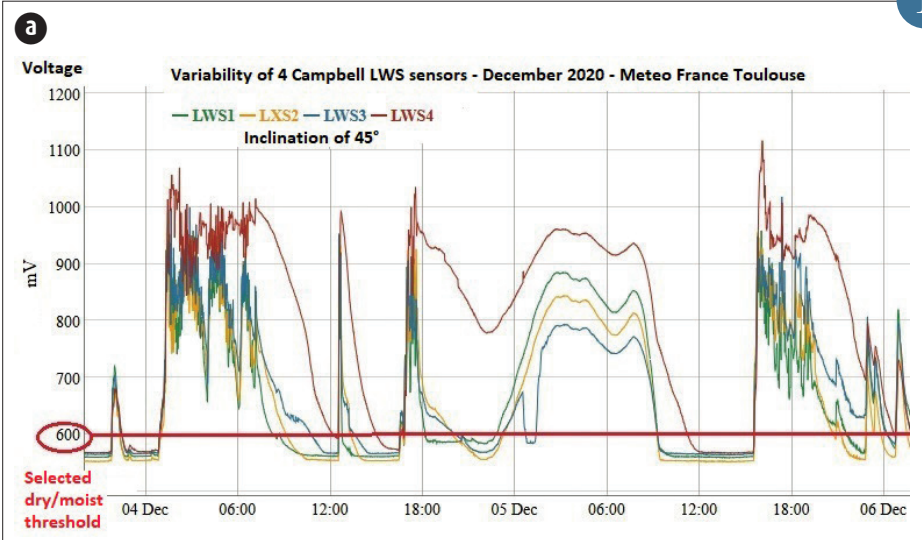
- RHT whose best statistical fit is obtained for the relative humidity (RH) threshold of 86%.
- CART, based on a decision tree whose most relevant predictors are relative humidity, rain, temperature and wind (figure b).

- a calibrated physical model considering the leaf as a reservoir; it gives the worst results. The CART model performs better despite an underestimation of the wetting duration. Due to its easy implementation, the RHT remains a quite good solution.

Sensors will be installed in other locations in 2021 to test the geographical portability of these results.

1

1



(a) Comparative measurements of 4 identical sensors  
 (b) Decision tree

---

## The 20Hz humidity under tethered balloon

Turbulent processes and in particular sensible and latent heat fluxes are mainly responsible for energy transfers between the surface and the atmosphere within the atmospheric boundary layer (ABL).

It is in this context that vertical observation of turbulent parameters is of interest. The probe shown in figure “a” was developed in 2010 in order to measure the thermodynamic parameters at very high frequencies (20Hz) and the sensible heat flux in order to know the heat exchanges within the ABL.

This lightweight instrument, weighing less than 3 kilograms, measures the thermodynamic parameters during vertical profiles carried out under a tethered balloon between the ground and 800m. These measurements are complementary to the measurements on mast and/or research aircraft during field campaigns dedicated to ABL.

In order to increase our knowledge on moisture exchanges within the boundary layer, in cooperation with the GSMA laboratory in Reims we have associated to the existing fast sensor a mini spectrometer with a laser diode weighing less than one kilogram in order to measure moisture fluctuations to calculate the latent heat flow. During the experimental campaign of the SOFOG3D project, this probe was used to carry out tests. Since then, corrections have been necessary such as the position of the mirrors in relation to the orientation of the probe and the sun. Soon other tests will be carried out, notably in a calibration chamber to ensure that the humidity measurement is comparable to conventional measurements. In July 2021, it will be deployed during the LIAISE field campaign in Spain to complement the measurements provided on a 50m mast and those on an aircraft.

The deployment of this probe will represent a strong asset in this measurement campaign where the understanding of the redistribution of humidity brought by irrigation on the vertical is essential.

2

## Water phase detection at cloud top from geostationary satellite

Cloud thermodynamic phase detection is essential for cloud optical properties estimation. Cloud phase is currently determined using brightness temperature difference from infrared channels at 8.7 and 10.8  $\mu\text{m}$  for the radiometer seviri onboard MSG1. The satellite MTG2 will carry a radiometer with a channel at 10.5  $\mu\text{m}$  that will have a negative impact on the cloud phase algorithm.

Indeed, the absorption properties of ice and liquid water are very similar at 10.5  $\mu\text{m}$  compared to 10.8  $\mu\text{m}$ . As a result, the ability of the 10.5  $\mu\text{m}$  band to separate the cloud phase is significantly reduced. It is confirmed by the simulations represented in the figure where it can be noted that the scatter plot at 10.8  $\mu\text{m}$  (see figure A) has a much higher variability than the one at 10.5  $\mu\text{m}$  (see figure B), and that the overlap between ice water clouds and liquid water clouds is less significant for the band at 10.8  $\mu\text{m}$  than for the band at 10.5  $\mu\text{m}$ .

The Beta-ratio is computed as a ratio of the cloud effective absorption coefficients at different wavelengths. The simulation results of this parameter are represented in the figure C for MSG (10.8  $\mu\text{m}$  band) and in figure D for MTG (10.5  $\mu\text{m}$  band). It can be highlighted that the liquid and ice water phase are much better separated with the Beta-ratio, thus offering interesting perspectives for the classification of the cloud phase.

3

---

## New observing systems of the Urban Heat Island at infra-urban scale

The observing networks of the National Meteorological Services primarily aim to observe the weather at synoptic and meso-scales. The meteorological stations are then, most often, located outside cities. However, in the goal to improve the weather forecasting in cities at hectometric scale, one need to have access to meteorological observations at high resolution within cities.

A network of approximately 70 meteorological stations has been co-constructed between Toulouse Metropole agglomeration and the CNRM, and has been fully operationally integrated within the city administration services. The Internet of Things is used to transfer in real-time the data, in order to realize maps of the Urban Heat Island. This network (figure a) allowed to analyze the infra-urban variability of the Urban Heat Island. For example, industrial and commercial zones, which are often considered as being hot-spots during day by city stakeholders, are in fact slightly cooler than the city center and other suburban areas, except in late afternoon.

On the other hand, cities are a source of many opportunistic data that can be of interest for the meteorology. The personal connected cars are increasingly present in the French vehicle fleet. During night, the embedded thermometers are of particularly good quality (less than 1°C of difference with meteorological urban stations). These data are particularly rich to study the urban microclimate. A PhD thesis has started on this subject, and allowed to map the Urban Heat Island on several cities (e.g. Paris, on figure b).

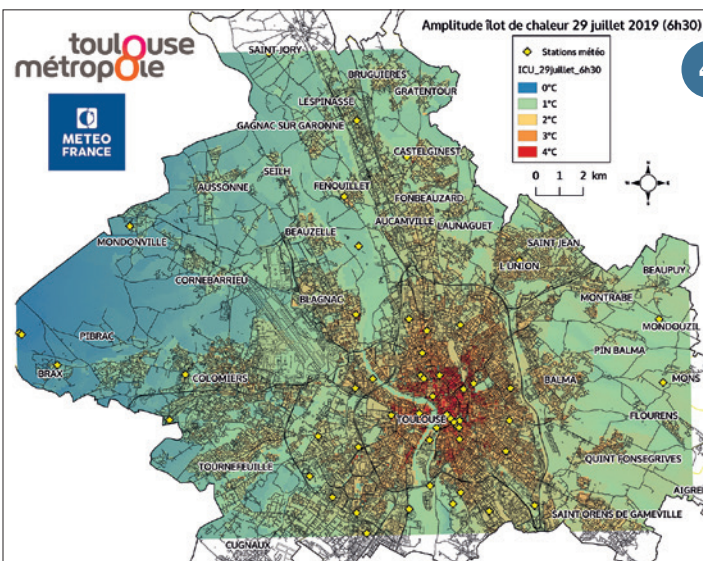
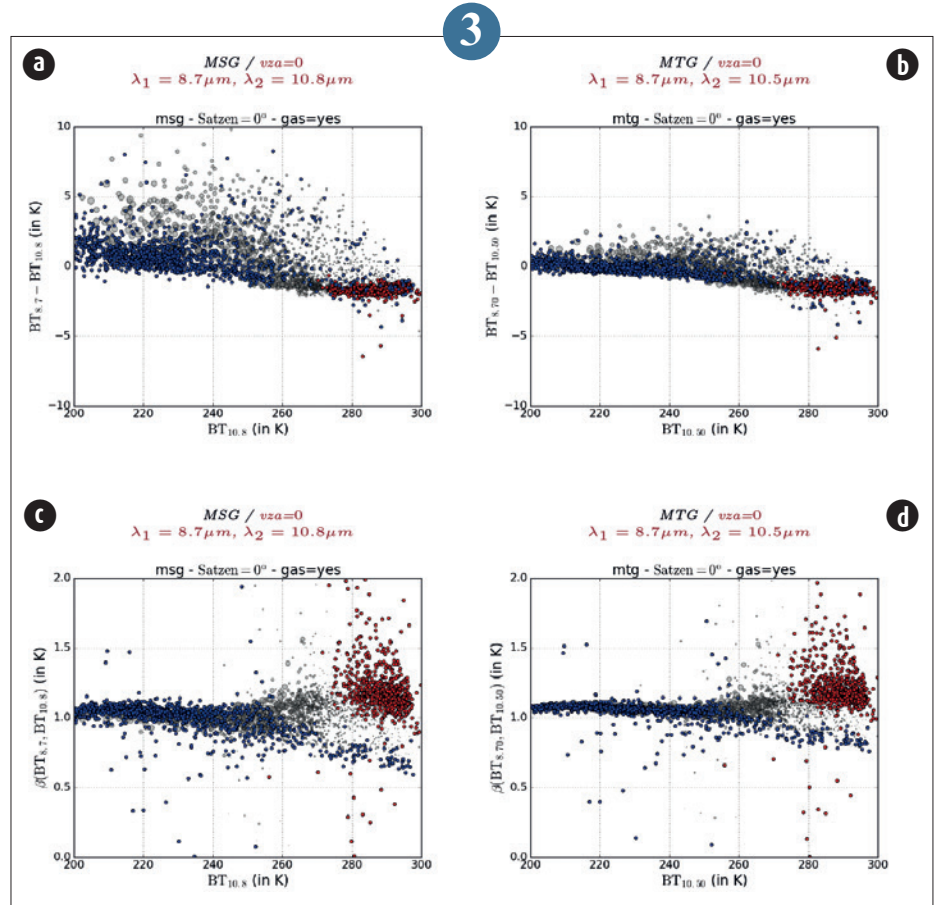
4





Turbulence probe under tethered balloon during a test flight. The mini spectrometer that measures fast humidity is installed on the right arm of the sonic anemometer.

Simulations of brightness temperature difference and Beta-ratio for liquid water cloud and ice water cloud as seen by Meteosat Second Generation (a and c) and Meteosat Third Generation (b and d). On each graph we represent liquid water clouds in red, ice water clouds in blue and mixed phase clouds in grey. We notice that in the plane (Beta-ratio - Brightness Temperature) the liquid and ice phases are better separated than in the plane (Brightness Temperature Difference - Brightness Temperature).



(a) Urban Heat Island observed by the meteorological stations urban network co-constructed with Toulouse Métropole (data of 29th July 2019, at 6h30). Source : PhD thesis of G. Dumas.  
 (b) Urban Heat Island observed by connected on Paris agglomeration the 3rd of August 2019 at 21 UTC. Source : PhD thesis of E. Marquès.

## Campaigns

### The Southwest FOGs 3D experiment for processes study (SOFOG3D) field campaign 2019-2020

Fog strongly perturbs transportation and accurate forecasts are thus required to reduce its impact on human activities. The main objective of the SOFOG3D project, funded by Météo-France and ANR, is to advance our understanding of fog processes to improve fog forecasts. The project, coordinated by the CNRM, involves LMD/IPSL and LATMOS/IPSL. The experiment seeks an international dimension with participation of the Met Office, the Köln University, MeteoSwiss and industrial partners.

A six months field experiment has been conducted from October 2019 to March 2020 in the Landes plain to provide 3D mapping of the boundary layer during fog events.

Three nested domains has been instrumented to collect observations from regional scale down to local scale on the super-site (Figure 1). The super-site has been selected in an agricultural exploitation to contrast large open area with pine forest slots. Detailed measurements of meteorological conditions, aerosol properties, fog microphysics, water deposition, radiation budget, heat and momentum fluxes on flux-masts were performed on four areas with different characteristics to investigate the impacts of surface heterogeneities on fog processes.

Two 94 GHz cloud radars were operated. In addition in situ measurements of turbulence and droplet size distribution were performed under a tethered balloon. Such a unique configuration allowed for the first time a volume sampling of a fog layer. Combination of cloud radar and microwave radiometer (MWR) measurements will allow optimal retrieval of temperature, humidity and liquid water content profiles. At the regional scale, a network of 8 MWR on 6 sites was deployed to investigate their impact on fog forecast through assimilation.

During intensive observation periods, 15 fog events were sampled with the tethered balloon, including 7 with UAV flights with some legs reaching ~5 km long, and 180 radiosoundings were launched.

Process studies will now be conducted on very well documented situations, using synergy between 3D high-resolution Large Eddy Simulation and unprecedented 3D detailed observations.

5

### Study of trade wind cumuli using UAS during EURECA

In February and March 2020, CNRM deployed unmanned aerial systems (UAS) in Barbados during an international field campaign, EURECA, co-led by the Max Planck Institute (Germany), the Laboratoire de Meteorologie et Dynamique (France) and the Caribbean Institute for Meteorology & Hydrology (Barbados). The objective of this campaign is to study the processes of cloud formation in tropical regions, which constitute a major source of uncertainty in estimates of climate change.

Two types of UAS were used:

- Lightweight Skywalker X6 UAS (2.5 kg, 1h endurance) carried out autonomous adaptive flights as a fleet to follow the life cycle of trade wind cumuli as part of the NEPHELAE project: 17 adaptive flights were conducted using autonomous sampling strategies by following the evolution of individual clouds for more than 10 kilometers.

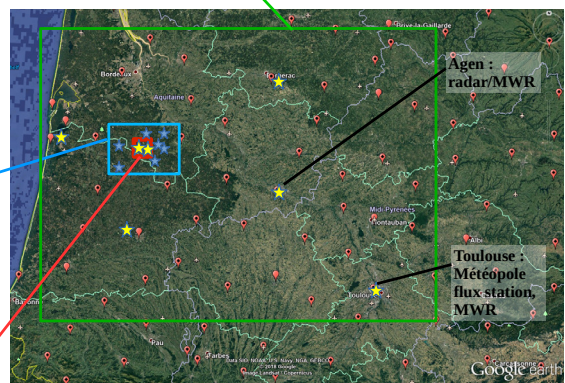
- The Boréal UAS (25 kg, 7h / 700 km of autonomy) flew over the Atlantic Ocean in the “Trade Wind Alley” to characterize the ocean-atmosphere exchanges. Equipped with sensors (aerosols, turbulence, wave height, temperature, humidity) and a transponder, the Boréal UAS coordinated flights with other research planes and oceanographic vessels for the first time, and flew for a total of 33 hours covering 3,260 km. The participation of the Boréal UAS was funded by an ANR (S. Bony, LMD) and Météo France.

These latest operations provide unprecedented meteorological observations to answer essential scientific questions (ocean-atmosphere exchanges, cloud life cycle), and demonstrate the complementarity of observations by UAS in a large-scale international project.

6

5

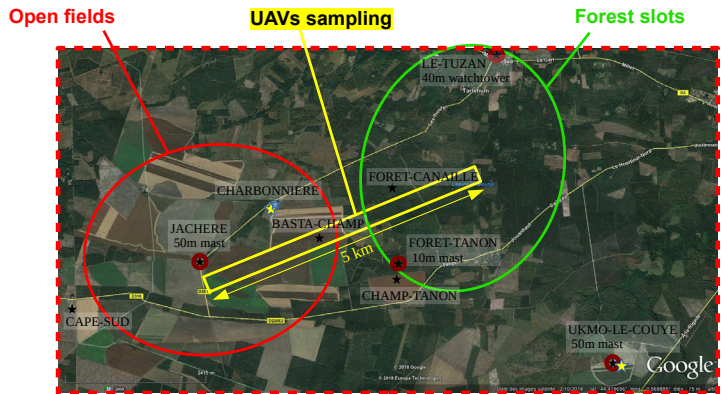
**Larger domain 300 x 200 km** (AROME-500m model) with in-situ sensors (~ 50 surface met. stations) and MWR (6 sites) networks



**Surrounding domain 30 x 50 km** with increased density in-situ sensors network (+8 surface met. stations with visibility, 40m watchtower, 10m mast flux and 2 ceilometers)

**Super-site 6 x 10 km**

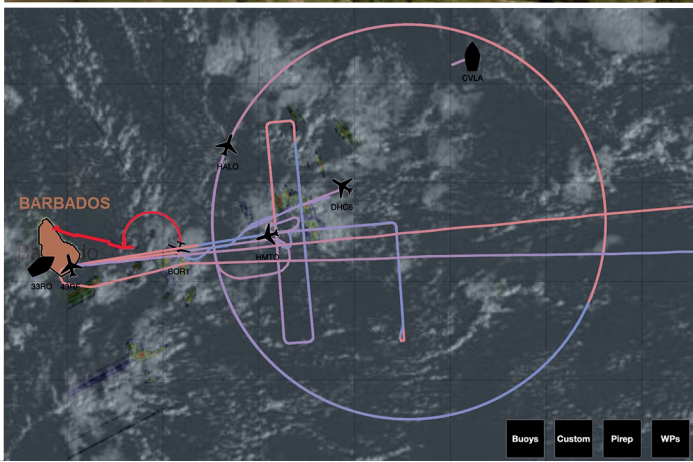
- tethered balloon, UAVs and RS operations,
- 2 cloud radars, 3 MWR, aerosol and wind lidars and 3 ceilometers,
- aerosol shelter, cloud microphysics, 9 surface met. stations, 10m and 50m masts and 40m watchtower



SOFOG3D experimental strategy : the 3 nested domains in the Southwest of France and the locations of the 9 instrumented sites on the super-site.

NEPHELAE - EUREC4A operations with lightweight Skywalker X6 UAS equipped with cloud, temperature and relative humidity sensors (left). A view of the trade wind cumuli during the field campaign (right). The Boréal UAS instrumented for measurements of ocean-atmosphere exchanges (left) and the trajectories of coordinated research aircraft flights during EUREC4A (right).

6



## EURECA, much closer to the cumulus of trade winds

The SAFIRE airborne research infrastructure, shared by Météo-France, CNRS and Cnes, was one of the pillars of the observation system of EURECA. This European project, initiated by researchers from the CNRS in France and the Max-Planck Institut in Germany, aims to better understand the functioning of trade winds and mid-scale oceanic eddies. These determining elements for the climate were therefore explored in detail from the island of Barbados by Météo-France ATR42 operated by SAFIRE, between January 26 and February 14, 2020. The experimental set-up of the project also included the German HALO aircraft, CNRM drones, plus French and German oceanographic vessels. American ship and plane, as well as an English plane joined the device because of the major interest of the research subject.

The SAFIRE ATR42 reached the Caribbean by taking the route of the Aéropostale pioneers: piloting the especially prepared plane, the crew joined Barbados in five flights, including one of 8 hours to cross the South Atlantic from Cape Verde to Brazil. Therefore at Bridgetown airport, the Safire experts had to apply a very unusual procedure by integrating back into the plane the many items of equipment that were transported by air or sea freight, to make the plane as light as possible.

Despite the unusual and difficult working conditions for the SAFIRE team, the scientific data is there, to the satisfaction of the project managers.

7

## SCARBO, an airborne demonstration of a new greenhouse gases detection technique for future space missions

SAFIRE (Research Infrastructure of CNRS, Météo-France and Cnes) have been involved with their Falcon 20 in a key milestone of the SCARBO project, its demonstration airborne campaign. The Horizon 2020 project SCARBO (Space CARBon Observatory) is implemented by a consortium of 10 European organisations led by Airbus Defence and Space. It aims at solving a key challenge of anthropogenic greenhouse gases (GHGs) monitoring from space: improve the temporal revisit over the various sites of interest while meeting the accuracy and spatial resolution requirements (as per the EU guidelines on anthropogenic GHGs monitoring).

The main objectives of the airborne campaign were to perform a proof of concept of the NanoCarb miniaturised prototype sensor - raising it from a technology concept (TRL2) to a validated technology in relevant environment (TRL5) - and to demonstrate, for the very first time, the improved aerosol correction for Green House Gas retrievals using real measurements.

In order to reach these objectives, two sensors have been installed on the SAFIRE Falcon 20:

- The NanoCarb airborne prototype, co-developed by the University of Grenoble and ONERA, for the monitoring of CO<sub>2</sub> plumes,
- SPEXairborne (Spectro-polarimeter for Planetary EXploration), co-developed by Airbus-NL and SRON for aerosol measurements. With co-located Spectrometer and Multi-Angle

Polarimeter measurements, the airborne campaign has been the first combined CO<sub>2</sub> and aerosol airborne remote sensing experiment. The SAFIRE Falcon 20 has performed different flights with the objective to monitor of strong CO<sub>2</sub> emitters over Poland and the monitoring of high aerosol loading (Aeronet stations) over Italy and Spain. Other flights over TCCON stations were originally scheduled for validation as well as flights over calibration scenes to support NanoCarb measurements. Due to the COVID-19 pandemic the demonstration campaign originally planned in May 2020 was finally performed during an alternative time slot in October. The flight conditions were not as good as initially expected and had an impact on the selection of the flight targets and on the exploitation of the measurements. Others flights will have to be organised later to get conclusive measurements and to confirm a significant scientific breakthrough with a direct benefit for future satellite GHG space-borne missions.

### ACKNOWLEDGEMENTS

The SCARBO project has received funding from the European Union's H2020 research and innovation program under grant agreement No 769032, <http://scarbo-h2020.eu>.

8

## A Proven it architecture for the MAP-IO programme

LACy's ambition is to make the MAP-IO (Marion Dufresne Atmospheric Program - Indian Ocean) programme sustainable by turning the ship into a real mobile laboratory.

MAP-IO's IT had to take up real challenges to meet the difficult constraints of harsh marine conditions and the limitations of the network link.

The ship is subject to vibrations from its engines and storms where 10m high waves cause violent shocks from which the instruments and computers must be protected.

Two high-availability servers are installed in the centre of the ship where movements are less abrupt. Their resistance to accelerations of several Gs is guaranteed by the manufacturer. The acquisition PCs are "hardened". They are installed in the "weather" room where the mechanical constraints are more intense and are fixed on a damping table designed by LACy. As the humidity, temperature and salinity in this room are not constant, these PCs can

withstand wide variations in temperature or humidity and their casings are made of aluminium.

All connections are interlocked to prevent cable detachment in heavy seas.

The (very expensive) bandwidth granted to MAP-IO by the shipowner is 50 Mb per day.

MAP-IO concentrators analyse the data and select the data to be transmitted in real time. The others are retrieved during stopovers.

A great deal of work has been done to adapt the acquisition software to autonomous operation. The data is monitored and the system already offers FTP accounts to the PIs.

These first months of operation have enabled the validation of the system set up.

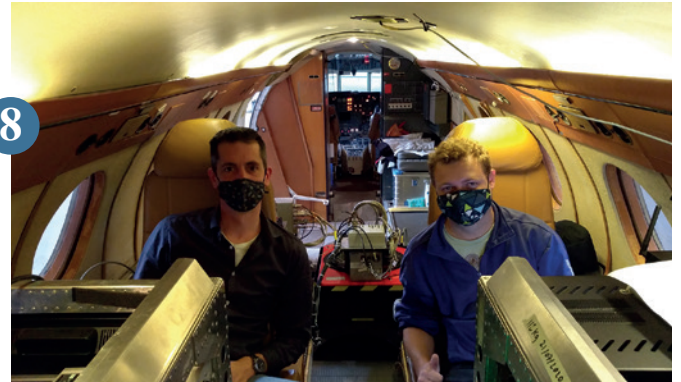
9



7

Back to hangar at sunset for the ATR42 of SAFIRE (JC Canonici)

Part of the SRON team onboard of SAFIRE Falcon 20 with SPEXairborne and NanoCarb instruments behind.  
Credits : SRON



8



9



stationMeteo.jpg: Vaisala weather station  
antenna\_GPS.jpg: Alloy GPS antenna, grease-protected  
tableAmortissange.jpg: cushioning table for the weather room

# Research and aeronautics

---

Météo-France is deeply involved in the meteorological component of the SESAR European program, which is aiming at modernising the European system for air traffic management.

After the research work carried out in 2019, which led to the operational provision to forecasters of a new index derived from ARPEGE deterministic forecasts for the diagnostic of turbulence undergone by planes, a study completed in 2020 demonstrated the added value when using ARPEGE ensemble forecasts to estimate turbulence risk. Moreover, another activity focused on reduced visibility, another weather-related hazard with great impact on air traffic, and its forecast based on the post-processing of AROME model outputs using Machine Learning methods.

In another area, the SAFIRE Research Infrastructure, which is operating the French national float of research planes, enabled in 2020 the evaluation and the qualification of the new Global Aeronautical Distress and Safety System (GADSS), showing the importance of these airborne means, not only for the activities of the research community, but also for the developments to improve air safety.

---

## HELIOS, test flights to improve aviation safety

The Safire Falcon 20 (Research Infrastructure of CNRS, Météo-France and Cnes) was used in late 2020 to demonstrate and qualify to demonstrate and qualify capabilities of the GADSS global aircraft safety program's end-to-end Emergency Locator Transmitter Distress Tracking (ELT-DT) system. This major European initiative was carried out with the financial support of the European GNSS Agency (GSA) in the framework of the H2020 Helios project, bringing together several industrial partners (Orolia, Air France, Airbus, etc.) and Cnes. The European GNSS Agency is the European Union agency responsible for managing the operations, security and service provision for the European Global Navigation Satellite Systems (GNSS), Galileo and EGNOS. It will soon become the European Union Space Programme Agency (EUSPA).

This was the first opportunity to evaluate a system-level implementation of the new Global Aviation Distress Safety System (GADSS), in particular its Autonomous Distress Tracking (ADT) component. The installation on board the Falcon 20 of a new type of distress beacon (Emergency Locator Transmitter Distress Tracking, ELT-DT) developed by Orolia allowed these tests to be carried out in real conditions, with the support of the Spanish and French Air Traffic Services, the Spanish and French Mission Control Centres, the Spanish and French Rescue Coordination Centres, as well as two major European Airline Operations Centres. Safire's Falcon 20 followed a trajectory through Spain and France, and the activation of the beacon was carried out according to a well-prepared scenario, in order to simulate a real activation of an aircraft in distress. The robustness of the alert and

location transmission, involving the Sarsat MEOSAR Cospas satellite constellation, as well as the performance of the reception and ground distribution, were confirmed - even with extreme aircraft attitudes. These tests also provided the opportunity to review some organizational and process aspects, in particular the insertion of the Distress Tracking process into the general aircraft alert management process, including communication between Air Traffic Service Units, Rescue Coordination Centres, and Airlines Operations Centres in France and Spain.

SAFIRE has thus participated in the improvement of air safety, by testing and validating the requirements of the GADSS programme for autonomous distress location, which will be required for new commercial aircraft to be built after January 2023.

---

## Use of the PEARP ensemble forecast for the prediction of aeronautical turbulence

A new diagnostic of EDR which forecasts turbulence suffered by planes has been available for forecasters and airlines since July 2019. This diagnostic is computed by the global model ARPEGE with a deterministic setup. During the internship of three engineer students from ENM, we could evaluate how ARPEGE ensemble forecasts may improve altitude turbulence forecast.

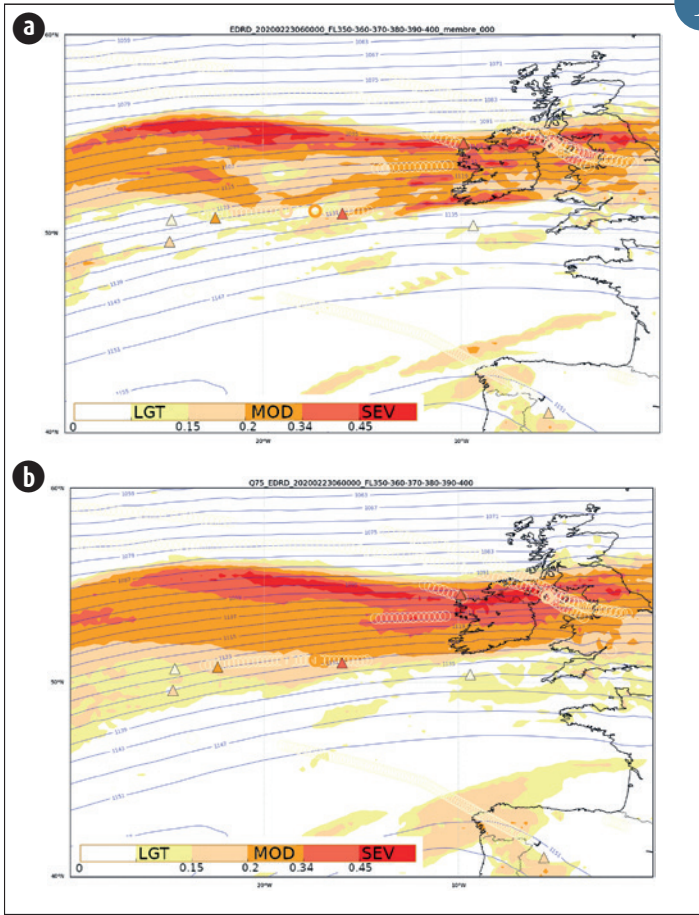
Although horizontal resolution is lower than the deterministic version, small differences between the 35 members provide added

value as early as 12h forecasting lead time. Thanks to 60 000 in-situ measurements of EDR performed by airliners during the second semester 2019, we have shown that moderate or severe turbulence detection (1 % of cases) is improved by 8 % compared to the deterministic version by using ensemble, without degrading the false alarm rate. As usual regarding rare events, cases of turbulence predicted with a high probability are too rarely detected in the observations: the reliability is low.

Some case studies have shown that statistics about ensemble, like quantiles for example, would help aeronautical forecasters. A decision matrix has been developed in order to help users, comparing risks versus associated probability.

1

1



EDR provided by the controlling member of ensemble (a) and value of quantile 75 (b). Triangles (resp. bold circles) represent pilot reports (resp. auto EDR). Maximum values taken in the vertical range FL350/450. The predicted and observed EDR values are shown with the color palette. Situation from 23/02/2020 at 06h simulated with the 00h run.

## Using random forests techniques to forecast visibility with AROME

Predicting visibility reduction phenomena is a major issue for the aviation operations. In order to meet the needs of this industry, Météo-France continues a research effort on improving the quality of NWP visibility forecasts.

The aim of this study is to explore the potential of supervised machine learning techniques such as “random forests” to forecast visibility by post-processing model outputs. The learning step is based on the visibility observations of the french RADOME network and uses several parameters of the regional model AROME as predictors. Two approaches are compared: a 2D approach using only weather ground level predictors, and a 3D approach using predictors from different vertical levels of the atmosphere.

The scores obtained for winter 2019-2020 show gains in detection of low visibility events of + 10% to + 15% for the 2D and 3D approaches, compared to the existing visibility diagnostics at Météo-France. We also note an over-performance for the 3D approach. The case studies show a good behavior of the new diagnosis (Figure - fog situation over Western Europe January 2021).

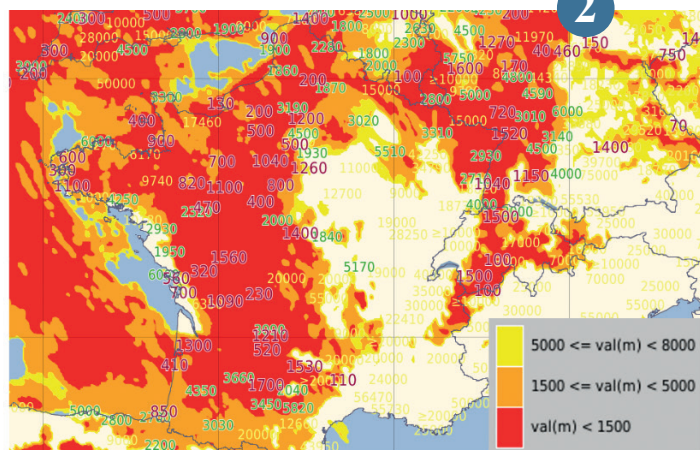
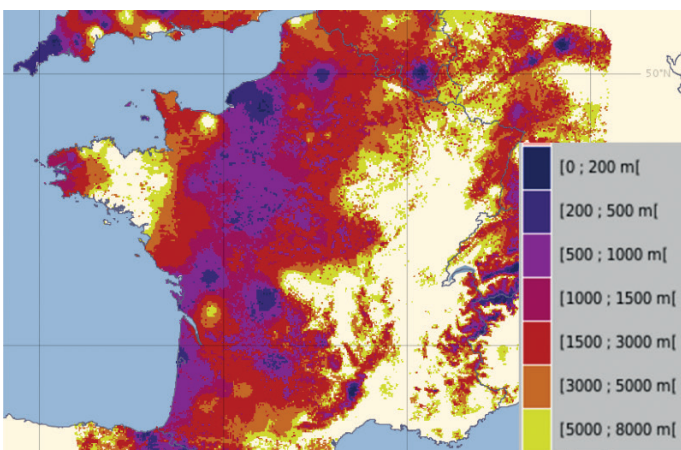
Moving towards an operational application is the next step. The use of the 2D approach is currently being validated by forecasters. The 3D approach requires additional research actions to optimize the inclusion of vertical information: the use of neural networks is being considered.

2

Low visibility situation over western Europe on January 27, 2021 at 9UTC.

Left figure - Satellite + Radar + Surface visibility fusion - Météo France product CERVUS. Right figure - Color ranges: Visibility diagnosis with machine random forest technique (2D approach) based on AROME NWP model - run 00UTC. Numerical values: visibility observations from RADOME, SYNOP and SOLOMM networks

(red: <1600 m, green: [1600 - 6000 m], yellow: > 6000 m.



# Appendix

## 2020 Scientific papers list

- Abeig, B., Morin, S., Demiroglu O., C., François, H., Rothleitner, M. and Strasser, U.: "Overloaded! Critical revision and a new conceptual approach for snow indicators in ski tourism," *Int. J. Biometeorol.*, 2020.
- Adebiyi, A. A., Kok, J. F., Wang, Y., Ito, A., Ridley, D. A., Nabat, P. and Zhao, C.: "Dust Constraints from joint Observational-Modelling-experiMental analysis (DustCOMM): comparison with measurements and model simulations," *Atmos. Chem. Phys.* (20:2), 2020, pp. 829-863.
- Albergel, C., Zheng, Y., Bonan, B., Dutra, E., Rodriguez-Fernandez, N., Munier, S., Draper, C., de Rosnay, P., Muñoz-Sabater, J., Balsamo, G., Fairbairn, D., Meurey, C. and Calvet, J.-C.: "Data assimilation for continuous global assessment of severe conditions over terrestrial surfaces," *Hydrol. Earth Syst. Sci.* (24:9), 2020, pp. 4291-4316.
- Alkama, R., Taylor, P. C., Martin, L. G.-S., Douville, H., Duveiller, G., Forzieri, G., Swingedouw, D. and Cescatti, A.: "Clouds damp the radiative impacts of polar sea ice loss," *The Cryosphere* (14:8), 2020, pp. 2673-2686.
- Allan, R. P., Barlow, M., Byrne, M. P., Cherchi, A., Douville, H., Fowler, H. J., Gan, T. Y., Pendergrass, A. G., Rosenfeld, D., Swann, A. L. S., Wilcox, L. J. and Zolina, O.: "Advances in understanding large-scale responses of the water cycle to climate change," *Ann. N.Y. Acad. Sci.* (1472:1), 2020, pp. 49-75.
- Allen, R. J., Turnock, S., Nabat, P., Neubauer, D., Lohmann, U., Olivieri, D., Oshima, N., Michou, M., Wu, T., Zhang, J., Takemura, T., Schulz, M., Tsigaridis, K., Bauer, S. E., Emmons, L., Horowitz, L., Naik, V., van Noije, T., Bergman, T., Lamarque, J.-F., Zanis, P., Tegen, I., Westervelt, D. M., Sager, P. L., Good, P., Shim, S., O'Connor, F., Akritidis, D., Georgoulias, A. K., Deushi, M., Sentman, L. T., John, J. G., Fujimori, S. and Collins, W. J.: "Climate and air quality impacts due to mitigation of non-methane near-term climate forcers," *Atmos. Chem. Phys.* (20:16), 2020, pp. 9641-9663.
- Amiri-Farhany, A., Allen, R. J., Li, K.-F., Nabat, P. and Westervelt, D. M.: "A La Niña-Like Climate Response to South African Biomass Burning Aerosol in CESM Simulations," *Journal of Geophysical Research: Atmospheres* (125:6), 2020.
- Amraoui, L. E., Sic, B., Piacentini, A., Marécal, V., Frebourg, N. and Attié, J.-L.: "Aerosol data assimilation in the MOCAGE chemical transport model during the TRAQA/ChArMEx campaign: lidar observations," *Atmos. Meas. Tech.* (13:9), 2020, pp. 4645-4667.
- Andersen, J. K., Andreassen, L. M., Baker, E. H., Ballinger, T. J., Berner, L. T., Bernhard, G. H., Bhatt, U. S., Bjerke, J. W., Box, J. E., Britt, L., Brown, R., Burgess, D., Cappelen, J., Christiansen, H. H., Decharme, B., Derksen, C., Drozdov, D. S., Epstein, H. E., Farquharson, L. M., Farrell, S. L., Fausto, R. S., Fettweis, X., Fioletov, V. E., Forbes, B. C., Frost, G. V., Gerland, S., Goetz, S. J., Grooßs, J.-U., Hanna, E., Hanssen-Bauer, I., Hendricks, S., Ialongo, I., Isaksen, K., Johnsen, B., Kaleschke, L., Kholodov, A. L., Kim, S.-J., Kohler, J., Labe, Z., Ladd, C., Lakkala, K., Lara, M. J., Loomis, B., Luks, B., Luoju, K., Macander, M. J., Malkova, G. V., Mankoff, K. D., Manney, G. L., Marsh, J. M., Meier, W., Moon, T. A., Mote, T., Mudryk, L., Mueter, F. J., Müller, R., Nyland, K. E., O'Neel, S., Overland, J. E., Perovich, D., Phoenix, G. K., Reynolds, M. K., Reijmer, C. H., Ricker, R., Romanovsky, V. E., Schuur, E. A. G., Sharp, M., Shiklomanov, N. I., Smeets, C. J. P. P., Smith, S. L., Streletskiy, D. A., Tedesco, M., Thoman, R. L., Thorson, J. T., Tian-Kunze, X., Timmermans, M.-L., Tømmervik, H., Tschudi, M., van As, D., van de Wal, R. S. W., Walker, D. A., Walsh, J. E., Wang, M., Webster, M., Winton, Ø., Wolken, G. J., Wood, K., Wouters, B. and Zador, S.: "The Arctic," *Bull. Amer. Meteor. Soc.* (101:8), 2020, pp. S239-S286.
- Andresen, C. G., Lawrence, D. M., Wilson, C. J., McGuire, A. D., Koven, C., Schaefer, K., Jafarov, E., Peng, S., Chen, X., Gouttevin, I., Burke, E., Chadburn, S., Ji, D., Chen, G., Hayes, D. and Zhang, W.: "Soil Moisture and Hydrology Projections of the Permafrost Region: A Model Intercomparison," *The Cryosphere* (14), 2020, pp. 445-459.
- Aouade, G., L. Jarlan, J. Ezzahar, S. Er-Raki, A. Napoly, A. Benkaddour, S. Khabba, G. Boulet, S. Garrigues, A. Chehbouni, A. Boone: 2020: "Evapotranspiration partition using the multiple energy balance version of the ISBA-A-gs land surface model within the SURFEX platform v8.1 over two irrigated crops in a semi-arid Mediterranean region (Marrakech, Morocco)" *Hydrol. Earth Syst. Sci.*, 24, 3789-3814
- Aouf L., D. Hauser, B. Chapron, A. Toffoli, C. Tourrain, C. Peureux: "New directional wave satellite observations: Towards improved-waveforecasts and climate description in Southern Ocean", *Geophysical Research Letters*, 10.1029/2020GL091187
- Ardilouze, C., Materia, S., Batté, L., Benassi, M. and Prodhomme, C.: "Precipitation response to extreme soil moisture conditions over the Mediterranean," *Climate Dyn.*, 2020.
- Arora, V. K., Katavouta, A., Williams, R. G., Jones, C. D., Brovkin, V., Friedlingstein, P., Schwinger, J., Bopp, L., Boucher, O., Cadule, P., Chamberlain, M. A., Christian, J. R., Delire, C., Fisher, R. A., Hajima, T., Ilyina, T., Joetzjer, E., Kawamiya, M., Koven, C. D., Krasting, J. P., Law, R. M., Lawrence, D. M., Lenton, A., Lindsay, K., Pongratz, J., Raddatz, T., Séférian, R., Tachiiri, K., Tjiputra, J. F., Wiltshire, A., Wu, T. and Ziehn, T.: "Carbon concentration and carbon climate feedbacks in CMIP6 models and their comparison to CMIP5 models," *Biogeosciences* (17:16), 2020, pp. 4173-4222.
- Audouin, O., Roehrig, R., Couvreur, F. and Williamson, D.: "Modeling the GABLS4 strongly-stable boundary layer with a GCM turbulence parameterization: parametric sensitivity or intrinsic limits?," *J. Adv. Model. Earth Syst.*, 2020.
- Auguste, F., Lac, C., Masson, V. and Cariolle, D.: "Large-Eddy Simulations with an Immersed Boundary Method: Pollutant Dispersion over Urban Terrain," *Atmosphere* (11:1), 2020, pp. 113.
- Baklanov, A., Cardenas, B., Lee, T.-c., Leroyer, S., Masson, V., Molina, L. T., Müller, T., Ren, C., Vogel, F. R. and Voogt, J. A.: "Integrated urban services: Experience from four cities on different continents," *Urban Clim.* (32), 2020, pp. 100610.
- Baray J.-L., Deguillaume L., Colomb A., Sellegrì K., Freney E. et al.: "Cézeaux-Aulnat-Opme-Puy De Dôme: a multi-site for the long-term survey of the tropospheric composition and climate change", *Atmospheric Measurement Techniques*, 2020, 13 (6), pp.3413-3445. 10.5194/amt-13-3413-2020
- Batté, L., Välisuo, I., Chevallier, M., Navarro, J. C. A., Ortega, P. and Smith, D.: "Summer predictions of Arctic sea ice edge in multi-model seasonal re-forecasts," *Climate Dyn.* (54:11-12), 2020, pp. 5013-5029.
- Bègue N., Shikwambana L., Bencherif H., Pallotta J., Sivakumar V. et al.: "Statistical analysis of the long-range transport of the 2015 Calbuco volcanic plume from ground-based and space-borne observations", *Annales Geophysicae*, 2020, 38 (2), pp.395 - 420. 10.5194/angeo-38-395-2020
- Bélaïr, S. and Boone, A. : « La représentation des surfaces continentales pour la prévision numérique du temps », *La Météorologie* (:108), 2020, pp. 059.
- Belke-Brea, M., Domine, F., Barrere, M., Picard, G., & Arnaud, L. (2020): "Impact of Shrubs on Winter Surface Albedo and Snow Specific Surface Area at a Low Arctic Site: In Situ Measurements and Simulations", *Journal of Climate*, 33(2), 597-609. Retrieved May 26, 2021, from <https://journals.ametsoc.org/view/journals/clim/33/2/jcli-d-19-0318.1.xml>



- Belke-Brea, M., Domine, F., Boudreau, S., Picard, G., Barrere, M., Arnaud, L., & Paradis, M. (2020). "New Allometric Equations for Arctic Shrubs and Their Application for Calculating the Albedo of Surfaces with Snow and Protruding Branches", *Journal of Hydrometeorology*, 21(11), 2581-2594. Retrieved May 26, 2021, from <https://journals.ametsoc.org/view/journals/hydr/21/11/jhm-d-20-0012.1.xml>
- Bencherif H., Bègue N., Kirsch Pinheiro D., Du Preez D., Cadet J.-M. Et al.: "Investigating the Long-Range Transport of Aerosol Plumes Following the Amazon Fires (August 2019): A Multi-Instrumental Approach from Ground-Based and Satellite Observations", *Remote Sensing*, 2020, *Advances in Remote Sensing of Biomass Burning*, 12 (22), pp.3846. 10.3390/rs12223846
- Bencherif H., Tohir A., Mbatha N., Sivakumar V., Du Preez D., Bègue N., Coetzee G.: "Ozone Variability and Trend Estimates from 20-Years of Ground-Based and Satellite Observations at Irene Station, South Africa", *Atmosphere*, 2020, *Tropospheric Ozone Observations*, 11, 10.3390/atmos11111216
- Berard-Chenu, L., Cognard, J., François, H., Morin, S. and George, E.: "Do changes in snow conditions have an impact on snowmaking investments in French Alps ski resorts?," *Int. J. Biometeorol.*, 2020.
- Bergot, T., Bessemoulin, P. and Sarraz, C. : « Apport des campagnes de mesures pour la compréhension des interactions sol-végétation-atmosphère », *La Météorologie* (:108), 2020, pp. 046.
- Bigeard, G., Arteta, J. and Plu, M.: "Improving the Representation of Agricultural Ammonia Emissions for a Better Air Quality Forecasting Over France: A Simple Model to Estimate Fertilization Dates from Meteorological Constraints" *IGARSS 2019 - 2019 IEEE International Geoscience and Remote Sensing Symposium*, IEEE, 2020.
- Bigeard, G., Sic, B., Amraoui, L. E. and Plu, M.: "Monitoring Volcanic ASH with the Chemistry-Transport Model Mocage: Improvements of Source Term and Assimilation of Observations" *IGARSS 2019 - 2019 IEEE International Geoscience and Remote Sensing Symposium*, IEEE, 2020.
- Bleischmidt, A.-M., Arteta, J., Coman, A., Curier, L., Eskes, H., Foret, G., Gielen, C., Hendrick, F., Maréchal, V., Meleux, F., Parmentier, J., Peters, E., Pinardi, G., Piters, A. J. M., Plu, M., Richter, A., Segers, A., Sofiev, M., Valdebenito, A. M., Roozendael, M. V., Vira, J., Vlemmix, T. and Burrows, J. P.: "Comparison of tropospheric NO<sub>2</sub> columns from MAX-DOAS retrievals and regional air quality model simulations," *Atmos. Chem. Phys.* (20:5), 2020, pp. 2795-2823.
- Blein, S., Roehrig, R., Voldoire, A. and Faure, G.: "Meso-scale contribution to airsea turbulent fluxes at GCM scale," *Quart. J. Roy. Meteor. Soc.* (146:730), 2020, pp. 2466-2495.
- Blockley, E., Vancoppenolle, M., Hunke, E., Bitz, C., Feltham, D., Lemieux, J., Losch, M., Maisonnave, E., Notz, D., Rampal, P., Tietsche, S., Tremblay, B., Turner, A., Massonnet, F., Ólason, E., Roberts, A., Aksenov, Y., Fichefet, T., Garric, G., Iovino, D., Madec, G., Rousset, C., Salas y Melia, D., & Schroeder, D. (2020). "The Future of Sea Ice Modeling: Where Do We Go from Here?," *Bulletin of the American Meteorological Society*, 101(8), E1304-E1311.
- Boé, J., Somot, S., Corre, L. and Nabat, P.: "Large discrepancies in summer climate change over Europe as projected by global and regional climate models: causes and consequences," *Climate Dyn.*, 2020.
- Bogning, S., Frappart, F., Paris, A., Blarel, F., Niño, F., Saux Picart, S., Lanet, P., Seyler, F., Mahé, G., Onguene, R., Bricquet, J.-P., Etame, J., Paiz, M.-C. and Braun, J.-J.: "Hydro-climatology study of the Ogooué River basin using hydrological modeling and satellite altimetry," *Adv. Space Res.*, 2020.
- Bolibar, J., Rabatel, A., Gouttevin, I. and Galiez, C.: "A deep learning reconstruction of mass balance series for all glaciers in the French Alps: 1967–2015," *Earth Syst. Sci. Data* (12), 2020, pp. 1973-1983.
- Bolibar, J., Rabatel, A., Gouttevin, I., Galiez, C., Condom, T. and Sauquet, E.: "Deep learning applied to glacier evolution modelling," *The Cryosphere* (14), 2020, pp. 565-584.
- Bonan, B., Albergel, C., Zheng, Y., Barbu, A. L., Fairbairn, D., Munier, S. and Calvet, J.-C.: "An ensemble square root filter for the joint assimilation of surface soil moisture and leaf area index within the Land Data Assimilation System LDAS-Monde: application over the Euro-Mediterranean region," *Hydrol. Earth Syst. Sci.* (24:1), 2020, pp. 325-347.
- Bordoais, L., Nycander, J. and Paci, A.: "Computation of Density Perturbation and Energy Flux of Internal Waves from Experimental Data," *Fluids*, 2020.
- Boucher, O., Servonnat, J., Albright, A. L., Aumont, O., Balkanski, Y., Bastrikov, V., ...Rio, C, ... & Vuichard, N.: "Presentation and evaluation of the IPSL-CM6A-LR climate model", *Journal of Advances in Modeling Earth Systems*, 12(7), 2020.
- Bouin, M.-N. and Brossier, C. L.: "Impact of a medicane on the oceanic surface layer from a coupled, kilometre-scale simulation," *Ocean Sci.* (16:5), 2020, pp. 1125-1142.
- Bouin, M.-N. and Lebeau-pin Brossier, C.: "Surface processes in the 7 November 2014 medicane from air-sea coupled high-resolution numerical modelling," *Atmos. Chem. Phys.* (20), 2020, pp. 6861-6881.
- Bourdier a., Diels J.-C., Delage O.: "Calculation of the refractive index for plane waves propagating in ionized gas", *Results in Physics*, 2020, 18, pp.103250. 10.1016/j.rinp.2020.103250
- Bousquet O., Barbary D., Bielli S., Kébir S., Raynaud L., Malardel S., Faure G.: "An evaluation of tropical cyclone forecast in the Southwest Indian Ocean basin with AROME-Indian Ocean convection-permitting numerical weather predicting system", *Atmospheric Science Letters*, 2020, 21 (3), pp.e950. 10.1002/asl.950
- Bousquet O., Lees E., Durand J., Peltier A., Duret A., et al.: "Densification of the Ground-Based GNSS Observation Network in the Southwest Indian Ocean: Current Status, Perspectives, and Examples of Applications in Meteorology and Geodesy", *Frontiers in Earth Science*, 2020, 8, pp.566105. 10.3389/feart.2020.566105
- Bouttier, F. and Marchal, H.: "Probabilistic thunderstorm forecasting by blending multiple ensembles," *Tellus A: Dynamic Meteorology and Oceanography* (72:1), 2020, pp. 1-19.
- Boysen, L. R., Brovkin, V., Pongratz, J., Lawrence, D. M., Lawrence, P., Vuichard, N., Peylin, P., Liddicoat, S., Hajima, T., Zhang, Y., Rocher, M., Delire, C., Séférian, R., Arora, V. K., Nieradzki, L., Anthoni, P., Thiery, W., Laguë, M. M., Lawrence, D. and Lo, M.-H.: "Global climate response to idealized deforestation in CMIP6 models," *Biogeosciences* (17:22), 2020, pp. 5615-5638.
- Braud I., Chaffard V., Coussot C., Galle S., Juen P. et al.: "Building the information system of the French Critical Zone Observatories network: Theia/OZCAR-IS", *Hydrological Sciences Journal, In press*, pp.1-19. 10.1080/02626667.2020.1764568
- Brilouet, P.-E., Durand, P., Canut, G. and Fourrié, N.: "Organized Turbulence in a Cold-Air Outbreak: Evaluating a Large-Eddy Simulation with Respect to Airborne Measurements," *Boundary Layer Meteorol.* (175:1), 2020, pp. 57-91.
- Bromwich, D. H., Werner, K., Casati, B., Powers, J. G., Gorodetskaya, I. V., Massonnet, F., Vitale, V., Heinrich, V. J., Liggett, D., Arndt, S., Barja, B., Bazile, E., Carpentier, S., Carrasco, J. F., Choi, T., Choi, Y., Colwell, S. R., Cordero, R. R., Gervasi, M., Haiden, T., Hirasawa, N., Inoue, J., Jung, T., Kalesse, H., Kim, S.-J., Lazzara, M. A., Manning, K. W., Norris, K., Park, S.-J., Reid, P., Rigor, I., Rowe, P. M., Schmithüsen, H., Seifert, P., Sun, Q., Uttal, T., Zannoni, M. and Zou, X.: "The Year of Polar Prediction in the Southern Hemisphere (YOPP-SH)," *Bull. Amer. Meteor. Soc.* (101:10), 2020, pp. E1653-E1676.
- Brumer, S. E., Garnier, V., Redelsperger, J.-L., Bouin, M.-N., Arduin, F. and Accensi, M.: "Impacts of surface gravity waves on a tidal front: A coupled model perspective," *Ocean Modell.* (154), 2020, pp. 101677.
- Brunner, L., McSweeney, C., Ballinger, A. P., Befort, D. J., Benassi, M., Booth, B., Coppola, E., de Vries, H., Harris, G., Hegerl, G. C., Knutti, R., Lenderink, G., Lowe, J., Nogherotto, R., O'Reilly, C., Qasmi, S., Ribes, A., Stocchi, P. and Undorf, S.: "Comparing Methods to Constrain Future European Climate Projections Using a Consistent Framework," *J. Climate* (33:20), 2020, pp. 8671-8692.
- Cadet J.-M., Bencherif H., Cadet N., Lamy K., Portafaix T. et al.: "Solar UV Radiation in the Tropics: Human Exposure at Reunion Island (21° S, 55° E) during Summer Outdoor Activities" *International Journal of Environmental Research and Public Health*, 2020, 17 (21), 10.3390/ijerph17218105
- Cadet J.-M., Portafaix T., Bencherif H., Lamy K., Brogniez C. et al.: "Inter-Comparison Campaign of Solar UVR Instruments under Clear Sky Conditions at Reunion Island (21 • S, 55 • E)", *International Journal of Environmental Research and Public Health*, 2020, 17 (8), pp.2867. 10.3390/ijerph17082867
- Calonne, N., Richter, B., Löwe, H., Cetti, C., ter Schure, J., Herwijnen, A. V., Fierz, C., Jaggi, M. and Schneebeli, M.: "The RHOSSA campaign: multi-resolution monitoring of the seasonal evolution of the structure and mechanical stability of an alpine snowpack," *The Cryosphere* (14:6), 2020, pp. 1829-1848.
- Calvet, J.-C. and Champeaux, J.-L. : « L'apport de la télédétection spatiale à la modélisation des surfaces continentales », *La Météorologie* (:108), 2020, pp. 052.
- Cappelaere, B., Feurer, D., Vischel, T., Ottlé, C., Issoufou, H., Saux Picart, S., Mainassara, I., Oi, M.,

- Chazarin, J.-P., Barral, H., Coudert, B. & Demarty, J.: "Modeling land surface fluxes from uncertain rainfall: a case study in the Sahel with field-driven stochastic rainfields", *Atmosphere* 2020, 11(5), 465; <https://doi.org/10.3390/atmos11050465>
- Cattiaux, J., F. Chauvin, O. Bousquet, S. Malardel and C.-L. Tsai (2020): "Projected changes in the Southern Indian Ocean cyclone activity assessed from high-resolution experiments and CMIP5 models", *Journal of Climate*, 33 (12), 4975–4991. doi:10.1175/JCLI-D-19-0591.1
- Charles, E., Meyssignac, B. and Ribes, A.: "Observational Constraint on Greenhouse Gas and Aerosol Contributions to Global Ocean Heat Content Changes," *J. Climate* (33:24), 2020, pp. 10579-10591.
- Cimini, D., Haeffelin, M., Kotthaus, S., Löhnert, U., Martinet, P., O'Connor, E., Walden, C., Collaud-Coen, M. and Preissler, J.: "Towards the profiling of the atmospheric boundary layer at European scale—introducing the COST Action PROBE.," *Bulletin of Atmospheric Science and Technology*, 2020.
- Cluzet, B., Revuelto, J., Lafaysse, M., Tuzet, F., Cosme, E., Picard, G., Arnaud, L. and Dumont, M.: "Towards the assimilation of satellite reflectance into semi-distributed ensemble snowpack simulations," *Cold Reg. Sci. Technol.* (170), 2020, pp. 102918.
- Coopmann, O., Guidard, V., Fourrié, N. and Josse, B.: "Use of variable ozone in a radiative transfer model for the global Météo-France 4D-Var system," *Quart. J. Roy. Meteor. Soc.*, 2020.
- Coopmann, O., Guidard, V., Fourrié, N., Josse, B. and Marécal, V.: "Update of Infrared Atmospheric Sounding Interferometer (IASI) channel selection with correlated observation errors for numerical weather prediction (NWP)," *Atmos. Meas. Tech.* (13:5), 2020, pp. 2659-2680.
- Coppola, E., Nogherotto, R., Ciarlo, J. M., Giorgi, F., Meijgaard, E., Kadygrov, N., Iles, C., Corre, L., Sandstad, M., Somot, S., Nabat, P., Vautard, R., Levvasseur, G., Schwingshackl, C., Sillmann, J., Kjellström, E., Nikulin, G., Aalbers, E., Lenderink, G., Christensen, O. B., Boberg, F., Sørland, S. L., Demory, M.-E., Bülow, K., Teichmann, C., Warrach-Sagi, K. and Wulfmeyer, V.: "Assessment of the European climate projections as simulated by the large EURO-CORDEX regional and global climate model ensemble," *Journal of Geophysical Research: Atmospheres*, 2020.
- Coppola, E., Sobolowski, S., Pichelli, E., Raffaele, F., Ahrens, B., Anders, I., Ban, N., Bastin, S., Belda, M., Belusic, D., Caldas-Alvarez, A., Cardoso, R. M., Davolio, S., Dobler, A., Fernandez, J., Fita, L., Fumiere, Q., Giorgi, F., Goergen, K., Güttler, I., Halenka, T., Heinzeller, D., Hodnebrog, Ø., Jacob, D., Kartsios, S., Katragkou, E., Kendon, E., Khodayar, S., Kunstmann, H., Knist, S., Lavngullon, A., Lind, P., Lorenz, T., Maraun, D., Marelle, L., van Meijgaard, E., Milovac, J., Myhre, G., Panitz, H.-J., Piazza, M., Raffa, M., Raub, T., Rockel, B., Schär, C., Sieck, K., Soares, P. M. M., Somot, S., Srncac, L., Stocchi, P., Tölle, M. H., Truhetz, H., Vautard, R., de Vries, H. and Warrach-Sagi, K.: "A first-of-its-kind multi-model convection permitting ensemble for investigating convective phenomena over Europe and the Mediterranean," *Climate Dyn.*, 2020.
- Coursol, L., Libois, Q., Gauthier, P. and Blanchet, J.-P.: "Optimal Configuration of a Far-Infrared Radiometer to Study the Arctic Winter Atmosphere," *Journal of Geophysical Research: Atmospheres* (125:14), 2020.
- Couvreux, F., Bazile, E., Rodier, Q., Maronga, B., Matheou, G., Chinita, M. J., Edwards, J., van Stratum, B. J. H., van Heerwaarden, C. C., Huang, J., Moene, A. F., Cheng, A., Fuka, V., Basu, S., Bou-Zeid, E., Canut, G. and Vignon, E.: "Intercomparison of Large-Eddy Simulations of the Antarctic Boundary Layer for Very Stable Stratification," *Boundary Layer Meteorol.* (176:3), 2020, pp. 369-400.
- Couvreux, F., Hourdin, F., Williamson, D., Roehrig, R., Volodina, V., Villefranque, N., Rio, C., Audouin1, O., Salter, J., Bazile, E., Briant, F., Favot, F., Honnert, R., Lefebvre, M.-P., Madeleine, J.-B., Rodier, Q. and Xu, W.: "Process-based climate model development harnessing machine learning: I. a calibration tool for parameterization improvement," *J. Adv. Model. Earth Syst.*, 2020.
- Cussac, M., Marécal, V., Thouret, V., Josse, B. and Sauvage, B.: "The impact of biomass burning on upper tropospheric carbon monoxide: a study using MOCAGE global model and IAGOS airborne data," *Atmos. Chem. Phys.* (20:15), 2020, pp. 9393-9417.
- Cuxart, J. and A. Boone, 2020: "Evapotranspiration over land from a Boundary-Layer Meteorology perspective." *Boundary-Layer Meteorology*, doi:10.1007/s10546-020-00550-9
- de Rosnay, P., Muñoz-Sabater, J., Albergel, C., Isaksen, I., English, S., Drusch, M. and Wigneron, J.-P.: "SMOS brightness temperature forward modelling and long term monitoring at ECMWF," *Remote Sens. Environ.* (237), 2020, pp. 111424.
- Decharme, B., Delire, C. and Boone, A. : « La représentation des surfaces continentales dans la modélisation du climat à Météo-France », *La Météorologie* (:108), 2020, pp. 067.
- Delire, C., Séférian R., Decharme B., Alkama R., Calvet J.-C., Carrer D., Gibelin A.-L., Joetzer E., Morel X., Rocher M., Tzanos D.: "The global land carbon cycle simulated with ISBA-CTRIP : improvements over the last decade", *Journal of Advances in Modeling Earth Systems*, 12, <https://doi.org/10.1029/2019MS001886>, 2020.
- Denjean, C., Bourriane, T., Burnet, F., Mallet, M., Maury, N., Colomb, A., Dominutti, P., Brito, J., Dupuy, R., Sellegri, K., Schwarzenboeck, A., Flamant, C. and Knippertz, P.: "Overview of aerosol optical properties over southern West Africa from DACCWA aircraft measurements," *Atmos. Chem. Phys.* (20:8), 2020, pp. 4735-4756.
- Denjean, C., Brito, J., Libois, Q., Mallet, M., Bourriane, T., Burnet, F., Dupuy, R., Flamant, C. and Knippertz, P.: "Unexpected Biomass Burning Aerosol Absorption Enhancement Explained by Black Carbon Mixing State," *Geophys. Res. Lett.* (47:19), 2020.
- Derkani, M. H., A. Alberello, F. Nelli, L. G. Bennetts, K. G. Hessner, K. MacHutchon, K. Reichert, L. Aouf, S. S. Khan, and A. Toffoli: "Wind, waves, and surface currents in the Southern Ocean: Observations from the Antarctic Circumnavigation Expedition." *Earth System Science Data*, 2020, <https://doi.org/10.5194/essd-2020-255>.
- Deschamps-Berger, C., Gascoïn, S., Berthier, E., Deems, J., Gutmann, E., Dehecq, A., Shean, D. and Dumont, M.: "Snow depth mapping from stereo satellite imagery in mountainous terrain: evaluation using airborne laser-scanning data," *The Cryosphere* (14:9), 2020, pp. 2925-2940.
- Destouches, M., Montmerle, T., Michel, Y. and Ménétrier, B.: "Estimating optimal localization for sampled background-error covariances of hydrometeor variables," *Quart. J. Roy. Meteor. Soc.* (147:734), 2020, pp. 74-93.
- Di Girolamo P., de Rosa B., Flamant C., Summa D., Bousquet O., Chazette P., Totems J., Cacciani M.: "Water vapor mixing ratio and temperature inter-comparison results in the framework of the Hydrological Cycle in the Mediterranean Experiment-Special Observation Period 1", *Bulletin of Atmospheric Science and Technology*, 2020, 1, pp.113-153. 10.1007/s42865-020-00008-3
- Di Girolamo, Paolo, and Marie-Noelle Bouin: "Characterization of Complex Water Vapour Field Structures and their Genesis Based on the Combined use of Raman Lidar Measurements and MESO-NH Model Simulations." *EPJ Web of Conferences*. Vol. 237. *EDP Sciences*, 2020.
- Douville, H., Decharme, B., Delire, C., Colin, J., Joetzer, E., Roehrig, R., Saint-Martin, D., Oudar, T., Stchepounoff, R. and Voldoire, A.: "Drivers of the enhanced decline of land near-surface relative humidity to abrupt 4xCO<sub>2</sub> in CNRM-CM6-1," *Climate Dyn.*, 2020.
- Du Preez D. J., Bencherif H., Bègue N., Clarisse L., Hoffman R. et al.: "Investigating the Large-Scale Transport of a Volcanic Plume and the Impact on a Secondary Site", *Atmosphere*, 2020, 11 (5), pp.548. 10.3390/atmos11050548
- Du Preez D., Parisi A., Millar D., Bencherif H., Wright C.: "Comparison of GOME-2 UVA Satellite Data to Ground-Based UVA Measurements in South Africa", *Photochemistry and Photobiology*, 2020, 10.1111/php.13308
- Duongé, L., Lac, C., Vié, B., Bergot, T. and Price, J. D.: "Fog in heterogeneous environments: the relative importance of local and non-local processes on radiative-advective fog formation," *Quart. J. Roy. Meteor. Soc.* (146:731), 2020, pp. 2522-2546.
- Duflot, V., Tulet, P., Flores, O., Barthe, C., Colomb, A., Deguillaume, L., Vaitilingom, M., Perring, A., Huffman, A., Hernandez, M. T., Sellegri, K., Robinson, E., O'Connor D., J., Gomez, O. M., Burnet, F., Bourriane, T., Strasberg, D., Rocco, M., Bertram, A. K., Chazette, P., Totems, J., Fournel, J., Stamenoff, P., Metzger, J.-M., Chabasset, M., Rousseau, C., Bourriane, E., Sancelme, M., Delort, A.-M., Wegener, R. E., Chou, C. and Elizondo, P.: "Preliminary results from the FARCE 2015 campaign: multidisciplinary study of the forest-gas-aerosol-cloud system on the tropical island of La Réunion," *Atmos. Chem. Phys.*, 2020.
- Dumont, M., Tuzet, F., Gascoïn, S., Picard, G., Kutuzov, S., Lafaysse, M., Cluzet, B., Nheili, R. and Painter, T. H.: "Accelerated snow melt in the Russian Caucasus mountains after the Saharan dust outbreak in March 2018," *J. Geophys. Res. Earth Surf.* (125), 2020.
- Emery, C. M., A. Paris, S. Biancamaria, A. Boone, S. Calmant, P.-A. Garambois, J. Santos de Silva and C. David, 2020: "Discharge estimation via assimilation of multi-satellite-based discharge

- products: case study over the Amazon basin." *IEEE Geosci. and Remote Sens. Letters*, doi: 10.1109/LGRS.2020.3020285
- Emery, C. M., Biancamaria, S., Boone, A., Ricci, S., Rochoux, M. C., Pedinotti, V. and David, C. H.: "Assimilation of wide-swath altimetry water elevation anomalies to correct large-scale river routing model parameters," *Hydrol. Earth Syst. Sci.* (24:5), 2020, pp. 2207-2233.
- Erdmann, F., Defer, E., Caumont, O., Blakeslee, R. J., Pédeboy, S. and Coquillat, S.: "Concurrent satellite and ground-based lightning observations from the Optical Lightning Imaging Sensor (ISS-LIS), the low-frequency network Meteorage and the SAETTA Lightning Mapping Array (LMA) in the northwestern Mediterranean region," *Atmos. Meas. Tech.* (13:2), 2020, pp. 853-875.
- Essery, R., H. Kim, L. Wang, P. Bartlett, A. Boone, C. Brutel-Vuilmet, E. Burke, M. Cuntz, B. Decharme, E. Dutra, X. Fang, C. Fierz, Y. Gusev, S. Hagemann, V. Haverd, A. Kontu, G. Krinner, M. Lafaysse, Y. Lejeune, T. Marke, D. Marks, C. Marty, C. Ménard, O. Nasonova, T. Nitta, J. Pomeroy, G. Schadler, V. Semenov, T. Smirnova, S. Swenson, D. Turkov, N. Wever and H. Yuan, 2020: "Snow cover duration trends observed at sites and predicted by multiple models." *The Cryosphere*, 14, 4687-4698. doi:10.5194/tc-14-4687-2020
- Evan S., Brioude J., Rosenlof K., Davis S., Vömel H. et al.: "Effect of deep convection on the tropical tropopause layer composition over the southwest Indian Ocean during austral summer", *Atmospheric Chemistry and Physics*, 2020, 20 (17), pp.10565-10586. 10.5194/acp-20-10565-2020
- Faure, G., Chambon, P. and Brousseau, P.: "Operational Implementation of the AROME Model in the Tropics: Multiscale Validation of Rainfall Forecasts," *Weather Forecasting* (35:2), 2020, pp. 691-710.
- Fiolleau, T., Roca, R., Cloche, S., Bouniol, D. and Raberanto, P.: "Homogenization of Geostationary Infrared Imager Channels for Cold Cloud Studies Using Megha-Tropiques/ScaRaB," *IEEE Transactions on Geoscience and Remote Sensing* (58:9), 2020, pp. 6609-6622.
- Fitzpatrick, R. G. J., Parker, D. J., Marsham, J. H., Rowell, D. P., Guichard, F. M., Taylor, C. M., Cook, K. H., Vizy, E. K., Jackson, L. S., Finney, D., Crook, J., Stratton, R. and Tucker, S.: "What Drives the Intensification of Mesoscale Convective Systems over the West African Sahel under Climate Change?," *J. Climate* (33:8), 2020, pp. 3151-3172.
- Fontaine, E., Schwarzenboeck, A., Leroy, D., Delanoë, J., Protat, A., Dezitter, F., Strapp, J. W. and Lillie, L. E.: "Statistical analysis of ice microphysical properties in tropical mesoscale convective systems derived from cloud radar and in situ microphysical observations," *Atmos. Chem. Phys.* (20:6), 2020, pp. 3503-3553.
- Foucras, M., Zribi, M., Albergel, C., Baghdadi, N., Calvet, J.-C. and Pellarin, T.: "Estimating 500-m Resolution Soil Moisture Using Sentinel-1 and Optical Data Synergy," *Water* (12:3), 2020, pp. 866.
- Fourteau, K., Domine, F., & Hagenmuller, P. (2020): "Macroscopic water vapor diffusion is not enhanced in snow", *The Cryosphere*. In press. <https://doi.org/10.5194/tc-2020-183>, 2020.
- Francon, L., Corona, C., Till-Bottraud, I., Choler, P., Carlson, B. Z., Charrier, G., Améglie, T., Morin, S., Eckert, N., Roussel, E., Lopez-Saez, J. and Stoffel, M.: "Assessing the effects of earlier snow melt-out on alpine shrub growth: The sooner the better?," *Ecol. Indic.* (115), 2020.
- Fréville, H., Chami, M. and Mallet, M.: "Analysis of the Transport of Aerosols over the North Tropical Atlantic Ocean Using Time Series of POLDER/PARASOL Satellite Data," *Remote Sensing* (12:5), 2020, pp. 757.
- Friedlingstein, P., O'Sullivan, M., Jones, M. W., Andrew, R. M., Hauck, J., Olsen, A., Peters, G. P., Peters, W., Pongratz, J., Sitch, S., Le Quéré, C., Canadell, J. G., Ciais, P., Jackson, R. B., Alin, S., Aragão, L. E. O. C., Arneeth, A., Arora, V., Bates, N. R., Becker, M., Benoit-Cattin, A., Bittig, H. C., Bopp, L., Bultan, S., Chandra, N., Chevallier, F., Chini, L. P., Evans, W., Florentie, L., Forster, P. M., Gasser, T., Gehlen, M., Gilfillan, D., Gkritzalis, T., Gressor, L., Gruber, N., Harris, I., Hartung, K., Haverd, V., Houghton, R. A., Ilyina, T., Jain, A. K., Joetzjer, E., Kadono, K., Kato, E., Kitidis, V., Korsbakken, J. I., Landschützer, P., Lefèvre, N., Lenton, A., Lienert, S., Liu, Z., Lombardozzi, D., Marland, G., Metzl, N., Munro, D. R., Nabel, J. E. M. S., Nakaoka, S.-I., Niwa, Y., O'Brien, K., Ono, T., Palmer, P. I., Pierrot, D., Poulter, B., Resplandy, L., Robertson, E., Rödenbeck, C., Schwinger, J., Séférian, R., Skjelvan, I., Smith, A. J. P., Sutton, A. J., Tanhua, T., Tans, P. P., Tian, H., Tilbrook, B., van der Werf, G., Vuichard, N., Walker, A. P., Wanninkhof, R., Watson, A. J., Willis, D., Wiltshire, A. J., Yuan, W., Yue, X., and Zaehle, S.: "Global Carbon Budget 2020", *Earth Syst. Sci. Data Discuss.*, <https://doi.org/10.5194/essd-2020-286>, in press, 2020.
- Fumière, Q., Déqué, M., Nuissier, O., Somot, S., Alias, A., Caillaud, C., Laurantin, O. and Seity, Y.: "Extreme rainfall in Mediterranean France during the fall: added value of the CNRM-AROME Convection-Permitting Regional Climate Model," *Climate Dyn.* (55:1-2), 2020, pp. 77-91.
- Gainusa-Bogdan, A., D. Swingedouw, P. Yiou, J. Cattiaux, F. Codron and S. Michel (2020): "AMOC and summer sea ice as key drivers of the spread in Mid-Holocene winter temperature patterns over Europe in PMIP3 models", *Global and Planetary Change*, 184, 103055. doi :10.1016/j.gloplacha.2019.103055
- Gardes, T., Schoetter, R., Hidalgo, J., Long, N., Marques, E. and Masson, V.: "Statistical prediction of the nocturnal urban heat island intensity based on urban morphology and geographical factors - An investigation based on numerical model results for a large ensemble of French cities," *Science of The Total Environment* (737), 2020, pp. 139253.
- Garratt, J., Wilczak, J., Holtslag, A., Schmid, H., Grachev, A., Beljaars, A., Foken, T., Fairall, C., Hicks, B., Kusaka, H., Martilli, A., Masson, V., Mauder, M., Oncley, S., Rotach, M. and Tjernström, M.: "Commentaries on Top-Cited Boundary-Layer Meteorology Articles," *Boundary Layer Meteorol.* (177), 2020, pp. 169-188.
- Gascoïn, S., Barrou Dumont, Z., Deschamps-Berger, C., Marti, F., Salgues, G., López-Moreno, J. I., Revuelto, J., Michon, T., Schattan, P. and Hagolle, O.: "Estimating Fractional Snow Cover in Open Terrain from Sentinel-2 Using the Normalized Difference Snow Index," *Remote Sensing* (12), 2020, pp. 2904.
- Gehlen, M., Berthet, S., Séférian, R., Ethé, C. and Penduff, T.: "Quantification of Chaotic Intrinsic Variability of Sea-Air CO<sub>2</sub> Fluxes at Interannual Timescales," *Geophys. Res. Lett.* (47:22), 2020.
- Gerbaux, M., Spandre, P., François, H., George, E. and Morin, S.: « Fiabilité de l'enneigement et disponibilité des ressources en eau pour la production de neige dans les domaines skiables du Département de l'Isère (France), en conditions climatiques actuelles et futures », *Journal of Alpine Research* (Revue de géographie Alpine) (108-4), 2020.
- Giese, A., A. Boone, P. Wagon and R. Howley, 2020: "Incorporating moisture content in surface energy balance modeling of a debris-covered glacier". *The Cryosphere*, 14, 1555-1577.
- Giordani, H., Bourdallé-Badie, R. and Madec, G.: "An Eddy-Diffusivity Mass-Flux Parameterization for Modelling Oceanic Convection," *J. Adv. Model. Earth Syst.*, 2020.
- Good, P., Chadwick, R., Holloway, C. E., Kennedy, J., Lowe, J. A., Roehrig, R. and Rushley, S. S.: "High sensitivity of tropical precipitation to local sea surface temperature," *Nature* (589:7842), 2020, pp. 408-414.
- Gouhier, M., Deslandes, M., Guéhenneux, Y., Hereil, P., Cacault, P. and Josse, B.: "Operational Response to Volcanic Ash Risks Using HOTVOLC Satellite-Based System and MOCAGE-Accident Model at the Toulouse VAAC," *Atmosphere* (11:8), 2020, pp. 864.
- Granero-Belinchon, C., Adeline, K., Lemonsu, A. and Briottet, X.: "Phenological Dynamics Characterization of Alignment Trees with Sentinel-2 Imagery: A Vegetation Indices Time Series Reconstruction Methodology Adapted to Urban Areas," *Remote Sensing* (12:4), 2020, pp. 639.
- Grimmond, S., Bouchet, V., Molina, L. T., Baklanov, A., Tan, J., Schlünzen, K. H., Mills, G., Golding, B., Masson, V., Ren, C., Voogt, J., Miao, S., Lean, H., Heusinkveld, B., Hovespyan, A., Teruggi, G., Parrish, P. and Joe, P.: "Integrated urban hydrometeorological, climate and environmental services: Concept, methodology and key messages," *Urban Clim.* (33), 2020, pp. 100623.
- Gruber, A., Lannoy, G. D., Albergel, C., Al-Yaari, A., Brocca, L., Calvet, J.-C., Colliander, A., Cosh, M., Crow, W., Dorigo, W., Draper, C., Hirschi, M., Kerr, Y., Konings, A., Lahoz, W., McColl, K., Montzka, C., Muñoz-Sabater, J., Peng, J., Reichle, R., Richaume, P., Rüdiger, C., Scanlon, T., van der Schalie, R., Wigneron, J.-P. and Wagner, W.: "Validation practices for satellite soil moisture retrievals: What are (the) errors?," *Remote Sens. Environ.* (244), 2020, pp. 111806.
- Guieu, C., D'Ortenzio, F., Dulac, F., Taillandier, V., Doglioli, A., Petrenko, A., Barrillon, S., Mallet, M., Nabat, P. and Desboeufs, K.: "Introduction: Process studies at the airsea interface after atmospheric deposition in the Mediterranean Sea objectives and strategy of the PEACETIME oceanographic campaign (May/June 2017)," *Biogeosciences* (17:22), 2020, pp. 5563-5585.
- Gutiérrez, C., Somot, S., Nabat, P., Mallet, M., Corre, L., van Meijgaard, E., Perpiñan, O. and A. Gaertner, M.: "Future evolution of surface solar radiation and photovoltaic potential in Europe: investigating the role of aerosols," *Environ. Res. Lett.* (15:3), 2020, pp. 034035.

- Habets, F., Etchevers, P. and Le Moigne, P. : « La représentation des surfaces continentales pour la prévision hydrologique », *La Météorologie* (108), 2020, pp. 088.
- Hamidi, Y., Raynaud, L., Rottner, L. and Arbogast, P.: "Texture-based classification of high-resolution precipitation forecasts with machine-learning methods," *Quart. J. Roy. Meteor. Soc.* (146:732), 2020, pp. 3014-3028.
- Hanzer, F., Carmagnola, C., Ebner, P. P., Koch, F., Monti, F., Bavay, M., Bernhardt, M., Lafaysse, M., Lehning, M., Strasser, U., François, H. and Morin, S.: "Simulation of snow management in Alpine ski resorts using three different snow models," *Cold Reg. Sci. Technol.* (172), 2020.
- Hauck, J., Zeising, M., Le Quéré, C., Gruber, N., Bakker, D. C. E., Bopp, L., Chau, T. T. T., Gürses, Ö., Ilyina, T., Landschützer, P., Lenton, A., Resplandy, L., Rödenbeck, C., Schwinger, J., Séférian, R.: "Consistency and challenges in the ocean carbon sink estimate for the Global Carbon Budget". *Front. Mar. Sci.*, 7, 852. <https://www.frontiersin.org/article/10.3389/fmars.2020.571720>, 2020.
- Hauser D., C. Tourain, L. Hermozo, D. Alraddawi, L. Aouf, B. Chapron, A. Dalphiné, et al.: "Radar observation of surface oceanwaves and windfromspace: first results from the SWIM instrument on-board CFOSAT", *IEEE Transaction on Geoscience and RemoteSensing*, 10.1109/TGRS.2020.2994372, 2020
- Hauser, D., C. Tourain, L. Hermozo, D. Alraddawi, L. Aouf, B. Chapron, A. Dalphiné, L. Delaye, M. Dalila, E. Dormy, F. Gouillon, V. Gressani, A. Grouazel, G. Guitton, R. Husson, A. Mironov, A. Mouche, A. Ollivier, L. Oruba, F. Piras, R. Rodriguez Suquet, P. Schippers, C. Tison, Ngan Tran: "New Observations From the SWIM Radar On-Board CFOSAT: Instrument Validation and Ocean Wave Measurement Assessment", *IEEE Transactions on Geoscience and Remote Sensing*, 2020, 10.1109/tgrs.2020.2994372.
- Hdidou, F. Z., Mordane, S., Moll, P., Mahfouf, J.-F., Erraji, H. and Dahmane, Z.: "Impact of the variational assimilation of ground-based GNSS zenith total delay into AROME-Morocco model," *Tellus A: Dynamic Meteorology and Oceanography* (72:1), 2020, pp. 1-13.
- Héron D., Evan S., Brioude J., Rosenlof K., Posny F., Metzger J.-M., Cammas J. -P.: "Impact of convection on the upper-tropospheric composition (water vapor and ozone) over a subtropical site (Réunion island; 21.1°S, 55.5°E) in the Indian Ocean", *Atmospheric Chemistry and Physics*, 2020, 20 (14), pp.8611-8626. 10.5194/acp-20-8611-2020
- Hirtl, M., Arnold, D., Baro, R., Brenot, H., Coltelli, M., Eschbacher, K., Hard-Stremayer, H., Lipok, F., Maurer, C., Meinhard, D., Mona, L., Mulder, M. D., Papagiannopoulos, N., Pernsteiner, M., Plu, M., Robertson, L., Rokitsansky, C.-H., Scherllin-Pirscher, B., Sievers, K., Sofiev, M., de Cerff, W. S., Steinheimer, M., Stuefer, M., Theys, N., Uppstu, A., Wagenaar, S., Winkler, R., Wotawa, G., Zobl, F. and Zopp, R.: "A volcanic-hazard demonstration exercise to assess and mitigate the impacts of volcanic ash clouds on civil and military aviation," *Nat. Hazards Earth Syst. Sci.* (20:6), 2020, pp. 1719-1739.
- Honnert, R., Efstathiou, G. A., Beare, R. J., Ito, J., Lock, A., Neggers, R., Plant, R. S., Shin, H. H., Tomassini, L. and Zhou, B.: "The Atmospheric Boundary Layer and the Gray Zone of Turbulence: A Critical Review," *Journal of Geophysical Research: Atmospheres* (125:13), 2020.
- Hourdin, F., Rio, C., Grandpeix, J.Y., Madeleine, J.B., Cheruy, F., Rochetin, N., Jam, A., Musat, I., Idelkadi, A., Fairhead, L. and Foujols, M.A.: "LMDZ6A: The atmospheric component of the IPSL climate model with improved and better tuned physics" *Journal of Advances in Modeling Earth Systems*, 12(7), 2020
- Hourdin, F., Rio, C., Jam, A., Traore, A.-K. and Musat, I.: "Convective Boundary Layer Control of the Sea Surface Temperature in the Tropics," *J. Adv. Model. Earth Syst.* (12:6), 2020.
- Hourdin, F., Williamson, D., Rio, C., Couvreur, F., Roehrig, R., Villefranche, N., Musat, I., Fairhead, L., Diallo, F. B. and Volodina, V.: "Process-based climate model development harnessing machine learning: II: model calibration from single column to global," *J. Adv. Model. Earth Syst.*, 2020.
- Ilyina, T., H. Li, A. Spring, W. A. Muller, L. Bopp, M. O. Chikamoto, G. Danabasoglu, M. Dobrynin, J. Dunne, F. Fransner, P. Friedlingstein, W. Lee, N. S. Lovenduski, W.J. Merryeld, J. Mignot, J.Y. Park, Séférian, R., R. Sospedra-Alfonso, M. Watanabe, S.: "Yeager: Predictable variations of the carbon sinks and atmospheric CO<sub>2</sub> growth in a multi-model framework". *Geophysical Research Letters*, 47, <https://doi.org/10.1029/2020GL090695>, 2020.
- Ito, A., Hajima, T., Lawrence, D. M., Brovkin, V., Delire, C., Guenet, B., Jones, C. D., Malyshev, S., Matera, S., McDermid, S. P., Peano, D., Pongratz, J., Robertson, E., Shevliakova, E., Vuichard, N., Wärlind, D., Wiltshire, A. and Ziehn, T.: "Soil carbon sequestration simulated in CMIP6-LUMIP models: implications for climatic mitigation," *Environ. Res. Lett.* (15:12), 2020, pp. 124061.
- Jacob, D., Teichmann, C., Sobolowski, S., Katragkou, E., Anders, I., Belda, M., Benestad, R., Boberg, F., Buonomo, E., Cardoso, R. M., Casanueva, A., Christensen, O. B., Christensen, J. H., Coppola, E., Cruz, L. D., Davin, E. L., Dobler, A., Domnguez, M., Fealy, R., Fernandez, J., Gaertner, M. A., Garcia-Dez, M., Giorgi, F., Gobiet, A., Goergen, K., Gomez-Navarro, J. J., Aleman, J. J. G., Gutiérrez, C., Gutiérrez, J. M., Güttler, I., Haensler, A., Halenka, T., Jerez, S., Jiménez-Guerrero, P., Jones, R. G., Keuler, K., Kjellström, E., Knist, S., Kotlarski, S., Maraun, D., van Meijgaard, E., Mercogliano, P., Montavez, J. P., Navarra, A., Nikulin, G., de Noblet-Ducoudré, N., Panitz, H.-J., Pfeifer, S., Piazza, M., Pichelli, E., Pietikäinen, J.-P., Prein, A. F., Preuschmann, S., Rechid, D., Rockel, B., Romera, R., Sanchez, E., Sieck, K., Soares, P. M. M., Somot, S., Srnec, L., Sørland, S. L., Termonia, P., Truhetz, H., Vautard, R., Warrach-Sagi, K. and Wulfmeyer, V.: "Regional climate downscaling over Europe: perspectives from the EURO-CORDEX community," *Reg. Environ. Change* (20:2), 2020.
- Jafari, M., Gouttevin, I., Couttet, M., Wever, N., Michel, A., Sharma, V., Rossman, L., Maass, N., Nicolaus, M. and Lehning, M.: "The Impact of Diffusive Water Vapor Transport on Snow Profiles in Deep and Shallow Snow Covers and on Sea Ice," *Front. Earth Sci.* (8), 2020, pp. 249.
- Jenny, J.-P., Anneville, O., Arnaud, F. and et al.: "Scientists' Warning to Humanity: Rapid degradation of the world's large lakes," *J. Great Lakes Res.* (46:4), 2020, pp. 686-702.
- Joly, L., Coopmann, O., Guidard, V., Decarpenterie, T., Dumelié, N., Cousin, J., Burgalat, J., Chauvin, N., Albora, G., Maamary, R., Khair, Z. M. E., Tzanos, D., Barrié, J., éric Moulin, Aressy, P. and Belleudy, A.: "The development of the Atmospheric Measurements by Ultra-Light Spectrometer (AMULSE) greenhouse gas profiling system and application for satellite retrieval validation," *Atmos. Meas. Tech.* (13:6), 2020, pp. 3099-3118.
- Joshi V., Sharma S., Niranjana Kumard K., Patel N., Kumar P., Bencherif H. et al. « Analysis of the middle atmospheric ozone using SABER observations: a study over mid-latitudes in the northern and southern hemispheres », *Climate Dynamics*, 2020, 10.1007/s00382-020-05124-6Joulin, P.-A., Mayol, M. L., Masson, V., Blondel, F., Rodier, Q., Cathelain, M. and Lac, C.: "The Actuator Line Method in the Meteorological LES Model Meso-NH to Analyze the Horns Rev 1 Wind Farm Photo Case," *Front. Earth Sci.* (7), 2020.
- Krinner, G., Kharin, V., Roehrig, R., Scinocca, J. and Codron, F.: "Historically-based run-time bias corrections substantially improve model projections of 100 years of future climate change," *Communications Earth & Environment* (1:1), 2020.
- Kwiatkowski, L., Torres, O., Bopp, L., Aumont, O., Chamberlain, M., Christian, J. R., Dunne, J. P., Gehlen, M., Ilyina, T., John, J. G., Lenton, A., Li, H., Lovenduski, N. S., Orr, J. C., Palmieri, J., Santana-Falcón, Y., Schwinger, J., Séférian, R., Stock, C. A., Tagliabue, A., Takano, Y., Tjiputra, J., Toyama, K., Tsujino, H., Watanabe, M., Yamamoto, A., Yool, A., and Ziehn, T. : "Twenty-first century ocean warming, acidification, deoxygenation, and upper-ocean nutrient and primary production decline from CMIP6 model projections", *Biogeosciences*, 17, 3439–3470, <https://doi.org/10.5194/bg-17-3439-2020>, 2020.
- Kwok, Y. T., De-Munck, C., Schoetter, R., Ren, C. and Lau, K. K.-L.: "Refined dataset to describe the complex urban environment of Hong Kong for urban climate modelling studies at the mesoscale," *Theor. Appl. Climatol.* (142), 2020, pp. 129-150.
- Laj P., Bigi A., Rose C., Andrews E., Lund Myhre C. et al.: "A global analysis of climate-relevant aerosol properties retrieved from the network of Global Atmosphere Watch (GAW) near-surface observatories", *Atmospheric Measurement Techniques*, 2020, 13, pp.4353 - 4392. 10.5194/amt-13-4353-2020
- Lakkala K., Kujanpää J., Brogniez C., Henriot N., Arola A. et al.: "Validation of the Tropospheric Monitoring Instrument (TROPOMI) surface UV radiation product", *Atmospheric Measurement Techniques*, 2020, 13, pp.6999 - 7024. 10.5194/amt-13-6999-2020
- Lamare, M., Dumont, M., Picard, G., Larue, F., Tuzet, F., Delcourt, C. and Arnaud, L.: "Simulating optical top-of-atmosphere radiance satellite images over snow-covered rugged terrain," *The Cryosphere* (14:11), 2020, pp. 3995-4020.
- Langford A., Alvarez R., Brioude J., Caputi D., Conley S. et al.: "Ozone Production in the Soberanes Smoke Haze: Implications for Air Quality in the San Joaquin Valley During the California Baseline Ozone Transport Study", *Journal of Geophysical Research: Atmospheres*, 2020, 125 (11), 10.1029/2019JD031777
- Largerone, C., Dumont, M., Morin, S., Boone, A., Lafaysse, M., Metref, S., Cosme, E., Jonas, T., Winstral, A. and Margulis, S. A.: "Toward Snow Cover Estimation in Mountainous Areas Using

- Modern Data Assimilation Methods: A Review," *Front. Earth Sci.* (8), 2020.
- Largeron, Y., Guichard, F., Roehrig, R., Couvreur, F. and Barbier, J.: "The April 2010 North African heatwave: when the water vapor greenhouse effect drives nighttime temperatures," *Climate Dyn.* (54:9-10), 2020, pp. 3879-3905.
- Larue, F., Picard, G., Arnaud, L., Ollivier, I., Delcourt, C., Lamare, M., Tuzet, F., Revuelto, J. and Dumont, M.: "Snow albedo sensitivity to macroscopic surface roughness using a new ray-tracing model," *The Cryosphere* (14:5), 2020, pp. 1651-1672.
- Lavaud, L., Bertin, X., Martins, K., Arnaud, G. and Bouin, M.-N.: "The contribution of short-wave breaking to storm surges: The case Klaus in the Southern Bay of Biscay," *Ocean Modell.* (156), 2020.
- Le Moigne, P. and Minvielle, M.: « Surfex : une plateforme pour simuler les flux des surfaces océaniques et continentales », *La Météorologie* (:108), 2020, pp. 082.
- Le Page, M., L. Jarlan, M. El Hajj, M. Zribi, N. Baghdadi, and A. Boone, 2020: "Potential for the detection of irrigation events on maize plots using Sentinel-1 soil moisture products". *Remote Sens.*, 12, 1621, doi:10.3390/rs12101621
- Lees E., Bousquet O., Leclair de Bellevue J.: "Analysis of diurnal to seasonal variability of Integrated Water Vapour in the South Indian Ocean basin using ground-based GNSS and fifth-generation ECMWF reanalysis (ERA5) data", *Quarterly Journal of the Royal Meteorological Society*, 2020, pp.1-20. 10.1002/qj.3915
- Lellouch G, Carrer D, Vincent C, Pardé M, C. Frietas S, Trigo IF: "Evaluation of Two Global Land Surface Albedo Datasets Distributed by the Copernicus Climate Change Service and the EUMETSAT LSA-SAF". *Remote Sensing*. 2020; 12(11):1888.
- LeMoigne, P., Besson, F., Martin, E., Boé, J., Boone, A., Decharme, B., Etchevers, P., Faroux, S., Habets, F., Lafaysse, M., Leroux, D. and Rousset-Regimbeau, F.: "The latest improvements with SURFEX v8.0 of the Safran-Isba-Modcou hydrometeorological model for (France)," *Geosci. Model Dev.* (13), 2020, pp. 3925-3946.
- Libois, Q., C.-Labonnote, L. and Camy-Peyret, C. « Forum mesurera linfrarouge lointain émis par la Terre », *La Météorologie* (:108), 2020, pp. 004.
- Liddicoat, S. K., Wiltshire, A. J., Jones, C. D., Arora, V. K., Brovkin, V., Cadule, P., Hajima, T., Lawrence, D. M., Pongratz, J., Schwinger, J., Séférian, R., Tjiputra, J. F., & Ziehn, T.: "Compatible Fossil Fuel CO2 emissions in the CMIP6 Earth System Models' Historical and Shared Socioeconomic Pathway experiments of the 21st Century". *J. Clim.*, 1, 1–72, doi:10.1175/JCLI-D-19-0991.1, 2020.
- Lindsay, N., Libois, Q., Badosa, J., Migan-Dubois, A. and Bourdin, V.: "Errors in PV power modelling due to the lack of spectral and angular details of solar irradiance inputs," *Sol. Energy* (197), 2020, pp. 266-278.
- Lopez-Moreno, J. I., Soubeyroux, J. M., Gascoin, S., Alonso-Gonzalez, E., Duran-Gomez, N., Lafaysse, M., Vernay, M., Carmagnola, C. and Morin, S.: "Long-term trends (19582017) in snow cover duration and depth in the Pyrenees," *Int. J. Climatol.* (40:14), 2020, pp. 6122-6136.
- Lucas-Picher, P., Arsenault, R., Poulin, A., Ricard, S., Lachance-Cloutier, S. and Turcotte, R.: "Application of a High-Resolution Distributed Hydrological Model on a U.S.-Canada Transboundary Basin: Simulation of the Multiyear Mean Annual Hydrograph and 2011 Flood of the Richelieu River Basin," *J. Adv. Model. Earth Syst.* (12:4), 2020.
- Lucas-Picher, P., Lachance-Cloutier, S., Arsenault, R., Poulin, A., Ricard, S., Turcotte, R. and Brissette, F.: "Will Evolving Climate Conditions Increase the Risk of Floods of the Large U.S.-Canada Transboundary Richelieu River Basin?," *JAWRA Journal of the American Water Resources Association* (57:1), 2020, pp. 32-56.
- MacDougall, A. H., Frölicher, T. L., Jones, C. D., Rogelj, J., Matthews, H. D., Zickfeld, K., Arora, V. K., Barrett, N. J., Brovkin, V., Burger, F. A., Eby, M., Eliseev, A. V., Hajima, T., Holden, P. B., Jeltsch-Thömmes, A., Koven, C., Mengis, N., Menviel, L., Michou, M., Mokhov, I. I., Oka, A., Schwinger, J., Séférian, R., Shaffer, G., Sokolov, A., Tachiiri, K., Tjiputra, J., Wiltshire, A. and Ziehn, T.: "Is there warming in the pipeline? A multi-model analysis of the Zero Emissions Commitment from CO<sub>2</sub>", *Biogeosciences* (17:11), 2020, pp. 2987-3016.
- Madeleine, J.B., Hourdin, F., Grandpeix, J.Y., Rio, C., Dufresne, J.L., Vignon, E., Boucher, O., Konsta, D., Cheruy, F., Musat, I. and Idelkadi, A.: "Improved representation of clouds in the atmospheric component LMDZ6A of the IPSL-CM6A Earth system model", *Journal of Advances in Modeling Earth Systems*, 12(10), 2020.
- Mallet, M., Solmon, F., Nabat, P., Elguindi, N., Waquet, F., Bouniol, D., Sayer, A. M., Meyer, K., Roehrig, R., Michou, M., Zuidema, P., Flamant, C., Redemann, J. and Formenti, P.: "Direct and semi-direct radiative forcing of biomass-burning aerosols over the southeast Atlantic (SEA) and its sensitivity to absorbing properties: a regional climate modeling study," *Atmos. Chem. Phys.* (20:21), 2020, pp. 13191-13216.
- Mandement, M. and Caumont, O.: "Contribution of personal weather stations to the observation of deep-convection features near the ground," *Nat. Hazards Earth Syst. Sci.* (20:1), 2020, pp. 299-322.
- Mansour, K., Decesari, S., Facchini, M., Belosi, F., Pagliano, M., Sandrini, S., Bellacicco, M., Marullo, S., Santoleri, R., Ovadnevaite, J., Ceburnis, D., O'Dowd, C., Roberts, G., Sanchez, K. and Rinaldi, M.: "Linking Marine Biological Activity to Aerosol Chemical Composition and Cloud-Relevant Properties over the North Atlantic Ocean," *J. Geophys.*, 2020.
- Margirier, F., Testor, P., Heslop, E., Mallil, K., Bosse, A., Houpert, L., Mortier, L., Bouin, M.-N., Coppola, L., D'Ortenzio, F., de-Madron, X. D., Mourre, B., Prieur, L., Raimbault, P. and Taillandier, V.: "Abrupt warming and salinification of intermediate waters interplays with decline of deep convection in the Northwestern Mediterranean Sea," *Sci. Rep.* (10), 2020.
- Marquet, P., Mahfouf, J.-F. and Holdaway, D.: "Definition of the Moist-Air Exergy Norm: A Comparison with Existing Moist Energy Norms," *Mon. Weather Rev.* (148:3), 2020, pp. 907-928.
- Martinet, P., Cimini, D., Burnet, F., Ménétrier, B., Michel, Y. and Unger, V.: "Improvement of numerical weather prediction model analysis during fog conditions through the assimilation of ground-based microwave radiometer observations: a 1D-Var study," *Atmos. Meas. Tech.* (13:12), 2020, pp. 6593-6611.
- Masson V., E. Bocher, B. Bucher, Z. Chitu, S. Christophe, C. Fortelius, R. Hamdi, A. Lemonsu, A. Perrels, B. Van Schaeybroeck, B. Wichers Schreur, L. Velea, Y. Beddar, J.-C. Calvet, A. Delcloo, A. Druel, F. Duchêne, G. Dumas, J. Gautier, M. Goret, M. Horttanainen, R. Kouznetsov, A. Le Bris, S. Lecorre, B. Le Roy, Y. Palamarchuk, G. Petit, R. Ruuhela, O. Saranko, M. Sofiev, P. Siljamo, H. Van de Vyver, P. van Velthoven, A. Votsis (2020): "The Urban Climate Services URCLIM project", *Climate Services*, 20, 10.1016/j.cliser.2020.100194
- Masson, V. and Lemonsu, A. : « Comment Joël Noilhan a influencé la modélisation et les études en climat urbain », *La Météorologie* (:108), 2020, pp. 093.
- Masson, V., Heldens, W., Bocher, E., Bonhomme, M., Bucher, B., Burmeister, C., de Munck, C., Esch, T., Hidalgo, J., Kanani-Sühring, F., Kwok, Y.-T., Lemonsu, A., Lévy, J.-P., Maronga, B., Pavlik, D., Petit, G., See, L., Schoetter, R., Tornay, N., Votsis, A. and Zeidler, J.: "City-descriptive input data for urban climate models: Model requirements, data sources and challenges," *Urban Clim.* (31), 2020, pp. 100536.
- Masson, V., Lemonsu, A., Hidalgo, J. and Voogt, J.: "Urban Climates and Climate Change," *Annu. Rev. Environ. Resour.* (45), 2020, pp. 411-444.
- Matthews, H. D., K. Tokarska, Z. R. J. Nicholls, J. Rogelj, J. P. Canadell, P. Friedlingstein, T. L. Frölicher, P. M. Forster, N. P. Gillett, T. Ilyina, R. B. Jackson, C. D. Jones, C. Koven, R. Knutti, A. H. MacDougall, M. Meinshausen, N. Mengis, Séférian, R., K. Zickfeld: "Opportunities and challenges in using carbon budgets to guide climate policy". *Nat. Geosci.* 13, 769–779 (2020). <https://doi.org/10.1038/s41561-020-00663-3>
- Mbatha N., Bencherif H.: "Time Series Analysis and Forecasting Using a Novel Hybrid LSTM Data-Driven Model Based on Empirical Wavelet Transform Applied to Total Column of Ozone at Buenos Aires, Argentina (1966–2017)", *Atmosphere*, 2020, 11 (5), 10.3390/atmos11050457
- McFarquhar, G. M., Bretherton, C., Marchand, R., Protat, A., DeMott, P. J., Alexander, S. P., Roberts, G. C., Twohy, C. H., Toohey, D., Siems, S., Huang, Y., Wood, R., Rauber, R. M., Lasher-Trapp, S., Jensen, J., Stith, J., Mace, J., Um, J., Järvinen, E., Schnaiter, M., Gettelman, A., Sanchez, K. J., McCluskey, C. S., Russell, L. M., McCoy, I. L., Atlas, R., Bardeen, C. G., Moore, K. A., Hill, T. C. J., Humphries, R. S., Keywood, M. D., Ristovski, Z., Cravigan, L., Schofield, R., Fairall, C., Mallet, M. D., Kreidenweis, S. M., Rainwater, B., D'Alessandro, J., Wang, Y., Wu, W., Saliba, G., Levin, E. J. T., Ding, S., Lang, F., Truong, S. C. H., Wolff, C., Haggerty, J., Harvey, M. J., Klekociuk, A. and McDonald, A.: "Observations of clouds, aerosols, precipitation, and surface radiation over the Southern Ocean: An overview of CAPRICORN, MARCUS, MICRE and SOCRATES," *Bull. Amer. Meteor. Soc.*, 2020.
- Mede, T., Chambon, G., Nicot, F. and Hagenmuller, P.: "Micromechanical investigation of snow failure under mixed-mode loading," *Int. J. Solids Struct.* (199), 2020, pp. 95-108.

- Ménard, C., R. Essery, G. Krinner, G. Arduini, P. Bartlett, A. Boone, C. Brutel-Vuilmet, E. Burke, J. Colin, M. Cuntz, Y. Dai, B. Decharme, E. Dutra, L. Fang, C. Fierz, Y. Gusev, S. Hagemann, V. Haverd, H. Kim, M. Lafaysse, T. Marke, O. Nasonova, T. Nitta, M. Niwano, J. Pomeroy, G. Schaedler, V. Semenov, T. Smirnova, U. Strasser, S. Swenson, D. Turkov, N. Wever, and H. Yuan, 2020: "Scientific and human errors in a snow model intercomparison". *Bull. Amer. Meteor. Soc.*, doi:10.1175/BAMS-D-19-0329.1
- Ménégoz, M., Valla, E., Jourdain, N. C., Blanchet, J., Beaumet, J., Wilhelm, B., Gallée, H., Fettweis, X., Morin, S. and Anquetin, S.: "Contrasting seasonal changes in total and intense precipitation in the European Alps from 1903 to 2010," *Hydrol. Earth Syst. Sci.* (24:11), 2020, pp. 5355-5377.
- Merchant, C. J., Saux-Picart, S. and Waller, J.: "Bias correction and covariance parameters for optimal estimation by exploiting matched in-situ references," *Remote Sens. Environ.* (237), 2020, pp. 111590.
- Merryfield, W. J., Baehr, J., Batté, L., Becker, E. J., Butler, A. H., Coelho, C. A. S., Danabasoglu, G., Dirmeyer, P. A., Doblas-Reyes, F. J., Domeisen, D. I. V., Ferranti, L., Ilyina, T., Kumar, A., Müller, W. A., Rixen, M., Robertson, A. W., Smith, D. M., Takaya, Y., Tuma, M., Vitart, F., White, C. J., Alvarez, M. S., Ardilouze, C., Attard, H., Baggett, C., Balmaseda, M. A., Beraki, A. F., Bhattacharjee, P. S., Bilbao, R., de Andrade, F. M., DeFlorio, M. J., Daz, L. B., Ehsan, M. A., Fragkoulidis, G., Grainger, S., Green, B. W., Hell, M. C., Infanti, J. M., Isensee, K., Kataoka, T., Kirtman, B. P., Klingaman, N. P., Lee, J.-Y., Mayer, K., McKay, R., Mecking, J. V., Miller, D. E., Neddermann, N., Ng, C. H. J., Osso, A., Pankatz, K., Peatman, S., Pegion, K., Perlwitz, J., Recalde-Coronel, G. C., Reintges, A., Renkl, C., Solaraju-Murali, B., Spring, A., Stan, C., Sun, Y. Q., Tozer, C. R., Vigaud, N., Woolnough, S. and Yeager, S.: "Current and emerging developments in subseasonal to decadal prediction," *Bull. Amer. Meteor. Soc.*, 2020.
- Meyer D., R. Schoetter, V. Masson, S. Grimmond, 2020 : "Enhanced software and platform for the Town Energy Balance (TEB) model". *The Journal of Open Source Software*, doi:10.21105/joss.02008
- Meyer, D., Schoetter, R., Riechert, M., Verrelle, A., Tewari, M., Dudhia, J., Masson, V., van Renswoude, M. and Grimmond, S.: "WRF-TEB: Implementation and Evaluation of the Coupled Weather Research and Forecasting (WRF) and Town Energy Balance (TEB) Model," *J. Adv. Model. Earth Syst.* (12:8), 2020.
- Mezzina, B., Garca-Serrano, J., Bladé, I., Palmeiro, F. M., Batté, L., Ardilouze, C., Benassi, M. and Gualdi, S.: "Multi-model assessment of the late-winter extra-tropical response to El Niño and La Niña," *Climate Dyn.*, 2020.
- Michou, M., Nabat, P., Saint-Martin, D., Bock, J., Decharme, B., Mallet, M., Roehrig, R., Séférian, R., Sénési, S. and Voldoire, A.: "Present-Day and Historical Aerosol and Ozone Characteristics in CNRM CMIP6 Simulations," *J. Adv. Model. Earth Syst.* (12:1), 2020.
- Montagnat M., Löwe H., Calonne N., Schneebeli M., Matzl M. and Jaggi M. (2020): "On the Birth of Structural and Crystallographic Fabric Signals in Polar Snow: A Case Study From the EastGRIP Snowpack". *Front. Earth Sci.* 8:365. doi: 10.3389/feart.2020.00365
- Montagnat, M., Chambon, G., Gaume, J., Hagemuller, P. and Sandells, M.: "Editorial: About the Relevance of Snow Microstructure Study in Cryospheric Sciences," *Front. Earth Sci.* (8), 2020, pp. 571.
- Morales, M. S., Cook, E. R., Barichivich, J., Christie, D. A., Villalba, R., LeQuesne, C., Srur, A. M., Ferrero, M. E., González-Reyes, Á., Couvreur, F., Matskovsky, V., Aravena, J. C., Lara, A., Mundo, I. A., Rojas, F., Prieto, M. R., Smerdon, J. E., Bianchi, L. O., Masiokas, M. H., Urrutia-Jalabert, R., Rodríguez-Catón, M., Muñoz, A. A., Rojas-Badilla, M., Alvarez, C., Lopez, L., Luckman, B. H., Lister, D., Harris, I., Jones, P. D., Williams, A. P., Velazquez, G., Aliste, D., Aguilera-Betti, I., Marcotti, E., Flores, F., Muñoz, T., Cuq, E. and Boninsegna, J. A.: "Six hundred years of South American tree rings reveal an increase in severe hydroclimatic events since mid-20th century," *PNAS (Proceedings of the National Academy of Sciences of the United States of America)*, 2020.
- Morel, X., Hansen, B., Delire, C., Ambus, P., Mastepanov, M. and Decharme, B.: "A new dataset of soil carbon and nitrogen stocks and profiles from an instrumented Greenlandic fen designed to evaluate land-surface models," *Earth Syst. Sci. Data* (12:4), 2020, pp. 2365-2380.
- Morgenstern, O., OConnor, F. M., Johnson, B. T., Zeng, G., Mulcahy, J. P., Williams, J., Teixeira, J., Michou, M., Nabat, P., Horowitz, L. W., Naik, V., Sentman, L. T., Deushi, M., Bauer, S. E., Tsigaridis, K., Shindell, D. T. and Kinnison, D. E.: "Reappraisal of the Climate Impacts of Ozone-Depleting Substances," *Geophys. Res. Lett.* (47:20), 2020.
- Morin, S., Horton, S., Techel, F., Bavay, M., Coléou, C., Fierz, C., Gobiet, A., Hagenmuller, P., Lafaysse, M., Lizar, M., Mitterer, C., Monti, F., Müller, K., Olefs, M., Snook, J. S., van Herwijnen, A. and Vionnet, V.: "Application of physical snowpack models in support of operational avalanche hazard forecasting: A status report on current implementations and prospects for the future," *Cold Reg. Sci. Technol.* (170), 2020, pp. 102910.
- Moseid, K. O., Schulz, M., Storelvmo, T., Julsrud, I. R., Olivé, D., Nabat, P., Wild, M., Cole, J. N. S., Takemura, T., Oshima, N., Bauer, S. E. and Gastineau, G.: "Bias in CMIP6 models as compared to observed regional dimming and brightening," *Atmos. Chem. Phys.* (20:24), 2020, pp. 16023-16040.
- Mucia, A., Bonan, B., Zheng, Y., Albergel, C. and Calvet, J.-C.: "From Monitoring to Forecasting Land Surface Conditions Using a Land Data Assimilation System: Application over the Contiguous United States," *Remote Sensing* (12:12), 2020, pp. 2020.
- Nabat, P., Somot, S., Cassou, C., Mallet, M., Michou, M., Bouniol, D., Decharme, B., Drugé, T., Roehrig, R. and Saint-Martin, D.: "Modulation of radiative aerosols effects by atmospheric circulation over the Euro-Mediterranean region," *Atmos. Chem. Phys.* (20:14), 2020, pp. 8315-8349.
- Napoly, A., A. Boone and T. Welfringer, 2020: "ISBA-MEB: model snow evaluation for local-scale forest sites". *Geoscientific Model Development*, 13, 6523-6545, doi:10.5194/gmd-13-6523-2020.
- Navarro, J. C. A., Ortega, P., Batté, L., Smith, D., Bretonnière, P. A., Guemas, V., Massonnet, F., Sicardi, V., Torralba, V., Tourigny, E. and Doblas-Reyes, F. J.: "Link Between Autumnal Arctic Sea Ice and Northern Hemisphere Winter Forecast Skill," *Geophys. Res. Lett.* (47:5), 2020.
- Naveau, P., Hannart, A. and Ribes, A.: "Statistical Methods for Extreme Event Attribution in Climate Science," *Annual Review of Statistics and Its Application* (7:1), 2020, pp. 89-110.
- Nicely, J. M., Duncan, B. N., Hanisco, T. F., Wolfe, G. M., Salawitch, R. J., Deushi, M., Haslerud, A. S., Jöckel, P., Josse, B., Kinnison, D. E., Klekociuk, A., Manyin, M. E., Marécal, V., Morgenstern, O., Murray, L. T., Myhre, G., Oman, L. D., Pitari, G., Pozzer, A., Quaglia, I., Revell, L. E., Rozanov, E., Stenke, A., Stone, K., Strahan, S., Tilmes, S., Tost, H., Westervelt, D. M. and Zeng, G.: "A machine learning examination of hydroxyl radical differences among model simulations for CCM1-1," *Atmos. Chem. Phys.* (20:3), 2020, pp. 1341-1361.
- Niekerk, A., Sandu, I., Zadra, A., Bazile, E., Kanehama, T., Köhler, M., Koo, M.-S., Choi, H.-J., Kuroki, Y., Toy, M. D., Vosper, S. B. and Yudin, V.: "Constraining Orographic Drag Effects (COORDE): A Model Comparison of Resolved and Parametrized Orographic Drag," *J. Adv. Model. Earth Syst.* (12:11), 2020.
- Nogueira, M., Albergel, C., Boussetta, S., Johannsen, F., Trigo, I. F., Ermida, S. L., Martins, J. P. A. and Dutra, E.: "Role of vegetation in representing land surface temperature in the CHTESSEL (CY45R1) and SURFEX-ISBA (v8.1) land surface models: a case study over Iberia", 2020.
- Nuissier, O., F. Duffourg, M. Martinet, V. Ducrocq, and C.: "Lac, Hectometric-scale simulations of a Mediterranean heavy-precipitation event during the Hydrological cycle in the Mediterranean Experiment (HyMeX) first Special Observation Period (SOP1)", *Atmos. Chem. Phys.*, 20, 14649-14667, 2020.
- Orbe, C., Plummer, D. A., Waugh, D. W., Yang, H., Jöckel, P., Kinnison, D. E., Josse, B., Marecal, V., Deushi, M., Abraham, N. L., Archibald, A. T., Chipperfield, M. P., Dhomse, S., Feng, W. and Bekki, S.: "Description and Evaluation of the specified-dynamics experiment in the Chemistry-Climate Model Initiative," *Atmos. Chem. Phys.* (20:6), 2020, pp. 3809-3840.
- Oudar, T., Cattiaux, J. and Douville, H.: "Drivers of the Northern Extratropical Eddy-Driven Jet Change in CMIP5 and CMIP6 Models," *Geophys. Res. Lett.* (47:8), 2020.
- Oudar, T., Cattiaux, J., Douville, H., Geoffroy, O., Saint-Martin, D. and Roehrig, R.: "Robustness and drivers of the Northern Hemisphere extratropical atmospheric circulation response to a CO<sub>2</sub>-induced warming in CNRM-CM6-1," *Climate Dyn.* (54:3-4), 2020, pp. 2267-2285.
- Padron, R. S., Gudmundsson, L., Decharme, B., Ducharne, A., Lawrence, D. M., Mao, J., Peano, D., Krinner, G., Kim, H. and Seneviratne, S. I.: "Observed changes in dry-season water availability attributed to human-induced climate change," *Nat. Geosci.* (13:7), 2020, pp. 477-481.
- Pagès, R., Baklouti, M., Barrier, N., Ayache, M., Sevault, F., Somot, S. and Moutin, T.: "Projected Effects of Climate-Induced Changes in Hydrodynamics on the Biogeochemistry of the Mediterranean Sea Under the RCP 8.5 Regional Climate Scenario," *Front. Mar. Sci.* (7), 2020.
- Palchetti, L., Brindley, H., Bantges, R., Buehler, S. A., Camy-Peyret, C., Carli, B., Cortesi, U., Bianco, S. D., Natale, G. D., Dinelli, B. M., Feldman, D., Huang, X. L., C.-Labonnote, L., Libois, Q., Maestri, T., Mlynczak, M. G., Murray, J. E., Oetjen, H., Ridolfi,

- M., Riese, M., Russell, J., Saunders, R. and Serio, C.: "FORUM: unique far-infrared satellite observations to better understand how Earth radiates energy to space," *Bull. Amer. Meteor. Soc.*, 2020, pp. 1-52.
- Pannekoucke, O. and Fablet, R.: "PDE-NetGen 1.0: from symbolic partial differential equation (PDE) representations of physical processes to trainable neural network representations," *Geosci. Model Dev.* (13:7), 2020, pp. 3373-3382.
- Pedreras R., Idier D, Le Roy S., David A., Schaeffer C., Durand J., Desmazes F.: "Infragravity Waves in a Complex Macro-tidal Environment: High Frequency Hydrodynamic Measurements and Modelling", *Journal of Coastal Research*, Coastal Education and Research Foundation, 2020, 95 (sp1), pp.1235. 10.2112/SI95-239.1
- Peinke, I., Hagenmuller, P., Ando, E., Chambon, G., Flin, F. and Roule, J. "Experimental Study of Cone Penetration in Snow Using X-Ray Tomography," *Front. Earth Sci.* (8), 2020.
- Pellet, V., Aires, F., Papa, F., Munier, S. and Decharme, B.: "Long-term Total Water Storage Change from a Satellite Water Cycle (SAWC) reconstruction over large south Asian basins," *Hydrol. Earth Syst. Sci.* (24), 2020, pp. 3033-3055.
- Peng, J., C. Albergel, A. Balenzano, L. Brocca, O. Cartus, M.H. Cosh, W.T. Crow, K. Dabrowska-Zielinska, S. Dadson, M.W.J. Davidson, P. de Rosnay, W. Dorigo, A. Gruber, S. Hagemann, M. Hirschi, Y.H. Kerr, F. Lovergine, M.D. Mahecha, P. Marzahn, F. Mattia, J. Pawel Musial, S. Preuschmann, R.H. Reichle, G. Satalino, M. Silgram, P. M. van Bodegom, N.E.C. Verhoest, W. Wagner, J.P. Walker, U. Wegmüller, A. Loew: "A roadmap for high-resolution satellite soil moisture applications – confronting product characteristics with user requirements", *Remote Sens. Environ.*, 2020, 112162.
- Phillips V., Formenton M., Kanawade V., Karlsson L., Patade S., et al.: "Multiple Environmental Influences on the Lightning of Cold-Based Continental Cumulonimbus Clouds. Part I: Description and Validation of Model", *Journal of the Atmospheric Sciences*, 2020, 77 (12), pp.3999-4024. 10.1175/JAS-D-19-0200.1
- Picard, G., Dumont, M., Lamare, M., Tuzet, F., Larue, F., Pirazzini, R., and Arnaud, L.: "Spectral albedo measurements over snow-covered slopes: theory and slope effect corrections, The Cryosphere, 14, 1497–1517, <https://doi.org/10.5194/tc-14-1497-2020>, 2020.
- Pineau-Guillou, L., Bouin, M.-N., Arduin, F., Lyard, F., Bidlot, J.-R. and Chapron, B. "Impact of wave-dependent stress on storm surge simulations in the North Sea: Ocean model evaluation against in situ and satellite observations," *Ocean Modell.* (154), 2020, pp. 101694.
- Planton, Y.Y., Guilyardi, E., Wittenberg, A. T., Lee, J., Gleckler, P.J., Bayr, T., McGregor, S., McPhaden, M. J., Power, S., Roehrig, R., Vialard, J. and Voldoire, A. "Evaluating climate models with the CLIVAR 2020 ENSO metrics package," *Bull. Amer. Meteor. Soc.*, 2020, pp. 1-57.
- Qasmi, S., Sanchez-Gomez, E., Ruprich-Robert, Y., Boé, J. and Cassou, C. "Modulation of the occurrence of heatwaves over the Euro-Mediterranean region by the intensity of the Atlantic Multidecadal Variability," *J. Climate*, 2020, pp. 1-50.
- Quesada-Ruiz, S., Attié, J.-L., Lahoz, W. A., Abida, R., Ricaud, P., Amraoui, L. E., Zbinden, R., Piacentini, A., Joly, M., Eskes, H., Segers, A., Curier, L., de Haan, J., Kujanpää, J., Nijhuis, A. C. P. O., Tamminen, J., Timmermans, R. and Veeckind, P. "Benefit of ozone observations from Sentinel-5P and future Sentinel-4 missions on tropospheric composition," *Atmos. Meas. Tech.* (13:1), 2020, pp. 131-152.
- Reale, M., Salon, S., Somot, S., Solidoro, C., Giorgi, F., Crise, A., Cossarini, G., Lazzari, P. and Sevault, F. "Influence of large-scale atmospheric circulation patterns on nutrient dynamics in the Mediterranean Sea in the extended winter season (October-March) 1961-1999," *Climate Research* (82), 2020, pp. 117-136.
- Redon, E., Lemonsu, A. and Masson, V. "An urban trees parameterization for modeling microclimatic variables and thermal comfort conditions at street level with the Town Energy Balance model (TEB-SURFEX v8.0)," *Geosci. Model Dev.* (13:2), 2020, pp. 385-399.
- Revuelto, J., Billecocq, P., Tuzet, F., Cluzet, B., Lamare, M., Larue, F. and Dumont, M.: "Random forests as a tool to understand the snow depth distribution and its evolution in mountain areas," *Hydrol. Processes* (34:26), 2020, pp. 5384-5401.
- Ribes, A., Thao, S. and Cattiaux, J.: "Describing the Relationship between a Weather Event and Climate Change: A New Statistical Approach," *J. Climate* (33:15), 2020, pp. 6297-6314.
- Ricaud, P., Grigioni, P., Roehrig, R., Durand, P. and Veron, D. E.: "Trends in Atmospheric Humidity and Temperature above Dome C, Antarctica Evaluated from Observations and Reanalyses," *Atmosphere* (11:8), 2020, pp. 836.
- Ricaud, P., Guasta, M. D., Bazile, E., Azouz, N., Lupi, A., Durand, P., Attié, J.-L., Veron, D., Guidard, V. and Grigioni, P.: "Supercooled liquid water cloud observed, analysed, and modelled at the top of the planetary boundary layer above Dome C, Antarctica," *Atmos. Chem. Phys.* (20:7), 2020, pp. 4167-4191.
- Riette, S.: "Development of Physical Parameterizations with Python (PPY, version 1.1) and its usage to reduce the time-step dependency in a microphysical scheme," *Geosci. Model Dev.* (13:2), 2020, pp. 443-460.
- Rivière, G., Ricard, D. and Arbogast, P.: "The downward transport of momentum to the surface in idealized sting-jet cyclones," *Quart. J. Roy. Meteor. Soc.* (146:729), 2020, pp. 1801-1821.
- Robin, Y. and Ribes, A.: "Nonstationary extreme value analysis for event attribution combining climate models and observations," *Adv. Stat. Climatol. Meteorol. Oceanogr.* (6:2), 2020, pp. 205-221.
- Rocco M., Colomb A., Baray J.-L., Amelynck C., Verreyken B. et al.: "Analysis of Volatile Organic Compounds during the OCTAVE Campaign: Sources and Distributions of Formaldehyde on Reunion Island", *Atmosphere*, 2020, 11 (2), 10.3390/atmos11020140
- Roehrig, R., Beau, I., Saint-Martin, D., Alias, A., Decharme, B., Guérémy, J.-F., Voldoire, A., Abdel-Lathif, A. Y., Bazile, E., Belamari, S., Blein, S., Bouniol, D., Bouteloup, Y., Cattiaux, J., Chauvin, F., Chevallier, M., Colin, J., Douville, H., Marquet, P., Michou, M., Nabat, P., Oudar, T., Peyrillé, P., Piriou, J.-M., y Méliá, D. S., Sférian, R. and Sénési, S.: "The CNRM Global Atmosphere Model ARPEGE-Climate 6.3: Description and Evaluation," *J. Adv. Model. Earth Syst.* (12:7), 2020.
- Roux E., Ignotti E., Bègue N., Bencherif H., Catry T., et al.: "Toward an Early Warning System for Health Issues Related to Particulate Matter Exposure in Brazil: The Feasibility of Using Global PM 2.5 Concentration Forecast Products", *Remote Sensing*, 2020, *Remote Sensing for Health: from Fine-Scale Investigations towards Early-Warning Systems*, 12 (24), pp.4074. 10.3390/rs12244074
- Roux, E. L., Evin, G., Eckert, N., Blanchet, J. and Morin, S.: "Non-stationary extreme value analysis of ground snow loads in the French Alps: a comparison with building standards," *Nat. Hazards Earth Syst. Sci.* (20:11), 2020, pp. 2961-2977.
- Sabatier, T., Largeron, Y., Paci, A., Lac, C., Rodier, Q., Canut, G. and Masson, V.: "Semi-idealized simulations of wintertime flows and pollutant transport in an alpine valley. Part II : Passive tracer tracking.," *QJR Meteorol Soc.*, 2020.
- Sabatier, T., Paci, A., Lac, C., Canut, G., Largeron, Y. and Masson, V.: "Semi-idealized simulations of wintertime flows and pollutant transport in an Alpine valley : Origins of local circulations (Part I).," *QJR Meteorol Soc.*, 2020.
- Sahlaoui, Z., S. Mordane, E. Wattrelot & J.-F. Mahfouf (2020): "Improving heavy rainfall forecasts by assimilating surface precipitation in the convective scale model AROME : A case study of the Mediterranean event of November 4, 2017." *Meteorological Applications*, 27, e1869. <https://doi.org/10.1002/met.1860>.
- Saint-Martin, D., Geoffroy, O., Voldoire, A., Cattiaux, J., Brient, F., Chauvin, F., Chevallier, M., Colin, J., Decharme, B., Delire, C., Douville, H., Guérémy, J.-F., Joetzier, E., Ribes, A., Roehrig, R., Terray, L. and Valcke, S.: "Tracking changes in climate sensitivity in CNRM climate models," *J. Adv. Model. Earth Syst.*, 2020.
- Saliba, G., Sanchez, K., Russell, L., Twohy, C., Roberts, G., Lewis, S., Dedrick, J., McCluskey, C., Moore, K., DeMott, P. J. and Toohey, D.: "Organic Composition of Three Different Size Ranges of Aerosol Particles over the Southern Ocean," *Aerosol Sci. Technol.*, 2020.
- Sánchez-Zapero, J., F. Camacho, E. Martínez-Sánchez, R. Lacaze, D. Carrer, F. Pinault, I. Benhadj, J. Muñoz-Sabater: "Quality assessment of PROBA-V surface albedo V1 for the continuity of the Copernicus Climate Change service". *Remote Sens.*, 12, 2596, <https://doi.org/10.3390/rs12162596>, 2020.
- Sanchez, K. J., Roberts, G. C., Diao, M. and Russell, L. M.: "Measured Constraints on Cloud-Top Entrainment to Reduce Uncertainty of Stratocumulus Shortwave Radiative Forcing in the Southern Ocean," *Geophys. Res. Lett.*, 2020.
- Sanchez, K. J., Roberts, G. C., Saliba, G., Russell, L. M., Twohy, C., Reeves, M., Humphries, R. S., Keywood, M. D., Ward, J. P. and McRobert, I. M.: "Measurement report: Cloud Processes and the Transport of Biological Emissions Regulate Southern Ocean Particle and Cloud Condensation Nuclei Concentrations," *Atmos. Chem. Phys. Disc.*, 2020.
- Sauvage, C., Lebeaupin Brossier, C., Bouin, M.-N. and Ducrocq, V.: "Characterization of the air-sea

exchange mechanisms during a Mediterranean heavy precipitation event using realistic sea state modelling," *Atmos. Chem. Phys.* (20), 2020, pp. 1675-1699.

Saux Picart, S., Marsouin, A., Legendre, G., Roquet, H., Péré, S., Nano-Ascione, N. and Gianelli, T.: "A Sea Surface Temperature data record (2004-2012) from Meteosat Second Generation satellites," *Remote Sens. Environ.* (240), 2020, pp. 111687.

Schoetter, R., Hidalgo, J., Jouglu, R., Masson, V., Rega, M. and Pergaud, J.: "A Statistical Dynamical Downscaling for the Urban Heat Island and Building Energy Consumption Analysis of Its Uncertainties," *Journal of Applied Meteorology and Climatology* (59:5), 2020, pp. 859-883.

Schoetter, R., Kwok, Y. T., de Munck, C., Lau, K. K. L., Wong, W. K. and Masson, V.: "Multi-layer coupling between SURFEX-TEB-V9.0 and Meso-NH-v5.3 for modelling the urban climate of high-rise cities," *Geosci. Model Dev.* (13), 2020, pp. 5609-5643.

Séférian, R., Berthet, S., Yool, A., Palmiéri, J., Bopp, L., Tagliabue, A., Kwiatkowski, L., Aumont, O., Christian, J., Dunne, J., Gehlen, M., Ilyina, T., John, J. G., Li, H., Long, M., Luo, J. Y., Nakano, H., Romanou, A., Schwinger, J., Stock, C., Santana-Falcón, Y., Takano, Y., Tjiputra, J., Tsujino, H., Watanabe, M., Wu, T., Wu, F. and Yamamoto, A.: "Tracking improvement in simulated marine biogeochemistry between CMIP5 and CMIP6," *Current Climate Change Reports*, 2020.

Ser-Giacomi, E., Jorda-Sanchez, G., Soto-Navarro, J., Thomsen, S., Mignot, J., Sevault, F. and Rossi, V.: "Impact of Climate Change on Surface Stirring and Transport in the Mediterranean Sea," *Geophys. Res. Lett.* (47:22), 2020.

Shaw, T. E., Deschamps-Berger, C., Gascoin, S. and McPhee, J.: "Monitoring Spatial and Temporal Differences in Andean Snow Depth Derived From Satellite Tri-Stereo Photogrammetry," *Front. Earth Sci.* (8), 2020.

Shinozuka, Y., Saide, P. E., Ferrada, G. A., Burton, S. P., Ferrare, R., Doherty, S. J., Gordon, H., Longo, K., Mallet, M., Feng, Y., Wang, Q., Cheng, Y., Dobracki, A., Freitag, S., Howell, S. G., LeBlanc, S., Flynn, C., Segal-Rosenhaimer, M., Pistone, K., Podolske, J. R., Stith, E. J., Bennett, J. R., Carmichael, G. R., da Silva, A., Govindaraju, R., Leung, R., Zhang, Y., Pfister, L., Ryo, J.-M., Redemann, J., Wood, R. and Zuidema, P.: "Modeling the smoky troposphere of the southeast Atlantic: a comparison to ORACLES airborne observations from September of 2016," *Atmos. Chem. Phys.* (20:19), 2020, pp. 11491-11526.

Siebert, H., Szodry, K.-E., Egerer, U., Wehner, B., Henning, S., Chevalier, K., Lückner, J., Welz, O., Weinhold, K., Fialho, P., Roberts, G., Allwayin, N., Schum, S., Shaw, R. A., Mazzoleni, C., Mazzoleni, L., Nowak, J. L., Malinowski, S., Karpinska, K., Kumala, W., Czyzewska, D., Luke, E. P., Kollias, P., Wood, R. and Mellado, J. P.: "Observations of aerosol, cloud, turbulence, and radiation properties at the top of the marine boundary layer over the Eastern North Atlantic Ocean: The ACORES campaign," *Bull. Amer. Meteor. Soc.*, 2020.

Smith, C. J., Kramer, R. J., Myhre, G., Alterskjær, K., Collins, W., Sima, A., Boucher, O., Dufresne, J.-L., Nabat, P., Michou, M., Yukimoto, S., Cole, J., Paynter, D., Shiogama, H., O'Connor, F. M.,

Robertson, E., Wiltshire, A., Andrews, T., Hannay, C., Miller, R., Nazarenko, L., Kirkevåg, A., Olivé, D., Fiedler, S., Lewinschal, A., Mackallah, C., Dix, M., Pincus, R. and Forster, P. M.: "Effective radiative forcing and adjustments in CMIP6 models," *Atmos. Chem. Phys.* (20:16), 2020, pp. 9591-9618.

Sow, M., Diakhaté, M., Dixon, R. D., Guichard, F., Dieng, D. and Gaye, A. T.: "Uncertainties in the Annual Cycle of Rainfall Characteristics over West Africa in CMIP5 Models," *Atmosphere* (11:2), 2020, pp. 216.

Specq, D. and Batté, L.: "Improving sub-seasonal precipitation forecasts through a statistical dynamical approach: application to the southwest tropical Pacific," *Climate Dyn.*, 2020.

Specq, D., Batté, L., Déqué, M. and Ardilouze, C.: "Multimodel Forecasting of Precipitation at Subseasonal Timescales Over the Southwest Tropical Pacific," *Earth Space Sci.* (7:9), 2020.

Stoffelen, A., Benedetti, A., Borde, R., Dabas, A., Flamant, P., Forsythe, M., Hardesty, M., Isaksen, I., Källén, E., Körnich, H., Reitebuch, O., Rennie, M., Riishøjgaard, L.-P., Schyberg, H., Straume, A. G. and Vaughan, M.: "Wind Profile Satellite Observation Requirements and Capabilities," *Bull. Amer. Meteor. Soc.*, 2020.

Taillardat, M. and Mestre, O.: "From research to applications – examples of operational ensemble post-processing in France using machine learning," *Nonlin. Processes Geophys.*, 27, 329–347, <https://doi.org/10.5194/npg-27-329-2020>, 2020.

Tato Loua R., Bencherif H., Bègue N., Mbatha N., Portafaix T. et al.: "Surface Temperature Trend Estimation over 12 Sites in Guinea Using 57 Years of Ground-Based Data" *Climate*, 2020, 8 (6), 10.3390/cli8060068

Thomas, G., J.-F. Mahfouf & T. Montmerle (2020): "Toward a variational assimilation of polarimetric radar observations in a convective-scale numerical weather (NWP) model". *Atmos. Meas. Tech.*, 13, 2279-2298. <https://doi.org/10.5194/amt-13-2279-2020>

Tian, H., Xu, R., Canadell, J. G., Thompson, R. L., Winiwarter, W., Suntharalingam, P., Davidson, E. A., Ciais, P., Jackson, R. B., Janssens-Maenhout, G., Prather, M. J., Regnier, P., Pan, N., Pan, S., Peters, G. P., Shi, H., Tubiello, F. N., Zaehle, S., Zhou, F., Arneeth, A., Battaglia, G., Berthet, S., Bopp, L., Bouwman, A. F., Buitenhuis, E. T., Chang, J., Chipperfield, M. P., Dangal, S. R. S., Dlugokencky, E., Elkins, J. W., Eyre, B. D., Fu, B., Hall, B., Ito, A., Joos, F., Krummel, P. B., Landolfi, A., Laruelle, G. G., Lauerwald, R., Li, W., Lienert, S., Maavara, T., MacLeod, M., Millet, D. B., Olin, S., Patra, P. K., Prinn, R. G., Raymond, P. A., Ruiz, D. J., van der Werf, G. R., Vuichard, N., Wang, J., Weiss, R. F., Wells, K. C., Wilson, C., Yang, J. and Yao, Y.: "A comprehensive quantification of global nitrous oxide sources and sinks," *Nature* (586:7828), 2020, pp. 248-256.

Tokarska, K. B., Arora, V. K., Gillett, N. P., Lehner, F., Rogelj, J., Schleussner, C.-F., Séférian, R. and Knutti, R.: "Uncertainty in carbon budget estimates due to internal climate variability," *Environ. Res. Lett.*, 2020.

Tramblay, Y., A. Koutroulis, L. Samaniego, S. Vicente-Serrano, F. Volaire, A. Boone, M. Le Page,

M. Carmen Llasat, C. Albergel, Z. Selmin Burak, M. Cailleret, K. Cindric Kalin, H. Davi, J.-L. Dupuy, P. Greve, M. Grillakis, L. Hanich, L. Jarlan, N. Martin-StPaul, J. Martinez Vilalta, D. Pulido Velazquez, P. Quintana Segui, D. Renard, M. Turco, M. Turkes, R. Trigo, J.-P. Vidal, A. Vilagrosa, M. Zribi, J. Polcher, 2020: "Future Mediterranean droughts: Current scenarios and research perspectives", *Earth-Science Reviews*, 103348, ISSN 0012-8252, doi:10.1016/j.earscirev.2020.103348

Turnock, S. T., Allen, R. J., Andrews, M., Bauer, S. E., Deushi, M., Emmons, L., Good, P., Horowitz, L., John, J. G., Michou, M., Nabat, P., Naik, V., Neubauer, D., O'Connor, F. M., Olivé, D., Oshima, N., Schulz, M., Sellar, A., Shim, S., Takemura, T., Tilmes, S., Tsigaridis, K., Wu, T. and Zhang, J.: "Historical and future changes in air pollutants from CMIP6 models," *Atmos. Chem. Phys.* (20:23), 2020, pp. 14547-14579.

Tuzet, F., Dumont, M., Picard, G., Lamare, M., Voisin, D., Nabat, P., Lafaysse, M., Larue, F., Revuelto, J. and Arnaud, L.: "Quantification of the radiative impact of light-absorbing particles during two contrasted snow seasons at Col du Lautaret (20580.167emm0.167ema.s.l., French Alps)," *The Cryosphere* (14:12), 2020, pp. 4553-4579.

Udina, M., Bech, J., González, S., Soler, M. R., Paci, A., Miró, J. R., Trapero, L., Donier, J. M., Douffet, T., Codina, B. and Pineda, N.: "Multi-sensor observations of an elevated rotor during a mountain wave event in the Eastern Pyrenees.," *Atmospheric Research*, 2020.

Vanderbecken, P. J., Mahfouf, J.-F. and Millet, C.: "Bayesian selection of atmospheric profiles from an ensemble data assimilation system using infrasonic observations of May 2016 Mount Etna eruptions," *Journal of Geophysical Research: Atmospheres*, 2020.

Vautard, R., Kadyrov, N., Iles, C., Boberg, F., Buonomo, E., Bülow, K., Coppola, E., Corre, L., Meijgaard, E., Nogherotto, R., Sandstad, M., Schwingshackl, C., Somot, S., Aalbers, E., Christensen, O. B., Ciarlo, J. M., Demory, M.-E., Giorgi, F., Jacob, D., Jones, R. G., Keuler, K., Kjellström, E., Lenderink, G., Levvasseur, G., Nikulin, G., Sillmann, J., Solidoro, C., Sørland, S. L., Steger, C., Teichmann, C., Warrach-Sagi, K. and Wulfmeyer, V.: "Evaluation of the large EURO-CORDEX regional climate model ensemble," *Journal of Geophysical Research: Atmospheres*, 2020.

Vautard, R., van Aalst, M., Boucher, O., Drouin, A., Haustein, K., Kreienkamp, F., van Oldenborgh, G. J., Otto, F. E. L., Ribes, A., Robin, Y., Schneider, M., Soubeyrou, J.-M., Stott, P., Seneviratne, S. I., Vogel, M. M. and Wehner, M.: "Human contribution to the record-breaking June and July 2019 heatwaves in Western Europe," *Environ. Res. Lett.* (15:9), 2020, pp. 094077.

Vergnes, J.-P., Roux, N., Habets, F., Ackerer, P., Amraoui, N., Besson, F., Caballero, Y., Courtois, Q., de Dreuzy, J.-R., Etchevers, P., Gallois, N., Leroux, D., Longuevergne, L., Le Moigne, P., Morel, T., Munier, S., Regimbeau, F., Thiéry, D. and Viennot, P.: "The Aquifer hydrometeorological modelling platform as a tool for improving groundwater resource monitoring over France: evaluation over a 60 year period," *Hydrol. Earth Syst. Sci.* (24), 2020, pp. 633-654.

Verreyken B., Amelynck C., Brioude J., Müller J.-F., Schoon N. et al. : "Characterisation of African biomass burning plumes and impacts on the



atmospheric composition over the south-west Indian Ocean", *Atmospheric Chemistry and Physics, European Geosciences Union*, 2020, 20 (23), pp.14821-14845. 10.5194/acp-20-14821-2020

Viallon-Galinier, L., Hagenmuller, P. and Lafaysse, M.: "Forcing and evaluating detailed snow cover models with stratigraphy observations," *Cold Reg. Sci. Technol.* (180), 2020.

Viguié, V., Lemonsu, A., Hallegatte, S., Beaulant, A.-L., Marchadier, C., Masson, V., Pigeon, G. and Salagnac, J.-L.: "Early adaptation to heat waves and future reduction of air-conditioning energy use in Paris," *Environ. Res. Lett.* (15:7), 2020, pp. 075006.

Volpi, D., Batté, L., Guérémy, J.-F. and Déqué, M.: "Teleconnection-based evaluation of seasonal forecast quality," *Climate Dyn.*, 2020.

Wang J. K., Aouf L., Jia Y. J., Zhang Y.: "Validation and Calibration of Significant Wave Height and wind speed retrievals from HY2B altimeter based on deep learning", *Remote Sensing*, 2020, 12, 2858; doi:10.3390/rs12172858.

Wing, A. A., Stauffer, C. L., Becker, T., Reed, K. A., Ahn, M.-S., Arnold, N. P., Bony, S., Branson, M., Bryan, G. H., Chaboureaud, J.-P., Rood, S. R. D., Gayatri, K., Hohenegger, C., Hu, I.-K., Jansson, F., Jones, T. R., Khairoutdinov, M., Kim, D., Martin, Z. K., Matsugishi, S., Medeiros, B., Miura, H., Moon, Y., Müller, S. K., Ohno, T., Popp, M., Prabhakaran, T., Randall, D., Rios-Berrios, R., Rochetin, N., Roehrig, R., Romps, D. M., Ruppert, J. H., Satoh, M., Silvers, L. G., Singh, M. S., Stevens, B., Tomassini, L., van Heerwaarden, C. C., Wang, S. and Zhao, M.: "Clouds and Convective Self-Aggregation in a Multimodel Ensemble of Radiative-Convective Equilibrium Simulations," *J. Adv. Model. Earth Syst.* (12:9), 2020.

Worou, K., Goosse, H., Fichet, T., Guichard, F. and Diakhaté, M.: "Interannual variability of rainfall in the Guinean Coast region and its links with sea surface temperature changes over the twentieth century for the different seasons," *Climate Dyn.* (55:3-4), 2020, pp. 449-470.

Wright C., Jean Preez D., Martincigh B., Allen M., Millar D. et al.: "A Comparison of Solar Ultraviolet Radiation Exposure in Urban Canyons in Venice, Italy and Johannesburg, South Africa", *Photochemistry and Photobiology*, 2020, 96 (5), pp.1148-1153. 10.1111/php.13291

Yiou, P., Cattiaux, J., Faranda, D., Kadyrov, N., Jézéquel, A., Naveau, P., Ribes, A., Robin, Y., Thao, S., van Oldenborgh, G. J. and Vrac, M.: "Analyses of the Northern European Summer Heatwave of 2018," *Bull. Amer. Meteor. Soc.* (101:1), 2020, pp. S35-S40.

Zanis, P., Akritidis, D., Georgoulas, A. K., Allen, R. J., Bauer, S. E., Boucher, O., Cole, J., Johnson, B., Deushi, M., Michou, M., Mulcahy, J., Nabat, P., Ollivier, D., Oshima, N., Sima, A., Schulz, M., Takemura, T. and Tsigaridis, K.: "Fast responses on pre-industrial climate from present-day aerosols in a CMIP6 multi-model study," *Atmos. Chem. Phys.* (20:14), 2020, pp. 8381-8404.

Zgheib, T., Giacoma, F., Granet-Abisset, A.-M., Morin, S. and Eckert, N.: "One and a half century of avalanche risk to settlements in the upper Maurienne valley inferred from land cover and socio-environmental changes," *Global Environ. Change* (65), 2020, pp. 102149.

Zheng, Y., Albergel, C., Munier, S., Bonan, B. and Calvet, J.-C.: "An offline framework for high-dimensional ensemble Kalman filters to reduce the time to solution," *Geosci. Model Dev.* (13:8), 2020, pp. 3607-3625.

Zhou M., Wang P., Langerock B., Vigouroux C., Hermans C. et al.: "Ground-based Fourier transform infrared (FTIR) O3 retrievals from the 3040 cm<sup>-1</sup> spectral range at Xianghe, China", *Atmospheric Measurement Techniques*, 2020, 13, pp.5379 - 5394. 10.5194/amt-13-5379-2020

Zribi, M.; Albergel, C.; Baghdadi, N. Editorial for the Special Issue: "Soil Moisture Retrieval using Radar Remote Sensing Sensors". *Remote Sens.*, 12, 1100, 2020.

---

## 2020 Scientific papers list (outside DESR)

Cantet, P., A. Belmadani, F. Chauvin, and P. Palany, 2020: "Projections of tropical cyclone rainfall over land with an Eulerian approach: Case study of three islands in the West Indies". *Int. J. Climatol.*, doi:10.1002/joc.6760.

Chauvin F., Pilon R., Palany P., Belmadani A. (2020): "Future changes in Atlantic hurricanes with the rotated-stretched ARPEGE-Climat at very high resolution". *Clim Dyn* 54:947-972. doi:10.1007/s00382-019-05040-4.

Delrieu, G., Khanal, A. K., Yu, N., Cazenave, F., Boudevillain, B., and Gaussiat, N.: "Preliminary investigation of the relationship between differential phase shift and path-integrated attenuation at the X band frequency in an Alpine environment", *Atmos. Meas. Tech.*, 13, 3731-3749, <https://doi.org/10.5194/amt-13-3731-2020>, 2020.

Hemri, S., Lerch, S., Taillardat, M., Vannitsem, S., and Wilks, D. S.: "Preface: Advances in post-processing and blending of deterministic and ensemble forecasts", *Nonlin. Processes Geophys.*, 27, 519-521, <https://doi.org/10.5194/npg-27-519-2020>, 2020.

Marzieh H. Derkani, A. Alberello, F. Nelli, L. G. Bennetts, K. G. Hessner, K. MacHutchon, K. Reichert, L. Aouf, S. Saeed Khan, and A. Toffoli : "Wind, waves, and surface currents in the Southern Ocean : Observations from the Antarctic Circumnavigation Expedition". *Earth System Science Data*, <https://doi.org/10.5194/essd-2020-255>.

Tourain C., D. Hauser, L. Hermozo, R. Rodriguez Suquet, P. Schippers, L. Aouf, A. Dalphiné, A. Mouche, B. Chapron, F. Collard, C. Dufour, F. Gouillon, A. Ollivier, F. Piras, M. Dalila, G. Guitton, J.-M. Lachiver, C. Tison: "CAL/VAL Phase for the Swim Instrument Onboard cFOSAT", *Geoscience and Remote Sensing Symposium IGARSS 2020 - 2020 IEEE International*, pp. 5678-5681, 2020.

Triquenot A., Fu Ruget, F. Souverain (2020) : « Le suivi de la pousse des prairies par le Ministère en charge de l'agriculture : aspects institutionnels et fonctionnels », *Fourrages* 244, 93-100

Viatte C., C. Clerbaux, C. Maes, P. Daniel, R. Garello, S. Safieddine & F. Arduin, 2020: "Air Pollution and Sea Pollution Seen from Space", *Surveys in Geophysics*, June 2020.

Vinet, F., M. Peroche, P. Palany, F. Leone, M. Gherardi, D. Grancher, A. Moatty, and S. Defossez, 2020: « Collecte et gestion des débris post-cycloniques à Saint-Martin (Antilles françaises) après le passage du cyclone Irma (sept. 2017) ». *CyberGeo: European Journal of Geography, Environnement, Nature, Paysage*, 937, doi:10.4000/cybergeo.34154.

Wang J. K., L. Aouf, X. Wang, B. Li, J. J. Wang: Remotely cross-calibration of wave buoys based on significant wave height of altimeters", *Remote Sensing*, 2020.

## PHD defended in 2020

Aleksovska, I. : « Améliorer les prévisions à court et moyen termes des modèles agronomiques en prenant mieux en compte l'incertitude des prévisions météorologiques. » Université de Toulouse, 2020.

Cluzet, B.: "Assimilation of space-borne snowpack shortwave reflectances and in-situ snow depths into spatialised ensemble simulations of the seasonal snow cover". Université de Toulouse, 2020.

Cussac, M. : « La composition chimique de la haute troposphère : étude de l'impact des feux de biomasse et des processus de transports verticaux avec le modèle MOCAGE et les mesures IAGOS. » INPT, Toulouse, 2020.

Destouches, M. : « Prise en compte des hydro-météores dans un schéma d'assimilation variationnel ensembliste appliqué au modèle de prévision AROME. » Université de Toulouse, 2020.

Erdmann, F.: "Preparation for the use of Meteosat Third Generation Lightning Imager observations in short-term numerical weather prediction". Université de Toulouse, 2020.

Guinaldo, T. : « Paramétrisation de la dynamique lacustre dans un modèle de surface couplé pour une application à la prévision hydrologique à l'échelle globale. » INPT, Toulouse, 2020.

Hamidi, Y. : « Détection de la texture des précipitations et des nébulosités avec des méthodes d'apprentissage statistique : application aux prévisions du modèle Arome. » Université de Toulouse, 2020.

Mandement, M. : « Apport des données d'objets connectés pour l'étude de la convection profonde à fine échelle. » INPT, Toulouse, 2020.

Rigal, A. : « Déformation des cycles saisonniers de variables climatiques. » Université de Toulouse, 2020.

Rocher, M. : « Evaluation des pratiques agricoles comme levier d'action contre le réchauffement climatique : apport de la modélisation à l'échelle globale. » INPT, Toulouse, 2020.

Sassi, Z. : « Apport de la synergie des observations satellitaires pour la définition de la température de surface en prévision numérique. » Université de Toulouse, 2020.

Shamambo, D. : « Assimilation de données satellitaires pour le suivi des ressources en eau dans la zone Euro-Méditerranée. » Université de Toulouse, 2020.

Speck, D. : « Prévisibilité des fortes précipitations aux échéances infra-saisonnières sur le Pacifique Sud-Ouest tropical. » INPT, Toulouse, 2020.

---

## « Habilitations à diriger des recherches » defended in 2020

Chambon P., 2020 : « Apport des observations spatiales pour l'estimation et la prévision des précipitations tropicales »

Decharme B., 2020 : « Contribution à la modélisation des surfaces continentales pour l'échelle globale »

Raynaud L., 2020 : « Représentation des incertitudes en Prévision Numérique du Temps : de l'état initial aux applications »

Vidot J., 2020 : « Modélisation du transfert radiatif rapide pour la Prévision Numérique du Temps »

# Glossary

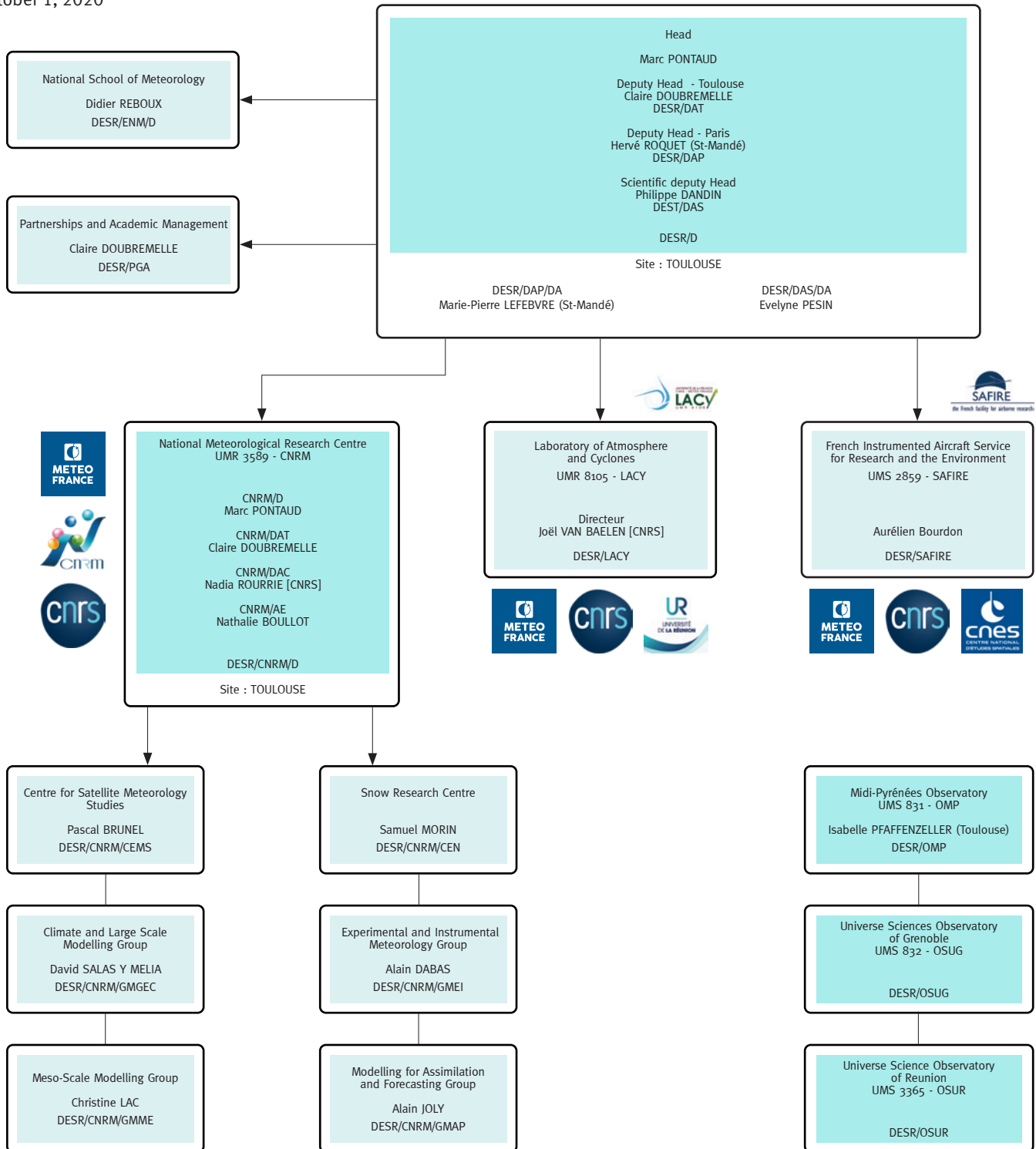
<b>3DnVar</b>	Schéma d'assimilation variationnel ensembliste tridimensionnel	<b>CNRM-ESM2-1</b>	Modèle du système Terre
<b>4DnVar</b>	Schéma associant l'approche variationnelle utilisée traditionnellement à Météo-France aux approches ensemblistes utilisées	<b>CNRM-RCSM6</b>	sixième version du système couplé de modélisation régionale
<b>ADAMONT</b>	Impacts du changement climatique et adaptation en territoire de montagne	<b>CNRS</b>	Centre National de Recherches Scientifiques
<b>ADEME</b>	Agence de l'Environnement et de la Maîtrise de l'Energie	<b>CO</b>	Monoxyde de Carbone
<b>ADM</b>	Atmospheric Dynamics Mission	<b>COMSI</b>	Comité scientifique
<b>ADT</b>	suivi autonome de la détresse	<b>COPERNICUS</b>	European Earth observation system <a href="http://www.copernicus.eu/pages-principales/services/climate-change/">http://www.copernicus.eu/pages-principales/services/climate-change/</a>
<b>AEMET</b>	Agencia Estatal de Meteorología (Espagne)	<b>CORDEX</b>	COordinated Regional climate Downscaling EXperiment
<b>AEOLUS</b>	Atmospheric Explorer Observations with a Lidar UV System	<b>CROCO</b>	modèle d'océan
<b>AERIS-GEO</b>	Aerosol and surface albedo Retrieval Using a directional Splitting method-application to GEOstationary data	<b>CROCUS</b>	Modèle de simulation numérique du manteau neigeux développé par Météo-France.
<b>AFAI</b>	Alternative Floating Algae Index	<b>CTRIP</b>	CNRM-Total Routing Integrated Pathway
<b>ALADIN</b>	Aire Limitée Adaptation Dynamique et développement InterNational	<b>DACCIWA</b>	Dynamics-Aerosol-Chemistry-Cloud Interactions in West Africa
<b>ALPHA</b>	Algorithmes et modèles pour la Production Homogène globale	<b>DCSC</b>	Direction de la Climatologie et des Services Climatiques
<b>AMSR</b>	Advanced Microwave Scanning Radiometer	<b>DEAL</b>	Direction de l'Environnement, de l'Aménagement et du Logement
<b>ANR</b>	Agence Nationale de la Recherche	<b>DESR</b>	Direction de l'Enseignement Supérieur et de la Recherche
<b>AOS</b>	Aérosols Organiques Secondaires	<b>DGPR</b>	Direction Générale de la Prévention des Risques
<b>AROME</b>	Application de la Recherche à l'Opérationnel à Mésos-Échelle	<b>DGSCGC</b>	Direction générale de la Sécurité Civile et de la Gestion de Crise
<b>AROME-PI</b>	Configuration AROME Prévision Immédiate	<b>Dianeige</b>	bureau d'études spécialisé dans l'aménagement touristique de la montagne
<b>ARPEGE</b>	Action de Recherche Petite Échelle Grande Échelle	<b>DIRAG</b>	Direction Inter-Régionale Antilles Guyane
<b>ASCAT</b>	Advanced SCATterometer	<b>DMSP</b>	Defense Meteorological Satellite Program
<b>AVHRR</b>	Advanced Very High Resolution Radiometer	<b>DRE</b>	Effet radiatif direct
<b>BIO Maïdo</b>	Bio-physicochemistry of tropical clouds at Maïdo	<b>DRIAS</b>	Portail d'accès à des données climatiques
<b>BSC</b>	Barcelona Supercomputing Center	<b>DSM</b>	Direction des Services Météorologiques
<b>BSRN</b>	Baseline Surface Radiation Network	<b>DSO</b>	Direction des Systèmes d'Observation
<b>C3S</b>	Copernicus Climate Change Service	<b>DSSF</b>	Downwelling surface short-wave radiation flux service météorologique allemand
<b>CALIOP</b>	Cloud-Aerosol Lidar with Orthogonal Polarization	<b>DWD</b>	service météorologique allemand
<b>CALIPSO</b>	Cloud-Aerosol Lidar and Infrared Pathfinder Satellite Observations	<b>ECMWF</b>	European Centre for Medium-range Weather Forecasts
<b>CAMS</b>	projet Européen Copernicus	<b>EcRad</b>	code de transfert radiatif
<b>CART</b>	Classification And Regression Trees	<b>ECUME</b>	ECUME paramétrisation des vagues
<b>CAT</b>	Clear Air Turbulence, Turbulence en Air Clair	<b>EDMF</b>	Eddy-Diffusivity-Mass-Flux
<b>CCM-I</b>	Chemistry-Climate Model Initiative	<b>EDR</b>	Eddy Dissipation Rate
<b>Cedre</b>	Centre de documentation, de recherche et d'expérimentations sur les pollutions accidentelles des eaux	<b>ENSO</b>	El Nino Southern Oscillation
<b>CEMS</b>	Centre d'Etude en Météorologie Satellitaire	<b>EOF</b>	Fonction Orthogonale Empirique
<b>CEN</b>	Centre d'Etudes de la Neige	<b>ERA</b>	European Re-Analysis
<b>CENPERM</b>	Center for Permafrost, University of Copenhagen	<b>ESA</b>	European Space Agency
<b>CEPMMT</b>	Centre Européen pour les Prévisions Météorologiques à Moyen Terme	<b>ESGF</b>	Earth System Grid Federation,
<b>CFOSAT</b>	Chinese-French SATellite	<b>EUMETSAT</b>	Organisation européenne pour l'exploitation de satellites météorologiques
<b>CLA</b>	Couche Limite Atmosphérique	<b>EUREC4A</b>	Elucidating the role of clouds-circulation coupling in climate
<b>CLIMSNOW</b>	Adaptation au changement climatique et projections de l'évolution de enneigement	<b>EUROCORDEX</b>	Modèle régional de climat
<b>CMCC</b>	Centre euro-Méditerranéen sur le Changement Climatique (Italie)	<b>EUSPA</b>	l'Agence du programme spatial de l'Union européenne
<b>CMIP</b>	Coupled Model Intercomparaison Project	<b>FEDER</b>	Fonds Européen de Développement Régional
<b>CMIP6</b>	Climate Models Intercomparison Project n°6	<b>FTP</b>	File Transfert Protocol
<b>CMO</b>	Couche Limite Océanique	<b>GADSS</b>	système global du programme mondial de sécurité aérienne
<b>CNES</b>	Centre National d'Études Spatiales	<b>GCM</b>	Modèle de circulation Générale
<b>CNRM</b>	Centre National de Recherches Météorologiques	<b>GELATO</b>	Global Experimental Leads and ice for Atmosphere and Ocean
<b>CNRM-CM6</b>	Version 6 du Modèle de Climat du CNRM	<b>GEO</b>	Group on Earth Observations
		<b>GEO-rng</b>	ceinture géostationnaire
		<b>GET</b>	laboratoire de Géosciences Environnement Toulouse
		<b>GHER</b>	GeoHydrodynamic and Environmental Research
		<b>GHF</b>	Green House Gazes

<b>GIEC</b>	Groupe Intergouvernemental d'experts sur l'Evolution du Climat	<b>MFWAM</b>	Météo-France Wave Model
<b>GIRAFE</b>	capteur Gravimétrique Interférométrique de Recherche à Atomes Froids Embarqué	<b>MJO</b>	Madden-Julian Oscillation
<b>GLDB</b>	Global Lake DataBase	<b>Mlake</b>	Modèle de bilan de masse des lacs
<b>GMAP</b>	Groupe de Modélisation et d'Assimilation pour la Prévision	<b>MOCAGE</b>	MOdélisation de la Chimie Atmosphérique de Grande Echelle (modélisation)
<b>GMEI</b>	Groupe de Météorologie Expérimentale et Instrumentale	<b>MODCOU</b>	MOdèle hydrologique COUplé surface-souterrain.
<b>GNSS</b>	systèmes mondiaux de navigation par satellite	<b>MODIS</b>	MOderate-resolution Imaging Spectro-radiometer (instrument)
<b>GOES</b>	Satellites météorologiques géostationnaires américains	<b>MOTHY</b>	Modèle Océanique de Transport d'HYdrocarbure
<b>GPCP</b>	Global Precipitation Climatology Project	<b>MRIR</b>	Medium Resolution Infrared Radiometer
<b>GSMA</b>	association internationale d'opérateurs télécoms	<b>MSG</b>	Météosat Seconde Génération
<b>GSX</b>	partenaire de Météo-France exploitant l'outil PROSNOW	<b>MSU</b>	Microwave Sounder Unit
<b>GTG</b>	Graphical Turbulence Guidance	<b>MTES</b>	Ministère de la Transition Ecologique et Solidaire
<b>HAMSTRAD</b>	H2O Antarctica Microwave Stratospheric and Tropospheric Radiometer	<b>MTG</b>	Météosat Troisième Génération
<b>HCERES</b>	Haut Conseil de l'évaluation de la recherche et de l'enseignement supérieur	<b>MTG-I</b>	Meteosat Third Generation – Imager
<b>HCL</b>	Hauteur de Couche Limite	<b>MUST</b>	Expérience climat urbain
<b>HIRLAM</b>	High Resolution Limited Area Model	<b>MW</b>	Micro Ondes
<b>HITRAN</b>	High-resolution TRANsmission molecular absorption database	<b>MWR</b>	radiomètre micro-ondes
<b>HOMONIM</b>	Historique Observation MOdélisation des Niveaux Marins	<b>NCAR</b>	National Center for Atmospheric Research
<b>HRIR</b>	High Resolution Infrared Radiometer	<b>NEMO</b>	Nucleus for European Modelling of Ocean
<b>HYCOM</b>	HYbrid Coordinate Ocean Model	<b>NEPHELAE</b>	Network for studying Entrainment and microPHysics of cLouds using Adaptive Exploration
<b>HyMeX</b>	Hydrological cYcle in the Mediterranean EXperiment	<b>NH3</b>	formule de l'ammoniac
<b>IAGOS</b>	In-service Aircraft for Global Observing System	<b>NOAA</b>	National Ocean and Atmosphere Administration
<b>IASI</b>	Interféromètre Atmosphérique de Sondage Infrarouge	<b>NWCSAF</b>	Satellite Application Facility for Nowcasting
<b>ICE3</b>	Schéma de nuages	<b>OACI</b>	Organisation de l'Aviation Civile Internationale
<b>ICICLE</b>	Campagne de mesures	<b>OAD</b>	Outils d'Aide à la Décision
<b>IFPEN</b>	Institut Français du Pétrole Energies Nouvelles	<b>OASIS-MCT</b>	Coupleur
<b>Ifremer</b>	Institut Français de Recherche pour l'Exploitation de la MER	<b>OLCI</b>	capteur satellitaire
<b>IFS</b>	Integrated Forecasting System	<b>OMM</b>	Organisation Météorologique Mondiale
<b>IGE</b>	Institut des Géosciences de l'Environnement	<b>ONERA</b>	Office national d'études et de recherches aérospatiales
<b>INRA</b>	Institut National de la Recherche Agronomique	<b>OPAR</b>	Observatoire de Physique de l'Atmosphère de la Réunion
<b>INRAE</b>	Institut National de Recherche pour l'Agriculture, l'alimentation et l'Environnement	<b>OPG</b>	Orages Points de Grille
<b>IODC</b>	Indian Ocean Data Coverage	<b>OSTIA</b>	Operational Sea surface Temperature sea Ice Analysis
<b>IPCC</b>	Intergovernmental Panel on Climate Change (Groupe d'experts intergouvernemental sur l'évolution du climat)	<b>PANGAEA</b>	Base de données climat
<b>IPSL</b>	Institut Pierre Simon Laplace	<b>PEARP</b>	Prévision d'Ensemble ARPège
<b>IR</b>	Infra Rouge	<b>PI</b>	Prévision Immédiate
<b>IRD</b>	Institut de Recherche pour le Développement	<b>PM10</b>	PM10 (particules aérosols de moins de 10 microns) ca
<b>IRIS</b>	InfraRed Interfometer Spectrometer	<b>PNT</b>	Prévision Numérique du Temps
<b>ISBA</b>	Interaction Sol-Biosphère-Atmosphère	<b>PROSNOW</b>	Provision of a prediction for Snow management
<b>KNMI</b>	Koninklijk Nederlands Meteorologisch Instituut	<b>RADOME</b>	Réseau d'Acquisition de Données d'Observations Météorologiques Etendu
<b>LA</b>	Laboratoire d'Aérodologie	<b>RCM</b>	Modèle de Climat Régional
<b>LACY</b>	Laboratoire de l'Atmosphère et des Cyclones – UMR 8105	<b>RCP</b>	Representative Concentration Pathway
<b>LAMP</b>	Laboratoire de Météorologie Physique	<b>RCP8.5</b>	8.5 W/m <sup>2</sup> Representative Concentration Pathway corresponding to a 8.5 W/m <sup>2</sup> radiative forcing at the end of the 21st century compared to preindustrial climate
<b>LARGE</b>	Laboratoire de recherche en géosciences et énergie	<b>ReNov'Risk</b>	Recherche intégrée et innovante sur les risques naturels : Impact Météorologique et Océanographique des Cyclones Tropicaux sur les territoires du Sud-Ouest de l'Océan Indien
<b>LATMOS</b>	Laboratoire Atmosphères, Observations Spatiales	<b>RGB</b>	Red Green Blue (satellite)
<b>LBLRTM</b>	Line-By-Line Radiative Transfer Model	<b>RHT</b>	Relative Humidity Threshold
<b>LEFE</b>	programme national « Les Enveloppes Fluides et l'Environnement »	<b>ROC</b>	Relative Operating Characteristic curve
<b>LIAISE</b>	Land surface Interactions with the Atmosphere over the Iberian Semi-arid Environment	<b>RTTOV</b>	Radiative Transfer for TOVS
<b>LIDAR</b>	light detection and ranging	<b>S2S</b>	Sub-seasonal to Seasonal
<b>LIMA</b>	schémas microphysiques	<b>SAF NSC</b>	Satellite Application Facility on support to Nowcasting
<b>LMD</b>	Laboratoire de Météorologie Dynamique	<b>SAF OWI</b>	Satellite Application Facility for Ocean and Sea Ice
<b>LMI</b>	Lifetime Maximum Intensity	<b>SAFIRE</b>	Service des Avions Français Instrumentés pour la Recherche en Environnement
<b>LSA</b>	Land Surface Analysis	<b>SAFRAN</b>	Système d'Analyse Fournissant des Renseignements Atmosphériques pour la Neige
<b>LSCE</b>	Laboratoire des Sciences du Climat et de l'Environnement	<b>SAR</b>	Synthetic Aperture Radar
<b>MAP-IO</b>	Marion Dufresne Atmospheric Program – Indian Ocean	<b>SBG</b>	Subgrid (phénomènes sous-grille)
<b>MCT</b>	Modèle de Chimie Transport	<b>SBUV-MOD</b>	Solar Backscatter UltraViolet -Merged Ozone Dataset
<b>MEB</b>	Multi-Energy-Balance	<b>SCARBO</b>	Space CARBon Observatory
<b>MEDSCOPE</b>	Mediterranean Services Chain based On climate Predictions	<b>SDI</b>	Sahara Dust Index
<b>Megha-Tropiques</b>	Satellite franco-indien dédié à l'étude du cycle de l'eau et des échanges d'énergie dans la zone tropicale	<b>Sentinel-2</b>	satellite optique Sentinel-2
<b>MERCATOR-OCEAN</b>	Société Civile Française d'océanographie opérationnelle	<b>SEsar</b>	Single European Sky ATM Research
<b>MERIT-DEM</b>	Modèle Numérique de terrain	<b>SEVIRI</b>	Spinning Enhanced Visible and Infra-Red Imager
<b>MERIT/HYDRO</b>	Modèle Numérique de Terrain à haute résolution	<b>Shom</b>	Service Hydrographique et Océanographique de la Marine
<b>MESO-NH</b>	Modèle à MESO-échelle Non Hydrostatique	<b>SIRS</b>	Satellite InfraRed Spectrometer
<b>METAR</b>	METEorological Aerodrome Report	<b>SLSTR</b>	Sea and Land Surface Temperature Radiometer
<b>METOP</b>	METEorological Operational Polar satellites	<b>SMMR</b>	Scanning Multichannel Microwave Radiometer
		<b>SOFOG3D</b>	SOuth westFOGs 3D (compréhension des processus de petites échelles pour améliorer les prévisions du brouillard)
		<b>SOLOMN</b>	Réseau de données météorologiques
		<b>SOOI</b>	Sud-Ouest Océan Indien
		<b>SROCC</b>	Rapport Spécial sur l'Océan et la Cryosphère dans un Climat Changeant

<b>SRON</b>	Space Research Organisation Netherlands	<b>TIROS</b>	Television InfraRed Operational Sounder
<b>SSM</b>	Special Sensor Microwave	<b>TRIP</b>	Total Runoff Integrating Pathways
<b>SSP</b>	Shared Socio-economic Pathway	<b>TRL</b>	Technology Readiness Level
<b>SURFEX</b>	code de SURFace EXternalisé	<b>TSM</b>	Températures de Surface de la Mer
<b>SURFEX/Flake</b>	Modèle d'évaporation	<b>UERRA</b>	Uncertainties in Ensembles of Regional Re-Analyses
<b>SWI</b>	Soil Wetness Index	<b>UK</b>	United Kingdom
<b>SWIM</b>	Surface Wave Investigation and Monitoring	<b>UMR</b>	Unité Mixte de Recherche
<b>SYNOP</b>	Données d'observations issues des messages internationaux d'observation en surface	<b>UTC</b>	Temps universel coordonné,
<b>TACTIC</b>	schéma interactif d'aérosols	<b>UTLS</b>	Haute Troposphère Basse Stratosphère
<b>TAF</b>	Terminal Aerodrome Forecast	<b>VAAC</b>	Volcanic Ash Advisory Centre
<b>TCCON</b>	Total Carbon Column Observing Network	<b>VIIRS</b>	Visible Infrared Imager Radiometer Suite
<b>TEB</b>	Town Energy Balance	<b>WASP</b>	Wave-Age dependent Stress Parameterization)
<b>TEMSI</b>	TEMps Significatif (aéronautique)	<b>WIRE</b>	Winter Risks for Energy
<b>THIR</b>	Temperature-Humidity Infrared Radiometer	<b>WMO/UNEP</b>	World Meteorological Organization / United Nations Environment Program

# DESR: Management structure

October 1, 2020



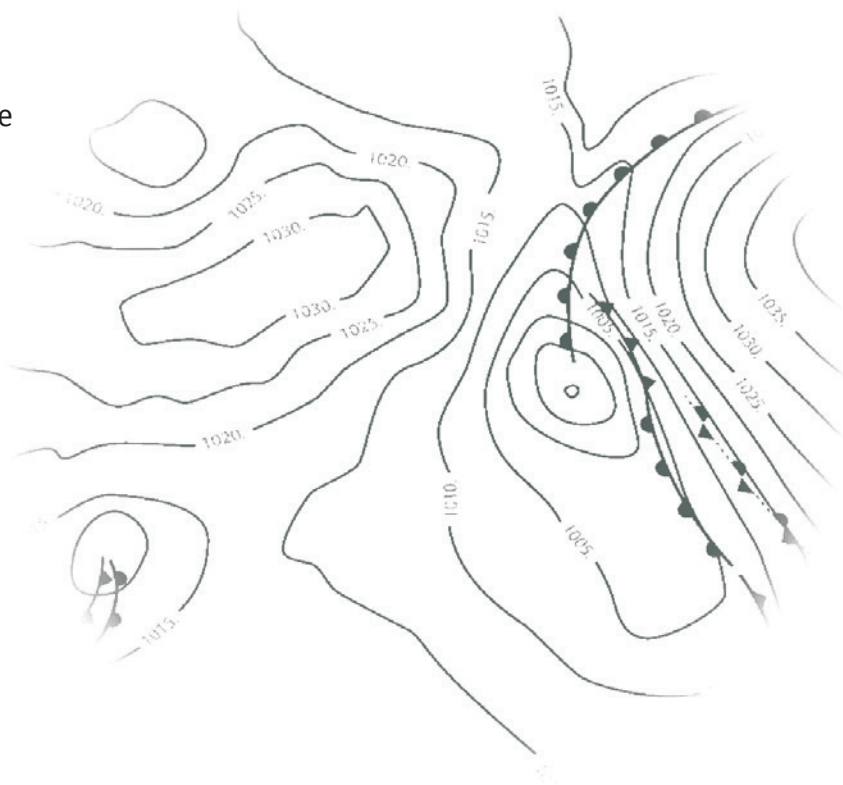


## Météo-France

73, avenue de Paris  
94165 Saint-Mandé Cedex  
Phone: +33 (0) 1 77 94 77 94  
Fax: +33 (0) 1 77 94 70 05  
[www.meteofrance.com](http://www.meteofrance.com)

## Higher Education and Research Department

42, avenue Gaspard Coriolis  
31057 Toulouse Cedex 1 France  
Phone: +33 (0) 5 61 07 93 70  
Fax: +33 (0) 5 61 07 96 00  
<http://www.meteofrance.fr/activites-recherche>  
Mail: [desr\\_contact@meteo.fr](mailto:desr_contact@meteo.fr)



Creation DIRCOM

Météo-France is certified to ISO 9001  
by AFNOR Certification  
© Météo-France 2021  
Copyright juin 2021  
ISSN : 2116-4541